広島大学学位請求論文

Alternating links and cubed complexes
（交代絡み目と立方複体）

学位取得年月2024 年 2 月

坂井駿介

目次

主論文

Alternating links and cubed complexes

Shunsuke Sakai

Abstract

An alternating link is a link that is represented by a diagram in which the crossings alternate under and over as one travels along each component of the link. Alternating links have various interesting properties. In particular, J. Greene and J. Howie independently gave an intrinsic characterization of alternating links, as an answer to R. H. Fox's problem, "What is an alternating knot?"

On the other hand, a cubed complex is a CW-complex obtained from a disjoint union of cubes by identifying the faces through Euclidean isometries. Cubed complexes play important roles in 3-manifold theory. In particular, it was proved by I. Aitchison that the exterior of a prime alternating link admits a natural non-positively curved cubed decomposition.

In this paper, we study alternating links from the view point of cubed complexes. This thesis consists of two parts. In the first part, we give a characterization of alternating link exteriors in terms of cubed complexes. In the second part, we give a rigorous proof to a result, announced by I. Agol in 2001, concerning two-parabolic-generator subgroups of hyperbolic alternating link groups. We also give a generalization of Agol's result to two-parabolic-generator subgroups of hyperbolic 3-manifold groups.

The content of the first part of the thesis was published in *Journal of Knot Theory and Its Ramifications* in vol. **27** (2018), published by World Scientific Publishing, and the second part will appear in *Hiroshima Mathematical Journal*, published by the Department of Mathematics, Hiroshima University.

Acknowledgements

I would like to express my deepest gratitude to Makoto Sakuma, for his guidance, encouragement and sharing his insights throughout this project. He was my supervisor during my time as an undergraduate and graduate student at Hiroshima University, until March 2020. Even after retirement, he continued to support me. This work would not have been possible without his support. I am grateful to Yuya Koda, who was my supervisor during the academic years April 2020 to March 2022, for his guidance and encouragement. I would like to thank my family for their support.

I would like to thank Ian Agol for making the slide of his talk available. I would also like to thank Iain Aitchison for teaching me the key ideas of polyhedral decompositions and cubical decompositions of alternating link exteriors and for numerous invaluable discussions. My thanks also go to Hirotaka Akiyoshi, Michel Boileau, Tetsuya Ito, Takuya Katayama, Yohei Komori, Ian Leary, Hideki Miyachi, Makoto Ozawa, and Yuta Taniguchi for enlightening conversations and encouragements.

Contents

Chapter 1

A characterization of alternating link exteriors in terms of cubed complexes

1.1 Introduction

Recently, Greene [23] and Howie [27], independently, established intrinsic characterizations of alternating links in terms of a pair of spanning surfaces, answering an old question of R. H. Fox. These results can be regarded as characterizations of alternating link exteriors which have marked meridians (see [27, Theorem 3.2]).

The purpose of this paper is to give a characterization of alternating link exteriors from the viewpoint of cubed complexes. Our starting point is a cubical decomposition of alternating link exteriors, which is originally due to Aitchison, and is used by Thurston [50], Yokota [53, 54], Agol [3], Adams [2] and Sakuma-Yokota [45]. Thus we call it the *Aitchison complex*. The Aitchison complex for an alternating link is actually a mapping cylinder of the natural map from the boundary of the exterior of the alternating link onto the Dehn complex. For a detailed description and historical background, see [45].

In this paper, we introduce the concepts of a *signed BW squared-complex* (or an *SBW squared-complex*, for short) and a *signed BW cubed-complex* (or an *SBW cubed-complex*, for short), and give a combinatorial description of the Dehn complex and the Aitchison complex as an SBW squared-complex and an SBW cubed-complex, respectively. The main theorem gives a necessary and sufficient condition for a given SBW cubed-complex to be isomorphic to the Aitchison complex of some alternating link exterior (Theorem 1.4.1). This implies a characterization of alternating link exteriors in terms of cubed complexes (Corollary 1.4.2).

This paper is organized as follows. In Section 1.2, we give an intuitive

description of the Aitchison complex and the Dehn complex following [50, 53]. In Section 1.3, we introduce the SBW squared-complex and the SBW cubed-complex, and describe the Dehn complex and the Aitchison complex in terms of the SBW squared-complex and the SBW cubed-complex, respectively. In Section 1.4, we prove the main theorem.

1.2 An intuitive description of the Aitchison complexes and the Dehn complexes for alternating links

In this section, we give an intuitive description of the Aitchison complexes and the Dehn complexes following [50, 53]. For detailed description, see [45].

Let $\Gamma \subset S^2$ be a connected alternating link diagram and $L \subset S^3$ the alternating link represented by Γ. We pick two points P_+ and P_- in the components of $S^3 \setminus S^2$ one by one. These points are regarded to lie above and below S^2, respectively. Identify $S^3 \setminus \{P_+, P_-\}$ with $S^2 \times \mathbb{R}$, and assume the following. The diagram Γ is regarded as a 4-valent graph in $S^2 \times \{0\}$, $L \subset \Gamma \times [-1,1] \subset S^2 \times [-1,1]$, and L intersects $S^2 \times \{0\}$ transversely in $2n$ points, where n is the crossing number of Γ.

For each vertex x of Γ, consider a square s in $S^2 = S^2 \times \{0\}$ which forms a relative regular neighborhood of x in (S^2, Γ) such that the four vertices of s lie in the four germs of edges around x. Let x^+ and x^- be the points of L which lie above and below x, respectively. Consider the two pyramids, $\Delta^\pm$, in S^3 which are obtained as the joins $x^\pm * s$. We may assume $\Delta^\pm \cap L = \{x^\pm\}$, $\Delta^+ \cap \Delta^- = s$. Note that $\Delta^+ \cup \Delta^-$ is an octahedron which contains the crossing arc of L determined by x (see Figure 1.1(b)). Let $\{\Delta_1^\pm, \dots, \Delta_n^\pm\}$ be the set of $2n$ pyramids in S^3 located around the vertices of Γ.

Pick an edge e of the graph Γ, and let x_1 and x_2 be the vertices of Γ joined by e, such that the arc $\tilde{e} = L \cap (e \times [-1,1])$ in L joins x_1^+ and x_2^- (see Figure 1.1(a)). Let a_i be the vertex of s_i contained in e $(i = 1, 2)$. Let R be one of the two regions of Γ in S^2 whose boundary contains the edge e, and let b_i be the vertex of s_i such that the edge $a_i b_i$ of s_i is contained in R.

Let $w = \tilde{e} \cap S^2$ be the "middle point" of $\tilde{e}$, and consider the vertical line segments wP_+ and wP_-. Then we have the following relative isotopies in (S^3, L) (see Figure 1.1(b)).

1. The edges $x_1^+ a_1$ and $x_1^+ b_1$ of the pyramid Δ_1^+ are isotopic to the vertical line segments wP_- and wP_+, respectively.

2. The edges $x_2^- a_2$ and $x_2^- b_2$ of the pyramid Δ_2^- are isotopic to the vertical line segments wP_+ and wP_-, respectively.

3. The edge $a_1 b_1$ of s_1 is isotopic to an almost vertical line segment which starts P_-, passes through a point in the interior of R and reaches P_+.

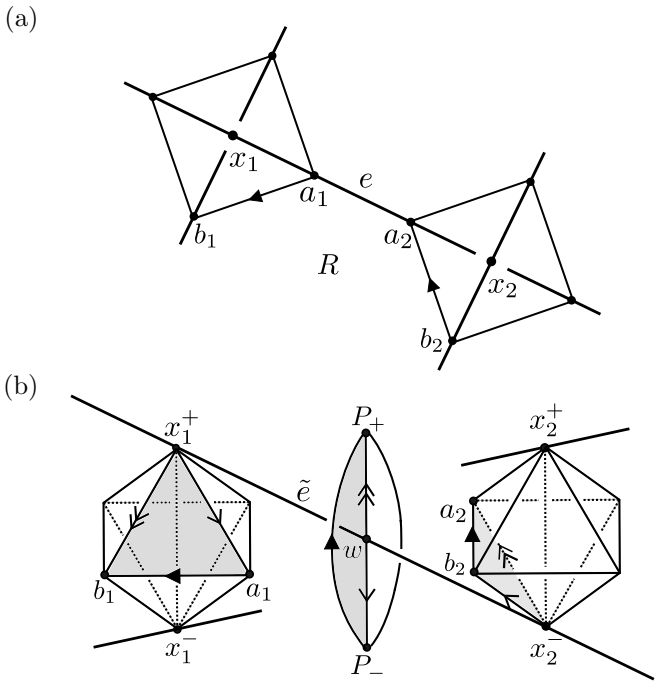

Figure 1.1

4. The edge b_2a_2 of s_2 is isotopic to an almost vertical line segment which starts P_-, passes through a point in the interior of R and reaches P_+.

These isotopies determine an isotopy (and so a homeomorphism) from the face $x_1^+a_1b_1$ of Δ_1^+ onto the face $x_2^-b_2a_2$ of Δ_2^-. In this way, we obtain a paring of faces of the octahedra $\{\Delta_i^+ \cup \Delta_i^-\}_i$ and a homeomorphism between the faces in each pair. Let $O_i^\pm$ be the cubes obtained from the pyramids $\Delta_i^\pm$ by chopping off a small regular neighborhoods of $x_i^\pm$. Then the above pairing and homeomorphisms determine a gluing information for the cubes $\{O_i^\pm\}_i$. Let $\mathcal{A}(\Gamma)$ be the resulting cubed complex and $\mathcal{D}(\Gamma)$ the subcomplex of $\mathcal{A}(\Gamma)$ obtained by gluing the squares $\{\Delta_i^+ \cap \Delta_i^-\}_i$. Then we have the following.

Proposition 1.2.1. *For a connected alternating diagram Γ, $\mathcal{A}(\Gamma)$ gives a cubical decomposition of the exterior $E(L)$ of the link L represented by Γ. Moreover, there is a deformation retraction of $\mathcal{A}(\Gamma)$ onto $\mathcal{D}(\Gamma)$, and so, $\mathcal{D}(\Gamma)$ is a spine of $E(L)$.*

We call $\mathcal{A}(\Gamma)$ the *Aitchison complex* of Γ. The subcomplex $\mathcal{D}(\Gamma)$ is isotopic to the Dehn complex of the diagram Γ, which is the two-dimensional cell complex defined as follows (see [16, 17, 55]). The 0-cells are P_+ and P_-, and the 1-cells are in one-to-one correspondence with the regions of the diagram; each 1-cell γ_i is a path going from P_+ to P_- and passing through a region R_i. The 2-cells are in one-to-one correspondence with the vertices of the diagram; for each vertex x, the 2-cell has a boundary of form $\gamma_{i_{x(1)}}\gamma_{i_{x(2)}}^{-1}\gamma_{i_{x(3)}}\gamma_{i_{x(4)}}^{-1}$, where $R_{i_{x(1)}}, R_{i_{x(2)}}, R_{i_{x(3)}}, R_{i_{x(4)}}$ are the regions of Γ that is located around x in this counterclockwise order, and γ^{-1} is the inverse path of γ.

1.3 Signed BW complexes

In this section, we introduce the concept of a *signed BW squared-complex* and that of a *signed BW cubed-complex*, and then describe the Dehn complexes and the Aitchison complexes for alternating links by using these concepts.

By a *signed BW square* (or an *SBW-square*, for short), we mean the square $s := [0,1]^2$ with the following information:

1. The vertices $(0,0)$ and $(1,1)$ are endowed with the sign $-$, and the vertices $(0,1)$ and $(1,0)$ are endowed with the sign $+$.

2. The horizontal edges $I \times \{0\}$ and $I \times \{1\}$ are endowed with the color B (Black), and the vertical edges $\{0\} \times I$ and $\{1\} \times I$ are endowed with the color W (White).

For an SBW-square s, we assume that each edge of s is oriented so that the initial point and the terminal point have the sign $-$ and $+$, respectively. Now consider a set $S = \{s_1, \ldots, s_n\}$ of n copies of the SBW-square, and let $V_+(S)$ and $V_-(S)$, respectively, be the sets of positive vertices and negative vertices of the SBW-squares in S.

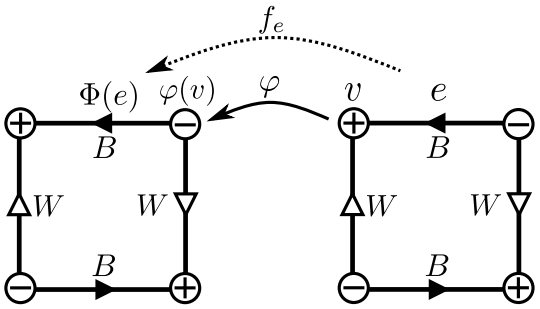

Figure 1.2

For each bijection $\varphi\colon V_+(S) \to V_-(S)$, we construct a squared complex (i.e. two-dimensional cubed complex), $\mathcal{C}^2(S,\varphi)$, as follows. Let $E_B(S)$ and $E_W(S)$, respectively, be the set of the black edges and the white edges of the SBW-squares in S. Then φ induces a bijection $\Phi_B\colon E_B(S) \to E_B(S)$ as follows. For a black edge $e \in E_B(S)$, let v be the positive vertex which forms the terminal point of e. Then $\Phi_B(e)$ is defined to be the unique black edge whose initial vertex is $\varphi(v)$ (see Figure 1.2). Similarly, φ induces a bijection $\Phi_W\colon E_W(S) \to E_W(S)$, such that $\Phi_W(e)$, for $e \in E_W(S)$, is the unique white edge whose initial vertex is the image of the terminal vertex of e by φ. Thus we obtain a bijection $\Phi := \Phi_B \sqcup \Phi_W$ from $E(S) := E_B(S) \sqcup E_W(S)$ to itself. For each $e \in E(S)$, let $f_e\colon e \to \Phi(e)$ be the unique orientation-preserving linear homeomorphism. We regard the family $\{f_e\colon e \to \Phi(e)\}_{e\in E(S)}$ as a gluing information for the SBW-squares $S = \{s_1, \dots, s_n\}$, and denote the resulting squared complex by $\mathcal{C}^2(S,\varphi)$. We call it the *signed BW squared-complex* (or the *SBW squared-complex*, for short) determined by the bijection $\varphi\colon V_+(S) \to V_-(S)$.

Remark 1.3.1. A signed BW squared-complex is a special case of a VH-complex introduced by Wise [55], which is defined to be a squared complex whose edges are partitioned into two classes V (vertical) and H (horizontal). Motivated by black/white checkerboard surfaces, we use W and B, instead of V and H.

For the SBW squared-complex $\mathcal{C}^2(S,\varphi)$, we define the associated SBW cubed-complex, $\mathcal{C}^3(S,\varphi)$, as follows. For the set $S = \{s_1, \dots, s_n\}$ of the SBW-squares, consider the set of the "upper SBW-cubes" $\{s_i \times [0,1]\}_{i=1}^n$ and the "lower SBW-cubes" $\{s_i \times [-1,0]\}_{i=1}^n$. Consider also the set of "upper side-faces" $F_+ := \{e \times [0,1]\}_{e\in E(S)}$ and the set of "lower side-faces" $F_- := \{e \times [-1,0]\}_{e\in E(S)}$. Then the bijection $\Phi\colon E(S) \to E(S)$ induces the bijection $\hat{\Phi}\colon F_- \to F_+$ defined by $\hat{\Phi}(e\times[-1,0]) = \Phi(e)\times[0,1]$. Moreover, the linear homeomorphism $f_e\colon e \to \Phi(e)$ induces the linear homeomorphism $\hat{f_e}\colon e \times [-1,0] \to \Phi(e) \times [0,1]$ defined by $\hat{f_e}(x,t) = (f_e(x), -t)$. By gluing the side-faces of the cubes $\{e \times [-1,0] \cup e \times [0,1]\}_{e\in E(S)}$ by the family of homeomorphisms $\{\hat{f_e}\colon e \times [-1,0] \to \Phi(e) \times [0,1]\}_{e\in E(S)}$, we obtain a three-dimensional cubed

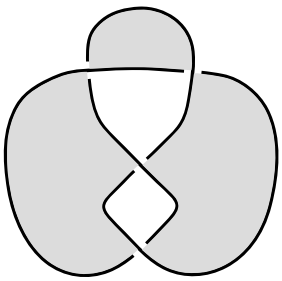

Figure 1.3

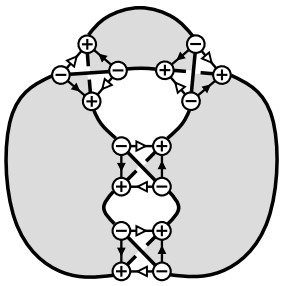

Figure 1.4

complex. We denote it by $\mathcal{C}^3(S,\varphi)$, and call it the *signed BW cubed-complex* (or the *SBW cubed-complex*, for short) determined by φ. It should be noted that $\mathcal{C}^2(S,\varphi)$ is a subcomplex of $\mathcal{C}^3(S,\varphi)$, and there is a natural deformation retraction of $\mathcal{C}^3(S,\varphi)$ onto $\mathcal{C}^2(S,\varphi)$.

For an alternating link $L \subset S^3$ represented by a connected alternating diagram $\Gamma \subset S^2$, the Dehn complex $\mathcal{D}(\Gamma)$ and the Aitchison complex $\mathcal{A}(\Gamma)$ are identified with the SBW squared-complex $\mathcal{C}^2(S,\varphi)$ and the SBW cubed-complex $\mathcal{C}^3(S,\varphi)$, respectively, where S and φ are defined as follows. Consider the checkerboard coloring of (S^2,Γ) such that the associated black surface for L has a positive half-twist at each crossing (see Figure 1.3). Let $\{x_1,\dots,x_n\}$ be the vertex set of Γ and let $S=\{s_1,\dots,s_n\}$ be the set of SBW-squares as illustrated in Figure 1.4. To be precise,

1. s_i is a square in S^2 which forms a relative regular neighborhood of x_i in (S^2,Γ), and the vertices of s_i are contained in Γ.

2. Each vertex of s_i has the sign $+$ or $-$ according to whether it lies in an underpass or an overpass.

3. Each edge of s_i is colored B or W according to whether it lies in a black region or a white region.

Observe that $\Gamma \setminus \bigcup_{i=1}^n \operatorname{int}(s_i)$ is a disjoint union of arcs and that the boundary of each of which consists of a vertex in $V_+(S)$ and a vertex in $V_-(S)$. This determines a bijection $\varphi\colon V_+(S) \to V_-(S)$. Then the following proposition is obvious from the construction of the Aitchison complex.

Proposition 1.3.2. *Under the above setting, the SBW squared-complex $\mathcal{C}^2(S,\varphi)$ and the SBW cubed-complex $\mathcal{C}^3(S,\varphi)$ are isomorphic to the Dehn complex $\mathcal{D}(\Gamma)$ and the Aitchison complex $\mathcal{A}(\Gamma)$, respectively.*

1.4 Main results

Proposition 1.3.2 shows that the Aitchison complex $\mathcal{A}(\Gamma)$ of a connected alternating diagram Γ can be described as the SBW cubed-complex $\mathcal{C}^3(S,\varphi)$. In this

section, we prove Theorem 1.4.1, which gives a characterization of the Aitchison complexes of connected alternating diagrams among the SBW cubed-complexes.

Let $S = \{s_1, \dots, s_n\}$ be a set of SBW-squares, and let $\varphi\colon V_+(S) \to V_-(S)$ be a bijection, where $V_\pm(S)$ are the sets of positive and negative vertices of the SBW-squares in S. Let $\Phi = \Phi_B \sqcup \Phi_W$ be the bijection from $E(S) = E_B(S) \sqcup E_W(S)$ to itself determined by φ.

Theorem 1.4.1. *Under the above setting, the SBW cubed-complex $\mathcal{C}^3(S, \varphi)$ is isomorphic to the Aitchison complex $\mathcal{A}(\Gamma)$ of a connected alternating diagram Γ, if and only if the bijection Φ satisfies*

$$|E(S)/\langle\Phi\rangle| = |S| + 2,$$

where $E(S)/\langle\Phi\rangle$ denotes the quotient space of the cyclic group action on $E(S)$ induced by Φ, and $|\cdot|$ denotes the cardinality of a set.

Proof. We first prove the only if part. Suppose that an SBW cubed-complex $\mathcal{C}^3(S, \varphi)$ is isomorphic to the Aitchison complex $\mathcal{A}(\Gamma)$ of a connected alternating diagram $\Gamma \subset S^2$. Then we may assume S and φ are constructed from Γ as in Section 1.3. Observe that there is a one-to-one correspondence between $E_B(S)/\langle\Phi\rangle$ (resp. $E_W(S)/\langle\Phi\rangle$) and the set of the black (resp. white) regions of Γ. Consider the cell decomposition of the projection plane S^2 obtained from Γ. Then the above observation implies that $|E(S)/\langle\Phi\rangle|$ is equal to the number of 2-cells of the cell decomposition. Since the cell decomposition has n vertices and each vertex has degree four, the number of 1-cells is equal to $2n$ when $n = |S|$. Hence, we have

$$2 = \chi(S^2) = n - 2n + |E(S)/\langle\Phi\rangle|.$$

This implies $|E(S)/\langle\Phi\rangle| = |S| + 2$, completing the proof of the only if part.

Next, we prove the if part. Suppose $|E(S)/\langle\Phi\rangle| = |S| + 2$. By using this condition, we construct a connected alternating diagram Γ such that $\mathcal{C}^3(S, \varphi) \cong \mathcal{A}(\Gamma)$. Consider the two-dimensional complex, X, obtained from the set $S = \{s_1, \dots, s_n\}$ of SBW-squares by attaching a 1-cell $\gamma = \langle v, \varphi(v)\rangle$ for each $v \in V_+(S)$, and we now attach black/white 2-cells to X, as follows.

Consider the action of the cyclic group $\langle\Phi_B\rangle$ on $E_B(S)$, and pick its orbit $\{e, \Phi_B(e), \dots, \Phi_B^{k-1}(e)\}$ with $\Phi_B^k(e) = e$. Then for each $i \in \{0, \dots, k-1\}$, the terminal vertex of $\Phi_B^i(e)$ is mapped by φ to the initial vertex of $\Phi_B^{i+1}(e)$, and so there is an edge, γ_i, of X joining these two points. Then,

$$e + \gamma_0 + \Phi_B(e) + \gamma_1 + \cdots + \Phi_B^{k-1}(e) + \gamma_{k-1}$$

determines a simple 1-cycle, where γ_i is given a natural orientation. We attach a black 2-cell to X along the 1-cycle. Similarly, each orbit of the action of $\langle\Phi_W\rangle$ on $E_W(S)$ determines a simple 1-cycle, and we attach a white 2-cell to X along the 1-cycle.

Let M be the two-dimensional cell complex obtained from X by attaching black/white 2-cells in this way. We can easily observe that M is an orientable 2-manifold. To compute the Euler characteristic $\chi(M)$, observe the following.

1. The number of vertices of M is $4n$ with $n = |S|$, since each vertex is contained in an SBW-square.

2. The edge set of M consists of $4n$ edges of the SBW-squares and $2n$ "connecting" edges. So, the number of edges of M is equal to $6n$.

3. The face set of M consists of n squares and $|E_B(S)/\langle\Phi_B\rangle|$ black 2-cells and $|E_W(S)/\langle\Phi_W\rangle|$ white 2-cells. So, the number of faces of M is $n + |E(S)/\langle\Phi\rangle|$.

Hence,

$$\chi(M) = 4n - 6n + (n + |E(S)/\langle\Phi\rangle|) = -n + |E(S)/\langle\Phi\rangle|,$$

and so, by the assumption, it is equal to 2. Therefore, M is homeomorphic to S^2.

Add an overpass connecting two negative vertices and an underpass connecting two positive vertices to each SBW-square. The union of connecting edges and overpasses and underpasses gives a connected link diagram Γ, which is clearly alternating. Moreover, it is obvious from the construction that $\mathcal{C}^3(S, \varphi)$ is isomorphic to $\mathcal{A}(\Gamma)$. □

Corollary 1.4.2. *A compact 3-manifold M is homeomorphic to the exterior of an alternating link L represented by a connected alternating diagram, if and only if M is homeomorphic to the underlying space of an SBW cubed-complex $\mathcal{C}^3(S, \varphi)$ such that $|E(S)/\langle\Phi\rangle| = |S| + 2$.*

Remark 1.4.3. If the identity in Theorem 1.4.1 is not satisfied, then the surface M in the proof is a closed orientable surface of genus ≥ 1, and Γ is an alternating diagram in the surface M. In this case the underlying space of $\mathcal{A}(\Gamma)$ is homomorphic to the *Dehn space* of the link L in $M \times [-1, 1]$ represented by the diagram Γ, namely the space obtained from the exterior of L by coning off $M \times \{\pm 1\}$ (see [17]). We note that the "Dehn complexes" of these spaces and related spaces are studied extensively in the works [26, 25, 17] by Harlander, Rosebrock, and Byrd.

Chapter 2

Two-parabolic-generator subgroups of hyperbolic 3-manifold groups

2.1 Introduction

Adams proved in [1, Theorem 4.3] that the fundamental group of a finite volume hyperbolic 3-manifold is generated by two parabolic elements if and only if the 3-manifold is homeomorphic to the complement of a 2-bridge link which is not a torus link. Moreover, he also proved that the pair consists of meridians. This refines the result of Boileau-Zimmermann [13, Corollary 3.3] that a link in S^3 is a 2-bridge link if and only if its link group is generated by two meridians. Adams also proved that (i) each hyperbolic 2-bridge link group admits only finitely many distinct parabolic generating pairs up to equivalence [1, Corollary 4.1] and (ii) for the figure-eight knot group, the upper and lower meridian pairs are the only parabolic generating pairs up to equivalence [1, Corollary 4.6]. Here, a *parabolic generating pair* of a non-elementary Kleinian group Γ is an unordered pair of two parabolic transformations that generates Γ. Two parabolic generating pairs $\{\alpha, \beta\}$ and $\{\alpha', \beta'\}$ of Γ are *equivalent* if $\{\alpha', \beta'\}$ is equal to $\{\alpha^{\epsilon_1}, \beta^{\epsilon_2}\}$ for some $\epsilon_1, \epsilon_2 \in \{\pm 1\}$ up to simultaneous conjugation.

Agol [3] announced the following theorem which generalizes and refines these results to all non-free Kleinian groups generated by two parabolic transformations.

Theorem 2.1.1 (Agol [3])**.** *Let Γ be a non-free Kleinian group generated by two non-commuting parabolic elements. Then one of the following holds.*

(1) *Γ is conjugate to a hyperbolic 2-bridge link group. Moreover, every hyperbolic 2-bridge link group has precisely two parabolic generating pairs up to equivalence.*

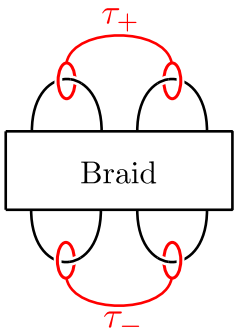

Figure 2.1: The upper and lower meridian pairs of a 2-bridge link group. The proper arcs τ_+ and τ_- in the exterior $M(L)$ of a 2-bridge link $L \subset S^3$ are the upper and lower tunnels, respectively. Each of the meridian pairs represented by τ_+ and τ_- generates the link group $G(L) = \pi_1(S^3 \setminus L)$.

(2) Γ *is conjugate to a Heckoid group. Moreover, every Heckoid group has a unique parabolic generating pair up to equivalence.*

For an explicit description of the theorem, including the definition of a Heckoid group, see Akiyoshi-Ohshika-Parker-Sakuma-Yoshida [9] and Aimi-Lee-Sakai-Sakuma [8] (cf. Lee-Sakuma [28]), which give a full proof of the classification of non-free, two-parabolic-generator Kleinian groups and an alternative proof of the classification of parabolic generating pairs, respectively. In the recent interesting articles [20] and [38] by Parker-Tan and Elzenaar-Martin-Schillewaert, respectively, we can find very beautiful pictures, produced by Yasushi Yamashita upon request of Caroline Series, that nicely illustrate Theorem 2.1.1 (see also Figure 0.2b in Akiyoshi-Sakuma-Wada-Yamashita [10]).

The two parabolic generating pairs of a hyperbolic 2-bridge link group in the second statement of Theorem 2.1.1(1) are the *upper* and *lower meridian pairs* illustrated in Figure 2.1 (cf. Section 2.2). The assertion was obtained in [3] as a consequence of the following more detailed result, together with Adams' result [1, Theorem 4.3] that every parabolic generating pair of a hyperbolic 2-bridge link group consists of meridians.

Theorem 2.1.2 (Agol [3])**.** *Let $L \subset S^3$ be a hyperbolic 2-bridge link. Then any non-commuting meridian pair in the link group $G(L)$ which is not equivalent to the upper nor lower meridian pair generates a free Kleinian group which is geometrically finite.*

The main purpose of this paper is to give a detailed account of Agol's beautiful proof of Theorem 2.1.2 included in the slide [3]. A key ingredient of the proof is non-positively curved cubed decompositions of alternating link exteriors in which the checkerboard surfaces are hyperplanes (Proposition 2.6.1). According to Rubinstein [45, p.3177], such cubed decompositions were first found by Aitchison, though he did not publish the result. They were rediscovered by D. Thurston [50] and described in detail by Yokota [54] (cf. [5, 45, 41]). The cubed

decompositions play essential roles in the proofs of (i) Proposition 2.3.1 which says that the checkerboard surfaces for hyperbolic alternating links are quasi-fuchsian and (ii) Propositions 2.7.4 and 2.8.3 concerning the disks bounded by the limit circles associated with checkerboard surfaces in the ideal boundary $\hat{\mathbb{C}}$ of the universal covering $\mathbb{H}^3$ of the hyperbolic alternating link complement. The proof of Theorem 2.1.2 is completed by applying Proposition 2.4.11 (a variant of Klein-Maskit combination theorem proved by using Maskit-Swarup [30]) to the action of meridian pairs on $\hat{\mathbb{C}}$ by using Proposition 2.8.3. (See Figures 2.16 and 2.17, which are copied from [3].)

Building on Theorems 2.1.1 and 2.1.2, we also prove the following generalization of Theorem 2.1.2.

Theorem 2.1.3. *Let $X = \mathbb{H}^3/G$ be an orientable, complete, hyperbolic 3-manifold, $\{\mu_1, \mu_2\}$ a pair of non-commuting parabolic elements of G, and $\Gamma = \langle \mu_1, \mu_2 \rangle$ the subgroup of G generated by $\{\mu_1, \mu_2\}$. Then one of the following holds.*

(1) *Γ is a rank 2 free group.*

(2) *Γ is equal to G, and it is a hyperbolic 2-bridge link group. Moreover, $\{\mu_1, \mu_2\}$ is equivalent to the upper or lower meridian pair.*

(3) *Γ is an index 2 subgroup of G, where Γ is the link group of a 2-component hyperbolic 2-bridge link, and G is the link group of a rational link in the projective 3-space P^3. Moreover, $\{\mu_1, \mu_2\}$, as a subset of Γ, is equivalent to the upper or lower meridian pair in the 2-bridge link group, and $\{\mu_1, \mu_2\}$, as a subset of G, consists of meridians of the rational link.*

Moreover, if X has finite volume, then the conclusion (1) is replaced with the following finer conclusion.

(1') *Γ is a rank 2 free Kleinian group which is geometrically finite.*

See Definition 2.10.2 for the definition of a rational link in P^3, and see Remark 2.10.6 for a detailed description of the statement (3) in the above theorem. This theorem gives a refinement of the result by Boileau-Weidmann [12, Proposition 2] concerning subgroups generated by two parabolic primitive elements of the fundamental group of an orientable, complete, hyperbolic 3-manifold of finite volume. The proof of Theorem 2.1.3 is based on (i) the result of Millichap-Worden [34] concerning the commensurable classes of 2-bridge link groups and (ii) the covering theorem of Canary [19] together with the tameness theorem established by Agol [4] and Calegari-Gabai [18] (see also Soma [47] and Bowditch [15]).

This paper is organized as follows. In Section 2.2, we reformulate the main Theorem 2.1.2 into Theorem 2.2.1, by using the correspondence between the meridian pairs up to equivalence and the proper arcs in the link exterior up to proper homotopy. We also state Theorem 2.2.2 concerning general alternating

links which is implicitly included in [3]. In Section 2.3, we recall the key fact that the checkerboard surfaces associated with prime alternating link diagrams of hyperbolic alternating links are quasi-fuchsian (Proposition 2.3.1). In Section 2.4, we describe the actions of meridians on the ideal boundary $\hat{\mathbb{C}}$ of the hyperbolic space $\mathbb{H}^3$, and give a sufficient condition for a meridian pair to generate a free Kleinian group which is geometrically finite (Proposition 2.4.11). The proposition is a basic tool for the proof of Theorems 2.2.1 and 2.2.2. In Section 2.5, we quickly recall fundamental facts concerning non-positively curved spaces, which is used in Sections 2.6 and 2.7. In Section 2.6, we describe non-positively curved cubed decompositions of alternating link exteriors (Proposition 2.6.1), and study relative positions of "checkerboard hyperplanes" and "peripheral hyperplanes", the components of the inverse images of checkerboard surfaces and peripheral tori, respectively, in the universal cover $\tilde{X}$ of a hyperbolic alternating link complement X (Proposition 2.6.6). In Section 2.7, we review the ideal polyhedral decomposition of X from the view point of the non-positively curved cubed decompositions. Then we prove Proposition 2.7.4 concerning relative positions of closed half-spaces in $\tilde{X}$ bounded by checkerboard hyperplanes. In Section 2.8, we use Proposition 2.7.4 to prove the key proposition, Proposition 2.8.3, concerning discs, in the ideal boundary $\hat{\mathbb{C}}$ of $\tilde{X} = \mathbb{H}^3$, bounded by the limit circles of checkerboard hyperplanes. In Section 2.9, we prove Theorems 2.2.1 and 2.2.2 (and so Theorem 2.1.2), by using Propositions 2.4.11 and 2.8.3. In Section 2.10, we prove Theorem 2.1.3 after introducing and studying rational links in P^3.

2.2 Reformulation of Theorem 2.1.2

Let L be a link in S^3, $X = X(L) := S^3 \setminus L$ the *link complement*, and $M = M(L) := S^3 \setminus \operatorname{int} N(L)$, the *link exterior*, where $N = N(L)$ is a regular neighborhood of L. The *link group* $G = G(L)$ of L is the fundamental group $\pi_1(M) = \pi_1(X)$. A *meridian* of L is an element μ of G which is represented by a based loop freely homotopic to a *meridional loop* in ∂N, i.e., a simple loop that bounds an essential disk in N.

A *meridian pair* is an unordered pair $\{\mu_1, \mu_2\}$ of meridians of L. Two meridian pairs $\{\mu_1, \mu_2\}$ and $\{\mu_1', \mu_2'\}$ are *equivalent* if $\{\mu_1', \mu_2'\}$ is equal to $\{g\mu_1^{\varepsilon_1}g^{-1}, g\mu_2^{\varepsilon_2}g^{-1}\}$ for some $\varepsilon_1, \varepsilon_2 \in \{\pm 1\}$ and $g \in G$.

Note that there is a bijective correspondence between the set of meridian pairs of L up to equivalence and the set of proper paths in M up to proper homotopy (cf. [1], [28, Section 2] and Lemma 2.4.9(2)). Here a *proper path* in M is a path (a continuous image of a closed interval) which intersects ∂M precisely at the endpoints. Two proper paths in M are *properly homotopic* in M if they are homotopic keeping the condition that the endpoints are contained in ∂M.

Assume that L is *hyperbolic*, i.e., the complement X admits a complete hyperbolic structure of finite volume. Then the meridian pair $\{\mu_1, \mu_2\}$ is *commuting* (i.e., $\mu_1\mu_2 = \mu_2\mu_1$) if and only if the corresponding proper path is *inessential*, i.e., properly homotopic to an arc in ∂M (cf. Lemma 2.4.2). In other words, $\{\mu_1, \mu_2\}$ is non-commuting if and only if the proper path is *es-*

sential, i.e., not inessential. If L is a 2-bridge link and if the arc is properly homotopic to the upper or lower tunnel of L, then $\{\mu_1, \mu_2\}$ generates the link group G (see Figure 2.1). Thus Theorem 2.1.2 is reformulated as follows.

Theorem 2.2.1. *Let $L \subset S^3$ be a hyperbolic 2-bridge link. Let γ be an essential proper path in the link exterior $M(L)$, and let $\{\mu_1, \mu_2\}$ be the meridian pair in the link group $G(L)$ represented by γ. Assume that γ is not properly homotopic to the upper nor lower tunnel of L. Then $\{\mu_1, \mu_2\}$ generates a rank 2 free Kleinian group which is geometrically finite.*

Agol's proof of Theorem 2.2.1 in [3] actually includes a proof of the following result concerning hyperbolic alternating links.

Theorem 2.2.2. *Let $L \subset S^3$ be a hyperbolic alternating link and D a prime alternating diagram of L. Let $\{\mu_1, \mu_2\}$ be a non-commuting meridian pair and γ an essential proper path in the link exterior $M(L)$ that represents the pair $\{\mu_1, \mu_2\}$. If γ is not properly homotopic to a crossing arc (with respect to the diagram D), then $\{\mu_1, \mu_2\}$ generates a rank 2 free Kleinian group which is geometrically finite.*

2.3 Checkerboard surfaces for alternating links

In the remainder of this paper, $L \subset S^3$ denotes a hyperbolic alternating link and $D \subset S^2$ denotes a prime alternating diagram of L, except in Sections 2.6 and 2.7, where we assume only that L is a prime alternating link. Here a link diagram is *prime* if (i) it contains at least one crossing and (ii) for every simple loop α in the projection plane, if α meets the diagram transversely in exactly two points, then α bounds a disk that contains no crossings of the diagram. It should be noted that a prime alternating diagram of a prime link is connected (as a plane graph) and reduced (i.e., contains no nugatory crossings.)

We pick two points v_+ and v_- in S^3, identify $S^3 \setminus \{v_+, v_-\}$ with $S^2 \times \mathbb{R}$ so that $\lim_{t\to\pm\infty}(x,t) = v_\pm$ for $x \in S^2$. The diagram D is regarded as a 4-valent graph in $S^2 \times \{0\}$, and we assume $L \subset D \times [-1,1]$. For each crossing c of D, we assume $L \cap (c \times [-1,1]) = c \times \{-1,1\}$. We call the point $c_+ := c \times 1$ (resp. $c_- := c \times (-1)$) the *over* (resp. *under*) *crossing point* of L at c, and call $c \times [-1,1]$ the *crossing arc of* L at c. The intersection of $c \times [-1,1]$ with the link exterior M (resp. the link complement X) is called the *crossing arc in* M (resp. the *open crossing arc in* X) at c. We assume that the crossing arc $c \times [-1,1]$ is oriented so that c_- and c_+, respectively, are the initial and terminal points.

We also assume that L coincides with D outside crossing balls, regular neighborhoods in S^3 of the crossing arcs at the crossings of D. We color the complementary regions of D in S^2 alternatively black and white. Then there is a compact, connected surface S_b (resp. S_w) bounded by L that coincides with the black (resp. white) regions outside the crossing balls and intersects each crossing ball in a twisted rectangle: it is called the *black* (resp. *white*) *surface* for L. It

should be noted that S_b and S_w intersect transversely along the crossing arcs (cf. Figure 2.4(a) in Section 2.6). Moreover, there is a natural bijective correspondence between the components of $(S_b \cup S_w) \setminus (S_b \cap S_w)$ and the regions of D. We occasionally refer to each of S_b and S_w as a *checkerboard surface* and denote it by S.

For each checkerboard surface S, we assume that S intersects the regular neighborhood N of L in a collar neighborhood of ∂S and so $S \cap M$ is properly embedded in M. We refer to $S \cap M \subset M$ (resp. $S \cap X \subset X$) a *checkerboard surface in* M (resp. an *open checkerboard surface in* X), and continue to denote it by S.

The following key proposition is implicitly included in the slide [3], and its proof following Agol's suggestion is given by Adams [2, Theorem 1.9]. The proof depends on the fact that every hyperbolic alternating link complement admits a non-positively curved cubed decomposition in which checkerboard surfaces are hyperplanes (see Section 2.6). Except for the existence of such a decomposition, essentially the same arguments had been given by Aitchison-Rubinstein [6, Lemma and its proof in p.146] in a more general setting. See Futer-Kalfagianni-Purcell [22, Theorem 1.6] for a generalization.

Proposition 2.3.1. *Let $L \subset S^3$ be a hyperbolic alternating link, and S a checkerboard surface obtained from a prime alternating diagram D of L. Then S is quasi-fuchsian.*

To explain the meaning of the proposition, let $p_u : \tilde{X} \to X$ be the universal covering, and identify the link group $G = \pi_1(X)$ with the covering transformation group $\mathrm{Aut}(\tilde{X})$. Since L is hyperbolic, $\tilde{X}$ is identified with the hyperbolic space $\mathbb{H}^3$ and $G = \mathrm{Aut}(\tilde{X})$ is regarded as a Kleinian group. Then S being *quasi-fuchsian* means that $\pi_1(S)$ injects into $\pi_1(X) = G$ and the Kleinian group $\pi_1(S) < G < \mathrm{PSL}(2, \mathbb{C})$ satisfies the following condition: if S is orientable then $\pi_1(S)$ is a quasi-fuchsian group (cf. [31, p.120, Definition]), and if S is non-orientable then the index 2 subgroup of $\pi_1(S)$ corresponding to the orientation double cover is a quasi-fuchsian group. Since the action of a quasi-fuchsian group on the 3-ball $\bar{\mathbb{H}}^3 = \mathbb{H}^3 \cup \hat{\mathbb{C}}$ is topologically conjugate to the action of a fuchsian group (see [31, Theorem 5.31]), we obtain the following corollary.

Corollary 2.3.2. *Let $L \subset S^3$ be a hyperbolic alternating link, and S a checkerboard surface obtained from a prime alternating diagram D of L. Let Σ be a component of the inverse image $p_u^{-1}(S) \subset \tilde{X} = \mathbb{H}^3$. Then Σ is an open disk properly embedded in $\mathbb{H}^3$, and it divides $\mathbb{H}^3$ into two half-spaces, B^- and B^+, which satisfy the following conditions.*

(1) *$\mathbb{H}^3 = B^- \cup B^+$ and $\Sigma = B^- \cap B^+$.*

(2) *The closure $\bar{\Sigma}$ of Σ in $\bar{\mathbb{H}}^3 = \mathbb{H}^3 \cup \hat{\mathbb{C}}$ is a disk properly embedded in $\bar{\mathbb{H}}^3$, and $(\bar{\mathbb{H}}^3, \bar{\Sigma})$ is homeomorphic to the standard ball pair (B^3, B^2), where B^3 is the unit 3-ball in $\mathbb{R}^3$ and B^2 is the intersection of B^3 with the x-y plane.*

(3) *The closures $\bar{B}^\pm$ of $B^\pm$ in $\bar{\mathbb{H}}^3$ are 3-balls, such that*

$$\bar{\mathbb{H}}^3 = \bar{B}^- \cup \bar{B}^+, \quad \bar{\Sigma} = \bar{B}^- \cap \bar{B}^+.$$

(4) *$\partial\bar{\Sigma}$ is a circle in $\hat{\mathbb{C}}$ which divides $\hat{\mathbb{C}}$ into two disks $\Delta^- := \bar{B}^- \cap \hat{\mathbb{C}}$ and $\Delta^+ := \bar{B}^+ \cap \hat{\mathbb{C}}$, such that $\hat{\mathbb{C}} = \Delta^- \cup \Delta^+$ and $\partial\bar{\Sigma} = \Delta^- \cap \Delta^+$.*

We call $\Sigma \subset \mathbb{H}^3$ and $\bar{\Sigma} \subset \bar{\mathbb{H}}^3$, respectively, a *checkerboard plane* and a *checkerboard disk*. The *color* of Σ (or $\bar{\Sigma}$) is defined to be black or white according to the color of the corresponding checkerboard surface S. We call each of $B^{\pm}$ a *checkerboard half-space* bounded by Σ.

2.4 The action of meridian pairs on the ideal boundary of the hyperbolic space

In the reminder of the paper, we assume for convenience that the hyperbolic alternating link L is *oriented*, and we use the terminology "meridian" and "meridian pair" in the following restricted sense: A *meridian* of L is an element of the link group G which is represented by an oriented closed path freely homotopic to a meridional loop in ∂N that has linking number $+1$ with L. A *meridian pair* is an unordered pair $\{\mu_1, \mu_2\}$ of meridians of L in the restricted sense. Then two meridian pairs are equivalent in the sense defined in Section 2.2 if and only if they are simultaneously conjugate. Of course, this does not affect the contents of Theorems 2.2.1 and 2.2.2.

Recall that $\tilde{X}$ is identified with the hyperbolic space $\mathbb{H}^3$ and $G = \mathrm{Aut}(\tilde{X})$ is identified with a Kleinian group. Thus a meridian $\mu \in G < \mathrm{PSL}(2, \mathbb{C})$ is parabolic, and its action on $\bar{\mathbb{H}}^3 = \mathbb{H}^3 \cup \hat{\mathbb{C}}$ has a unique fixed point, which lies in $\hat{\mathbb{C}}$. The point is called the *parabolic fixed point* of μ and denoted by $\mathrm{Fix}(\mu)$.

Let $\mathrm{PFix}(G) \subset \hat{\mathbb{C}}$ be the set of the parabolic fixed points of G, i.e., the set of the fixed points of the parabolic elements of G. For each $p \in \mathrm{PFix}(G)$, the stabilizer $\mathrm{Stab}_G(p)$ of p in G is a rank 2 free abelian group which belongs to the conjugacy class of the fundamental group of a component of ∂M. Since every component of ∂M contains a unique meridian loop (which has linking number $+1$ with L) up to isotopy, $\mathrm{Stab}_G(p)$ contains a unique meridian μ_p of the oriented link L. We call μ_p the *meridian of L at the parabolic fixed point p*.

Lemma 2.4.1. *The maps $\mu \mapsto \mathrm{Fix}(\mu)$ and $p \mapsto \mu_p$, respectively, determine the following bijective correspondence and its inverse:*

$$\{\textit{meridians of } L\} \to \mathrm{PFix}(G).$$

The following lemma is easily proved.

Lemma 2.4.2. *Let $\{\mu_1, \mu_2\}$ be a meridian pair represented by a proper path γ in the link exterior M. Then the following conditions are equivalent.*

(1) *$\{\mu_1, \mu_2\}$ is commuting.*

(2) $\mathrm{Fix}(\mu_1) = \mathrm{Fix}(\mu_2)$.

(3) *γ is inessential.*

We now describe the action of the meridian μ_p on $\bar{\mathbb{H}}^3$. To this end, we assume that $X \setminus M$ consists of open cusp neighborhoods, and therefore $\tilde{M} := p_u^{-1}(M)$ is a submanifold of $\tilde{X} = \mathbb{H}^3$ bounded by disjoint horospheres $\{H_p\}_{p \in \mathrm{PFix}(G)}$. Note that the Euclidean torus $H_p/\mathrm{Stab}_G(p)$ is a component of ∂M and every component of ∂M is of this form.

Now, let $S \subset X$ be an open checkerboard surface for L. We may assume that S intersects transversely each component of ∂M in a closed Euclidean geodesic. For each $p \in \mathrm{PFix}(G)$, $p_u^{-1}(S) \cap H_p$ is a disjoint union of Euclidean lines $\{\ell_j\}_{j \in \mathbb{Z}} = \{\ell_j(p)\}_{j \in \mathbb{Z}}$ such that $\mu_p(\ell_j) = \ell_{j+1}$. Let $\Sigma_j = \Sigma_j(p)$ be the checkerboard plane that is the component of $p_u^{-1}(S)$ such that $\ell_j \subset \Sigma_j \cap H_p$.

Lemma 2.4.3. *Under the above setting, $\Sigma_j \cap H_p = \ell_j$ for each $p \in \mathrm{PFix}(G)$ and $j \in \mathbb{Z}$. In other words, the checkerboard planes Σ_j $(j \in \mathbb{Z})$ are all different.*

Proof. Suppose to the contrary that $\Sigma_j = \Sigma_{j'}$ for some distinct integers j and j'. Let $\check{\Sigma}$ be the intersection of $\Sigma_j = \Sigma_{j'}$ and $\tilde{M}$. Then $\check{\Sigma}$ is properly embedded in $\tilde{M}$, and the image $\check{S} := p_u(\check{\Sigma}) = S \cap M$ is a checkerboard surface in M. Let $\tilde{\alpha}$ be a path in $\check{\Sigma}$ joining the boundary components ℓ_j and $\ell_{j'}$ of $\check{\Sigma}$. Since $\tilde{M}$ is simply connected, $\tilde{\alpha}$ is homotopic rel endpoints to a path in $H_p \subset \partial\tilde{M}$. Thus the path $\alpha := p_u \circ \tilde{\alpha}$ in $\check{S}$ is homotopic rel endpoints to a path in ∂M inside M. On the other hand, since $\ell_j \neq \ell_{j'}$, α is not homotopic rel endpoints to $\partial\check{S}$ in $\check{S}$. This contradicts [39, Theorem 11.31] which says that $\check{S}$ is π_1-essential, in particular, boundary π_1-injective (see [39, Definition 11.30]). □

Remark 2.4.4. See Proposition 2.6.6(2) for a direct geometric proof of the above lemma. The π_1-essentiality of checkerboard surfaces associated with prime alternating diagrams had been proved by Aumann [11] (cf. Menasco-Thistlethwaite [33, Proposition 2.3]). See Ozawa [36, Theorem 3] and [37, Theorem 2.8] for generalizations.

Lemma 2.4.5. (1) *There are checkerboard half-spaces $B_j^{\pm} = B_j^{\pm}(p)$ $(j \in \mathbb{Z})$ bounded by Σ_j which satisfy the following conditions:*

(a) $\bar{\mathbb{H}}^3 = \bar{B}_j^- \cup \bar{B}_j^+$ *and* $\bar{\Sigma}_j = \bar{B}_j^- \cap \bar{B}_j^+$.

(b) $\bar{B}_j^- \subset \bar{B}_{j+1}^-$ *and* $\bar{B}_j^+ \supset \bar{B}_{j+1}^+$.

(c) $\mu_p(\bar{B}_j^{\pm}) = \bar{B}_{j+1}^{\pm}$.

(2) *Set $\Delta_j^{\pm} = \Delta_j^{\pm}(p) := \bar{B}_j^{\pm}(p) \cap \hat{\mathbb{C}}$. Then $\Delta_j^{\pm}$ are disks in $\hat{\mathbb{C}}$ which satisfy the following conditions.*

(a) $\hat{\mathbb{C}} = \Delta_j^- \cup \Delta_j^+$ *and* $\partial\bar{\Sigma}_j = \Delta_j^- \cap \Delta_j^+$.

(b) $\Delta_j^- \subset \Delta_{j+1}^-$ *and* $\Delta_j^+ \supset \Delta_{j+1}^+$.

(c) $\mu_p(\Delta_j^{\pm}) = \Delta_{j+1}^{\pm}$.

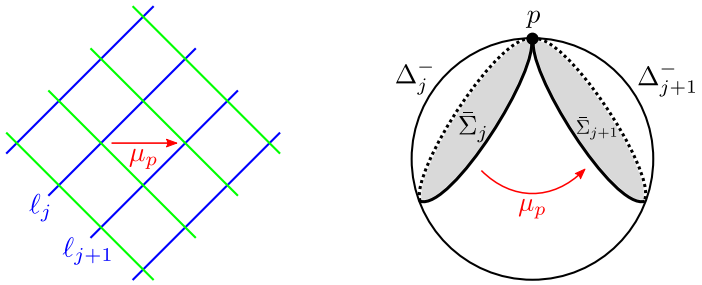

(a) (b)

Figure 2.2: (a) The action of μ_p on $(H_p, H_p \cap p_u^{-1}(S_b), H_p \cap p_u^{-1}(S_w))$. (b) A rough model of the action of μ_p on $(\bar{\mathbb{H}}^3, \{\bar{\Sigma}_j\}_j)$. This figure is not precise. In fact, $\Delta_j^- \cap \Delta_{j+1}^+ = \partial\Delta_j^- \cap \partial\Delta_{j+1}^+$ is generically strictly bigger than $\{p\}$ (cf. Remark 2.4.8).

In the above lemma, the symbol $\pm$ is used in the following way: for example, $\mu_p(\bar{B}_j^\pm) = \bar{B}_{j+1}^\pm$ means that $\mu_p(\bar{B}_j^\epsilon) = \bar{B}_{j+1}^\epsilon$ for each $\epsilon \in \{-,+\}$. We apply this convention throughout the paper.

Proof. By Lemma 2.4.3, $H_p \cap \Sigma_j$ is equal to the line ℓ_j. Observe that the line ℓ_j divides H_p into two closed half-spaces $H_{p,j}^-$ and $H_{p,j}^+$, where $\ell_{j\pm1} \subset H_{p,j}^\pm$ (see Figure 2.2(a)). By Corollary 2.3.2, $(\bar{\mathbb{H}}^3, \bar{\Sigma}_j)$ is a standard ball pair and there are checkerboard half-spaces B_j^ϵ ($\epsilon \in \{-,+\}$) bounded by Σ_j which satisfy the condition (1-a), such that $H_{p,j}^\epsilon \subset \bar{B}_j^\epsilon$. Since $H_{p,j}^- \subset H_{p,j+1}^-$ and $H_{p,j}^+ \supset H_{p,j+1}^+$, the condition (1-b) are satisfied. Since $\mu_p(H_{p,j}^\pm) = H_{p,j+1}^\pm$, the condition (1-c) is also satisfied, completing the proof of (1).

The assertion (2) follows from (1) and the fact that $(\bar{\mathbb{H}}^3, \bar{\Sigma}_j)$ is a standard ball pair. □

Definition 2.4.6. Under the above setting, a *butterfly* $\mathrm{BF}(p)$ *at* $p \in \mathrm{PFix}(G)$ is a pair of disks $\{\Delta_j^-, \Delta_{j+1}^+\} = \{\Delta_j^-(p), \Delta_{j+1}^+(p)\}$ in $\hat{\mathbb{C}}$ for some $j \in \mathbb{Z}$. The *color* of the butterfly is defined to be black or white according to the color of the checkerboard surface S. The underlying space $|\mathrm{BF}(p)|$ of $\mathrm{BF}(p)$ is defined by $|\mathrm{BF}(p)| := \Delta_j^- \cup \Delta_{j+1}^+ \subset \hat{\mathbb{C}}$ (see Figure 2.2(b)).

It should be noted that a butterfly $\mathrm{BF}(p)$ is determined by the parabolic fixed point p, the color (equivalently, the choice of a checkerboard surface S), and the choice of a component Σ_j of $p_u^{-1}(S)$ such that $p \in \bar{\Sigma}_j$.

Lemma 2.4.7. *For a butterfly* $\mathrm{BF}(p) = \{\Delta_j^-, \Delta_{j+1}^+\}$ *at* $p \in \mathrm{PFix}(G)$*, the following hold.*

(1) Δ_j^- *and* Δ_{j+1}^+ *are disks in* $\hat{\mathbb{C}}$ *which have disjoint interiors.*

(2) $\mu_p(\hat{\mathbb{C}} \setminus \operatorname{int}\Delta_j^-) = \Delta_{j+1}^+$.

Proof. (1) By Lemma 2.4.5(2-a, b), $\operatorname{int}\Delta_j^- \subset \operatorname{int}\Delta_{j+1}^- = \hat{\mathbb{C}} \setminus \Delta_{j+1}^+$. Hence

$$\operatorname{int}\Delta_j^- \cap \operatorname{int}\Delta_{j+1}^+ \subset (\operatorname{int}\Delta_j^-) \cap \Delta_{j+1}^+ = \emptyset.$$

(2) By Lemma 2.4.5(2-c), $\mu_p(\hat{\mathbb{C}} \setminus \operatorname{int}\Delta_j^-) = \mu_p(\Delta_j^+) = \Delta_{j+1}^+$. □

Remark 2.4.8. The parabolic fixed point p is contained in the intersection $\Delta_j^- \cap \Delta_{j+1}^+ = \partial\Delta_j^- \cap \partial\Delta_{j+1}^+$. However, in general, the intersection is strictly bigger than the singleton $\{p\}$; it is generically a Cantor set (cf. [31, Theorem 3.13]). We hope to give a more detailed description of the intersection in a subsequent paper.

Now, let $\{\mu_1, \mu_2\}$ be a non-commuting meridian pair, and set $p_i := \operatorname{Fix}(\mu_i) \in \operatorname{PFix}(G)$ $(i = 1, 2)$. Note that $p_1 \neq p_2$ and $\mu_i = \mu_{p_i}$ $(i = 1, 2)$ by Lemmas 2.4.1 and 2.4.2. Then the following lemma follows immediately from Lemma 2.4.1.

Lemma 2.4.9. (1) *The correspondence* $\{\mu_1, \mu_2\} \mapsto \{p_1, p_2\}$ *gives a bijective correspondence from the set of the non-commuting meridian pairs of* L *up to equivalence to the set of the unordered pairs of distinct points in* $\operatorname{PFix}(G)$ *up to the action of* G.

(2) *Let* $\{\mu_1, \mu_2\}$ *and* $\{p_1, p_2\}$ *be as in the above, and let* γ *be a proper path in* M *that represents the pair* $\{\mu_1, \mu_2\}$. *Then* γ *lifts to a proper path* $\tilde{\gamma}$ *in the universal cover* $\tilde{M} \subset \tilde{X} = \mathbb{H}^3$ *that joins the horospheres* H_{p_1} *and* H_{p_2}. *Conversely, if* γ *is a proper path in* M *which is the image of a proper path* $\tilde{\gamma}$ *in* $\tilde{M}$ *joining* H_{p_1} *and* H_{p_2}, *then* γ *represents the pair* $\{\mu_1, \mu_2\}$.

Notation 2.4.10. Under the above setting, when we consider two butterflies $\operatorname{BF}(p_1)$ and $\operatorname{BF}(p_2)$ simultaneously, we denote the butterfly $\operatorname{BF}(p_i)$ by $\{\Delta_i^-, \Delta_i^+\}$ for $i = 1, 2$, where Δ_i^- and Δ_i^+ correspond to $\Delta_j^-(p_i)$ and $\Delta_{j+1}^+(p_i)$, respectively, in Definition 2.4.6. Thus $\mu_i(\hat{\mathbb{C}} \setminus \operatorname{int}\Delta_i^-) = \Delta_i^+$ $(i = 1, 2)$. In this sense, we regard $\operatorname{BF}(p_i)$ as the ordered pair (Δ_i^-, Δ_i^+) of closed disks in $\hat{\mathbb{C}}$, though we continue to denote it by $\{\Delta_i^-, \Delta_i^+\}$.

The proof of Theorem 2.2.1 is based on the following proposition.

Proposition 2.4.11. *Let* $L \subset S^3$ *be a hyperbolic alternating link,* $\{\mu_1, \mu_2\}$ *a non-commuting meridian pair in the link group* $G(L)$, *and* $\{p_1, p_2\}$ *the corresponding pair of parabolic fixed points. Then the subgroup* $\Gamma = \langle \mu_1, \mu_2 \rangle$ *generated by* $\{\mu_1, \mu_2\}$ *is a rank 2 free Kleinian group which is geometrically finite, provided that there are butterflies* $\operatorname{BF}(p_i) = \{\Delta_i^-, \Delta_i^+\}$ *at* p_i $(i = 1, 2)$ *satisfying the following conditions.*

(i) *The underlying spaces* $|\operatorname{BF}(p_1)|$ *and* $|\operatorname{BF}(p_2)|$ *have disjoint interiors in* $\hat{\mathbb{C}}$, *equivalently, the four disks* Δ_1^-, Δ_1^+, Δ_2^- *and* Δ_2^+ *have disjoint interiors.*

(ii) *The complementary open set* $O := \hat{\mathbb{C}} \setminus (|\operatorname{BF}(p_1)| \cup |\operatorname{BF}(p_2)|)$ *is non-empty.*

Proof. By a standard ping-pong argument (see [35, Chapter 4] for a nice exposition with beautiful illustrations), we have $w(O) \cap O = \emptyset$ for any non-trivial reduced word w in $\{\mu_1, \mu_2\}$. Hence, the subgroup $\Gamma = \langle \mu_1, \mu_2 \rangle$ of $G(L)$ is a rank 2 free group and it has a non-empty domain of discontinuity. Since a two-parabolic-generator Kleinian group which has a non-empty domain of discontinuity is geometrically finite by Maskit-Swarup [30, Theorem 1], Γ is geometrically finite. □

Remark 2.4.12. Though [3] appeals to the Klein-Maskit combination theorem, we could not verify that the conditions in [29, Theorem C.2] is satisfied in the setting of Proposition 2.4.11. This is the reason why we use the result of Maskit and Swarup [30]. We thank Yohei Komori and Hideki Miyachi for suggesting this idea to us.

2.5 Basic facts concerning non-positively curved spaces

In this section, we recall fundamental facts concerning non-positively curved spaces, basically following Bridson-Haefliger [16].

Let $X = (X, d)$ be a metric space. In this paper, we mean by a *geodesic* in X an isometric embedding $g : J \to X$ where J is a connected subset of $\mathbb{R}$. If J is the whole $\mathbb{R}$ (resp. a closed interval), g is called a *geodesic line* (resp. a *geodesic segment*). We do not distinguish between a geodesic and its image. X is said to be a *geodesic space* if every pair of points can be joined by a geodesic in X. For points a and b in a geodesic space X, we denote by $[a, b]$ a geodesic segment joining a and b. The symbols (a, b), $[a, b)$ and $(a, b]$ represent open or half-open geodesic segments, respectively. Then the distance $d(a, b)$ is equal to the length, length$([a, b])$, of the geodesic segment $[a, b]$. (See [16, Definition I.1.18] for the definition of the length of a curve.)

A geodesic space X is called a *CAT(0) space* if any geodesic triangle is thinner than a comparison triangle in the Euclidean plane $\mathbb{E}^2$, that is, the distance between any points on a geodesic triangle is less than or equal to the corresponding points on a comparison triangle. A CAT(0) space is *uniquely geodesic*, i.e., for every pair of points, there is a unique geodesic joining them ([16, Proposition II.1.4(1)]). A geodesic space X is said to be *non-positively curved* if it is locally a CAT(0) space (cf. [16, Definitions II.1.1 and II.1.2]). The following (special case of) the Cartan-Hadamard theorem is fundamental.

Proposition 2.5.1. [16, Special case of Theorem II.4.1(2)] *Let X be a complete, connected, metric space. If X is non-positively curved, then the universal covering $\tilde{X}$ (with the induced length metric) is a CAT(0) space.*

A subset W of a uniquely geodesic space X is said to be *convex* if, for any distinct points a and b in W, the geodesic segment $[a, b]$ is contained in W. For a closed convex set W of a complete CAT(0) space X, let $\pi_W : X \to W$ be the *projection*, namely $\pi_W(x)$ for every $x \in X$ is the unique point in W such that

$d(x, \pi_W(x)) = d(x, W) := \inf\{d(x, y) \mid y \in W\}$ (see [16, Proposition II.2.4]). For points $x \in X \setminus W$ and $w \in W$ define

$$\angle_w(x, W) := \inf \{\angle_w(x, y) \mid y \in W \setminus \{w\}\},$$

where $\angle_w(x, y)$ is the Alexandrov angle $\angle_w([w, x], [w, y])$ between the geodesic segments $[w, x]$ and $[w, y]$ at w (see [16, Definition I.1.12 and Notation II.3.2]).

Remark 2.5.2. The angle $\angle_w(x, W)$ is determined by the local shape of (X, W) around w in the following sense. For any neighborhood U of w, and for any $x' \in (w, x] \cap U$, we have

$$\angle_w(x, W) = \angle_w(x', W \cap U) := \inf \{\angle_w(x', y') \mid y' \in (W \cap U) \setminus \{w\}\},$$

because for any $x' \in (w, x]$, $y \in W \setminus \{w\}$ and $y' \in (w, y]$, we have $\angle_w(x, y) = \angle_w(x', y')$.

Lemma 2.5.3. *Let X be a complete CAT(0) space and W a closed convex subset of X. Then for any $x \in X$ and $w \in W$, we have $w = \pi_W(x)$ if and only if $\angle_w(x, W) \geq \frac{\pi}{2}$.*

Proof. The only if part is nothing other than [16, Proposition II.2.4(3)]. To see the if part, suppose that the inequality $\angle_w(x, W) \geq \frac{\pi}{2}$ holds, and assume to the contrary that w is different from the point $w_0 := \pi_W(x)$. Let $\Delta(\bar{x}, \bar{w}, \bar{w}_0) \subset \mathbb{E}^2$ be the comparison triangle of the geodesic triangle $\Delta(x, w, w_0) \subset X$. Then $\angle_{\bar{w}}(\bar{x}, \bar{w}_0) \geq \angle_w(x, w_0) \geq \angle_w(x, W) \geq \frac{\pi}{2}$ by [16, Propositions II.1.7(4)] and the assumption. We also have $\angle_{\bar{w}_0}(\bar{x}, \bar{w}) \geq \angle_{w_0}(x, w) \geq \frac{\pi}{2}$ by [16, Propositions II.1.7(4) and II.2.4(3)]. Thus the Euclidean triangle $\Delta(\bar{x}, \bar{w}, \bar{w}_0)$ has two angles $\geq \frac{\pi}{2}$, a contradiction. □

Let W_1 and W_2 be closed convex subsets of a complete CAT(0) space X. The distance $d(W_1, W_2)$ between W_1 and W_2 is defined by

$$d(W_1, W_2) := \inf\{d(x_1, x_2) \mid x_1 \in W_1, x_2 \in W_2\}.$$

For a pair of distinct points $(x_1, x_2) \in W_1 \times W_2$, the geodesic segment $[x_1, x_2]$ is a *shortest path* between W_1 and W_2 if $d(W_1, W_2) = \text{length}([x_1, x_2])$. The geodesic segment $[x_1, x_2]$ is a *common perpendicular* to W_1 and W_2 if $\angle_{x_1}(x_2, W_1) \geq \frac{\pi}{2}$ and $\angle_{x_2}(x_1, W_2) \geq \frac{\pi}{2}$.

Lemma 2.5.4. *Let X be a complete CAT(0) space, and let W_1 and W_2 be closed convex subsets of X. Then, for a pair of distinct points $(x_1, x_2) \in W_1 \times W_2$, the geodesic segment $[x_1, x_2]$ is a shortest path between W_1 and W_2 if and only if it is a common perpendicular to W_1 and W_2. In particular, if a common perpendicular to W_1 and W_2 exists, then $d(W_1, W_2) > 0$ and so $W_1 \cap W_2 = \emptyset$.*

Proof. Assume that $[x_1, x_2]$ is a common perpendicular to W_1 and W_2. Consider the projection $\pi_s := \pi_{[x_1, x_2]}$ from X to the closed convex set $[x_1, x_2]$. Then for any pair of points $(y_1, y_2) \in W_1 \times W_2$, we see $x_1 = \pi_s(y_1)$ by the if part

of Lemma 2.5.3, because $\angle_{x_1}(y_1, [x_1, x_2]) = \angle_{x_1}(x_2, y_1) \geq \angle_{x_1}(x_2, W_1) \geq \frac{\pi}{2}$. Similarly $x_2 = \pi_s(y_2)$. Since the projection does not increase distances by [16, Proposition II.2.4(4)], we have

$$d(x_1, x_2) = d(\pi_s(y_1), \pi_s(y_2)) \leq d(y_1, y_2).$$

Hence $\mathrm{length}([x_1, x_2]) = d(x_1, x_2) = d(W_1, W_2)$. This completes the proof of the if part. The only if part immediately follows from (the if part of) Lemma 2.5.3. □

A *cubed complex* is a metric space $X = (X, d)$ obtained from a disjoint union of unit cubes $\hat{X} = \bigsqcup_{\lambda \in \Lambda}(I^{n_\lambda} \times \{\lambda\})$ by gluing their faces through isometries. To be precise, it is an M_κ-polyhedral complex with $\kappa = 0$ in the sense of [16, Definition I.7.37] that is made up of Euclidean unit cubes, i.e., the set $\mathrm{Shapes}(X)$ in the definition consists of Euclidean unit cubes. (See [16, Example (I.7.40)(4)].) The metric d on X is the length metric induced from the Euclidean metrics of the unit cubes (see [16, I.7.38] for a precise definition). We recall the following basic fact (cf. [16, Theorem in p.97 or I.7.33]).

Proposition 2.5.5. *Every finite dimensional cubed complex is a complete geodesic space.*

When we need to consider the combinatorial structure of the cubed complex X in addition to its metric, we denote it by using the corresponding calligraphic letter $\mathcal{X}$ and regard the metric space X as the underlying space $|\mathcal{X}|$ of $\mathcal{X}$. Otherwise, we do not distinguish symbolically among X, $\mathcal{X}$ and $|\mathcal{X}|$, and use a symbol which we think fit to the setting. We also call $\mathcal{X}$ a *cubed decomposition* of the metric space X.

For a point $x \in X = |\mathcal{X}|$, two non-trivial geodesics issuing from x are said to define the *same direction* if the Alexandrov angle between them is zero. This determines an equivalence relation on the set of non-trivial geodesics issuing from x, and the Alexandrov angle induces a metric on the set of the equivalence classes. The resulting metric space is called the *space of directions* at x and denoted by $S_x(X)$ (see [16, Definition II.3.18]).

Suppose x is a vertex v of the cubed complex $\mathcal{X}$. Then the space $S_v(\mathcal{X})$ is obtained by gluing the spaces $\{S_{v_\lambda}(I^{n_\lambda} \times \{\lambda\})\}$, where λ runs over the elements of the index set Λ such that $(v_\lambda, \lambda) \in I^{n_\lambda} \times \{\lambda\} \subset \hat{X}$ is mapped to v by the projection $\hat{X} \to X$. Here $S_{v_\lambda}(I^{n_\lambda} \times \{\lambda\})$ is the space of directions in the cube $I^{n_\lambda} \times \{\lambda\}$ at the vertex v_λ; so it is an *all-right spherical simplex*, a geodesic simplex in the unit sphere $S^{n_\lambda - 1}$ all of whose edges have length $\pi/2$. Hence $S_v(\mathcal{X})$ has a structure of a finite dimensional *all-right spherical complex*, namely an M_κ-polyhedral complex with $\kappa = 1$ in the sense of [16, Definition I.7.37] which is made up of all-right spherical simplices. This complex is called the *geometric link* of v in $\mathcal{X}$, and is denoted by $\mathrm{Lk}(v, \mathcal{X})$ (see [16, (I.7.38)]). It is endowed with the length metric $d_{\mathrm{Lk}(v,\mathcal{X})}$ induced from the spherical metrics of the all-right spherical simplices. Then the following holds (cf. [16, the second sentence in p.191]).

Lemma 2.5.6. *The metric $d_{S_v(\mathcal{X})}$ on $S_v(\mathcal{X}) = \mathrm{Lk}(v, \mathcal{X})$ determined by the Alexandrov angle is equal to the metric $d^{\pi}_{\mathrm{Lk}(v,\mathcal{X})}$ defined by*

$$d^{\pi}_{\mathrm{Lk}(v,\mathcal{X})}(g_1, g_2) := \min\{d_{\mathrm{Lk}(v,\mathcal{X})}(g_1, g_2), \pi\}.$$

Proof. By [16, Theorem I.7.39], there is a natural isometry f from the open ball $B_X(v, \epsilon) = \{x \in X \mid d(v, x) < \epsilon\}$, for some $\epsilon > 0$, onto the open ball of the same radius ϵ about the cone point of the Euclidean cone $C_0(\mathrm{Lk}(v, \mathcal{X}))$ over the metric space $\mathrm{Lk}(v, \mathcal{X})$. (See [16, Definition I.5.6] for the definition of the Euclidean cone (κ-cone with $\kappa = 0$) and its cone point.) The metric $d^{\pi}_{\mathrm{Lk}(v,\mathcal{X})}$ is recovered from the metric of the open ball about the cone point of the Euclidean cone $C_0(\mathrm{Lk}(v, \mathcal{X}))$ (see [16, Remark I.5.7]), whereas the metric $d_{S_v(\mathcal{X})}$ is determined by the metric on $B_X(v, \epsilon)$. Hence, by the naturality of the isometry f, we obtain the desired result. □

We recall the following well-known criterion for a cubed complex to be non-positively curved [16, Theorem II.5.20], where a *flag complex* is a *simplicial* complex in which every finite set of vertices that is pairwise joined by an edge spans a simplex.

Proposition 2.5.7 (Gromov's flag criterion)**.** *A finite dimensional cubed complex $\mathcal{X}$ is non-positively curved if and only if the geometric link of each vertex is a flag complex.*

2.6 Non-positively curved cubed decompositions of alternating link exteriors

The proof of Proposition 2.7.4, as well as that of Proposition 2.3.1 given by [2, 3, 6], is based on non-positively curved cubed decompositions of prime alternating link exteriors in which the checkerboard surfaces are *hyperplanes*, i.e., consist of midsquares of the cubes. Here a *midsquare* of a cube I^3 is a square properly embedded in I^3 which is parallel to a face of ∂I^3 and passes through the center $(\frac{1}{2}, \frac{1}{2}, \frac{1}{2})$. (See [24, Definition 2.2] for a precise definition of a hyperplane.) In this section, we quickly describe the cubed decompositions following the construction by D. Thurston [50] and the detailed description by Yokota [54] (cf. [5, 45, 41]).

For each crossing of a prime alternating diagram D of a prime alternating link L, consider an octahedron that contains the corresponding crossing arc as a vertical central axis (see Figure 2.3). Truncating each octahedron at its top and bottom vertices and splitting along the horizontal square containing the remaining four vertices, we obtain a pair of cubes in the link exterior M, each of which intersects ∂M along the top or bottom face and intersects the checkerboard surfaces in the vertical midsquares (see Figure 2.4). We can expand the cubes in M so as to obtain the desired cubed decomposition of M (see Figure 2.3 and its caption). Thus we obtain the following proposition.

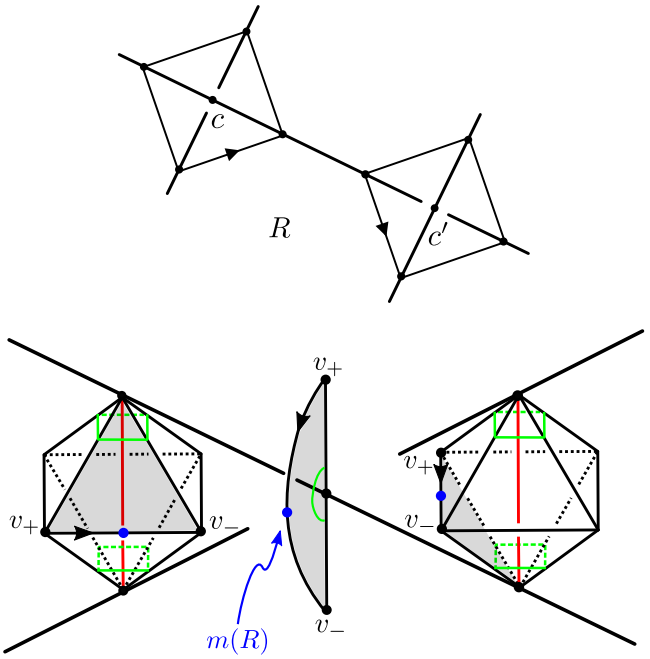

Figure 2.3: Local picture of the cubed complex $\mathcal{M}$. The partially truncated octahedra in M are expanded so that they cover the whole M. The shaded faces of the octahedra at the crossings c and c' are identified with the central bow-shaped face. In particular, the pair of the horizontal arrowed edges of the octahedra are identified with the arrowed edge of the bow-shaped face joining monotonically the top vertex v_+ and the bottom vertex v_-, passing through the center $m(R)$ of the region R.

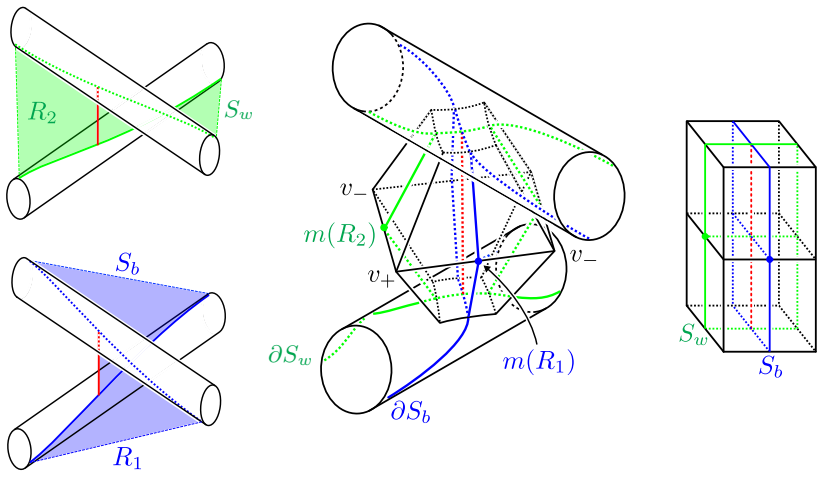

Figure 2.4: At each crossing, (a) S_b and S_w intersect transversely along the crossing arc, (b) each of S_b and S_w intersects the partially truncated octahedron in a vertical middle plate containing the crossing arc, and (c) each of the middle plate determines a pair of midsquares in the pair of cubes, and the two pairs of midsquares intersect orthogonally along the vertical axes of the cubes.

Proposition 2.6.1. *Let L be a prime alternating link and D a prime alternating diagram of L. Then there is a complete, non-positively curved, cubed complex $\mathcal{M}$ whose underlying space is the exterior M of L, which satisfies the following conditions.*

(1) *Each cube I^3 intersects ∂M in the top face $I^2 \times \{1\}$ or the bottom face $I^2 \times \{0\}$.*

(2) *There are hyperplanes $\mathcal{S}_b$ and $\mathcal{S}_w$ in $\mathcal{M}$ that represent the isotopy classes of the black and white surfaces, respectively, and satisfy the following conditions.*

   (a) *Each of $\mathcal{S}_b$ and $\mathcal{S}_w$ intersects each cube in one of the two vertical midsquares $\{\frac{1}{2}\} \times I^2$ and $I \times \{\frac{1}{2}\} \times I$.*

   (b) *$\mathcal{S}_b$ and $\mathcal{S}_w$ intersects "orthogonally" along $\mathcal{C} := \mathcal{S}_b \cap \mathcal{S}_w$, the disjoint union of geodesic segments representing crossing arcs.*

(3) *$\mathcal{M}$ has precisely two inner vertices v_+ and v_-.*

(4) *There is a bijective correspondence between the inner edges (edges contained in $\operatorname{int} \mathcal{M}$) of $\mathcal{M}$ and the regions of D: the inner edge $e(R)$ corresponding to a region R is a monotone path joining v_+ with v_- that intersects $\mathcal{S}_b \cup \mathcal{S}_w$ "orthogonally" at a single point $m(R)$ which is contained*

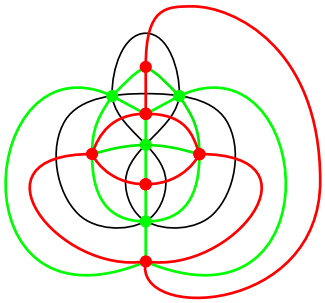

Figure 2.5: The geometric link $\mathrm{Lk}(v_\epsilon, \mathcal{M})$: The union of the thick red graph and the thick green graph forms the 1-skeleton of $\mathrm{Lk}(v_\epsilon, \mathcal{M})$.

in the component of $(\mathcal{S}_b \cup \mathcal{S}_w) \setminus \mathcal{C}$ *corresponding to* R. *We call* $m(R)$ *the center of* R.

(5) *For each* $\epsilon \in \{+, -\}$, *the geometric link* $\mathrm{Lk}(v_\epsilon, \mathcal{M})$ *is the all-right spherical complex whose combinatorial structure is obtained from the cell decomposition of* S^2 *determined by the dual graph* D^* *of* D, *by subdividing each region of* D^* *as follows. Each region of* D^* *contains a unique vertex, say* c, *of* D. *Subdivide the region by taking the join of* c *and the edge cycle of* D^* *forming the boundary of the region (see Figure 2.5). Here the vertex* $m^*(R)$ *of* $D^* \subset \mathrm{Lk}(v_\pm, \mathcal{M})$ *dual to the region* R *corresponds to the direction at* v_ϵ *determined by the geodesic* $[v_\epsilon, m(R)]$.

Remark 2.6.2. (1) In the statement (2-b), the adjective "orthogonally" means that every interior point of $\mathcal{C}$ has a neighborhood U in $\mathcal{M}$ such that the triple $(U, U \cap \mathcal{S}_b, U \cap \mathcal{S}_w)$ is isometric to a neighborhood of the origin in $(\mathbb{R}^3, 0 \times \mathbb{R}^2, \mathbb{R} \times 0 \times \mathbb{R})$.

(2) In the statement (4), the adjective "orthogonally" means that there is a CAT(0) neighborhood U of $m(R)$ in $\mathcal{M}$, such that for any point $x \in (e(R) \setminus \{m(R)\}) \cap U$ and $y \in ((\mathcal{S}_b \cup \mathcal{S}_w) \setminus \{m(R)\}) \cap U$, we have $\angle_{m(R)}(x, y) = \pi/2$.

(3) For each component T of ∂M, the restriction $\mathcal{M}|_T$ of $\mathcal{M}$ to T gives a cubed decomposition of T, whose 1-skeleton is the union of two longitudes ℓ_b and ℓ_w, where ℓ_b and ℓ_w are parallel to $S_b \cap T$ and $S_w \cap T$, respectively. In particular, for each square I^2 of $\mathcal{M}|_T$, exactly one of the two diagonals of the square projects to a meridional loop (cf. Figure 2.2(a)).

(4) The assertion (5) implies the following key fact. For distinct regions R_1 and R_2 of D, the distance $d_{\mathrm{Lk}(v_\epsilon, \mathcal{M})}(m^*(R_1), m^*(R_2))$ is $\pi/2$ or $\geq \pi$ according to whether R_1 and R_2 are adjacent or not. By Lemma 2.5.6, this implies that the Alexandrov angle $\angle_{v_\epsilon}(m(R_1), m(R_2))$ is equal to $\pi/2$ or π according to whether R_1 and R_2 are adjacent or not. This fact plays a key role in the proof of Proposition 2.7.4.

Let $\mathcal{X}$ be the cubed complex obtained by attaching the cubed complex $\bigcup_{n=1}^{\infty} \partial\mathcal{M} \times [n, n+1]$ to $\mathcal{M}$ along $\partial\mathcal{M}$. Then the underlying space is the

link complement X, and we have the following key proposition.

Proposition 2.6.3. *The cubed complexes $\mathcal{M}$ and $\mathcal{X}$ are complete and non-positively curved.*

Proof. By Proposition 2.5.5, $\mathcal{M}$ and $\mathcal{X}$ are complete. From the description of $\mathrm{Lk}(v_\pm, \mathcal{M})$ $(= \mathrm{Lk}(v_\pm, \mathcal{X}))$ given by Proposition 2.6.1(5), we can check that they are flag complexes as in [45, Proof of Proposition 3.3]. For any other vertex v of $\mathcal{M}$ and $\mathcal{X}$, we can easily see that the geometric link of v in $\mathcal{M}$ and $\mathcal{X}$, respectively, is a flag complex. Hence, $\mathcal{M}$ and $\mathcal{X}$ are non-positively curved by Gromov's flag criterion (Proposition 2.5.7). □

Let $\tilde{\mathcal{X}}$ (resp. $\tilde{\mathcal{M}}$) be the cubed decomposition of the universal covering space $\tilde{X}$ (resp. $\tilde{M}$) obtained by pulling back the cubed decompositions $\mathcal{X}$ of X (resp. $\mathcal{M}$ of M) through the covering projection $p_u : \tilde{X} \to X$. Then $\tilde{\mathcal{X}}$ and $\tilde{\mathcal{M}}$ are complete CAT(0) cubed complexes by Proposition 2.6.3 and the Cartan-Hadanard theorem (Proposition 2.5.1).

As in Proposition 2.6.1(2), the open checkerboard surfaces S_b and S_w in X are isotopic to hyperplanes in $\mathcal{X}$, which we also denote by $\mathcal{S}_b$ and $\mathcal{S}_w$, respectively. Then $\mathcal{S}_b$ and $\mathcal{S}_w$ intersects orthogonally along $\mathcal{C} := \mathcal{S}_b \cap \mathcal{S}_w$, the disjoint union of geodesic lines representing open crossing arcs. Set $\tilde{\mathcal{S}}_b := p_u^{-1}(\mathcal{S}_b)$ and $\tilde{\mathcal{S}}_w := p_u^{-1}(\mathcal{S}_w)$. Then every component Σ of $\tilde{\mathcal{S}}_b$ (resp. $\tilde{\mathcal{S}}_w$) is a hyperplane in $\tilde{\mathcal{X}}$, and it is regarded as the universal covering of $\mathcal{S}_b$ (resp. $\mathcal{S}_w$): we call Σ a *checkerboard hyperplane* in $\tilde{\mathcal{X}}$. Of course, a checkerboard hyperplane is a checkerboard plane defined in Section 2.3.

Proposition 2.6.4. *Every checkerboard hyperplane Σ is convex in the CAT(0) space $\tilde{\mathcal{X}}$. Moreover, Σ divides $\tilde{\mathcal{X}}$ into two closed convex subspaces, namely, there are convex subspaces $\mathcal{B}$ and $\mathcal{B}^\mathfrak{c}$ of $\tilde{\mathcal{X}}$ such that $\tilde{\mathcal{X}} = \mathcal{B} \cup \mathcal{B}^\mathfrak{c}$ and $\Sigma = \mathcal{B} \cap \mathcal{B}^\mathfrak{c}$.*

Proof. This follows from Farley's result [21, Theorem 4.4], that is motivated by Sageev's combinatorial study of hyperplanes in [40, Section 4]. See [42, Section 4.3] for another proof. □

We call each of the subspaces $\mathcal{B}$ and $\mathcal{B}^\mathfrak{c}$ of $\tilde{\mathcal{X}}$ in the above proposition a *checkerboard half-space* bounded by the checkerboard hyperplane Σ. Though every checkerboard half-space is also regarded as that defined in Section 2.3, we use the terminology in the above sense throughout the remainder of this paper.

By a *peripheral plane*, we mean a component of $\partial\tilde{\mathcal{M}} \subset \tilde{\mathcal{X}}$. Then we have the following proposition, which is easily proved by using [42, Theorem 1.1].

Proposition 2.6.5. *Under the above setting, every peripheral plane $H \subset \partial\tilde{\mathcal{M}}$ is convex in the CAT(0) space $\tilde{\mathcal{X}}$.*

Propositions 2.6.4 and 2.6.5 imply the following proposition.

Proposition 2.6.6. (1) *Let Σ_1 and Σ_2 be distinct checkerboard hyperplanes in $\tilde{\mathcal{X}}$. Then one of the following holds.*

(a) $\Sigma_1 \cap \Sigma_2 = \emptyset$.

(b) $\Sigma_1 \cap \Sigma_2$ *is a geodesic line. Moreover,* Σ_1 *and* Σ_2 *intersect orthogonally along* $\Sigma_1 \cap \Sigma_2$*, in the sense defined in Remark 2.6.2(1). Furthermore,* $\Sigma_1 \cap \Sigma_2$ *divides each of* Σ_1 *and* Σ_2 *into two convex subspaces.*

(2) *Let* Σ *be a checkerboard hyperplane and* H *a peripheral plane in* $\tilde{\mathcal{X}}$*. Then one of the following holds.*

(a) $\Sigma \cap H = \emptyset$*.*

(b) $\Sigma \cap H$ *is a geodesic line. Moreover,* Σ *and* H *intersect orthogonally along* $\Sigma \cap H$*, in the sense defined in Remark 2.6.2(1). Furthermore,* $\Sigma \cap H$ *divides each of* Σ *and* H *into two convex subspaces.*

Proof. The assertions except for the orthogonalities are consequences of Propositions 2.6.4, 2.6.5 and the fact that the intersection of two convex sets is again convex. The orthogonality of Σ_1 and Σ_2 in (1-b) follows from the fact that Σ_1 and Σ_2 are hyperplanes, and so their relative positions are as explained in Proposition 2.6.1(2) and illustrated in Figure 2.4(c). The orthogonality of Σ and H in (2-b) follows similarly from Proposition 2.6.1(1,2) and Figure 2.4(c). The additional assertions in (1-b) and (2-b) are proved by a (much simpler) argument similar to the proof of Proposition 2.6.4. □

The following technical corollary is used in Section 2.9.

Corollary 2.6.7. *Let* Σ_1 *and* Σ_2 *be distinct checkerboard hyperplanes such that* $\ell := \Sigma_1 \cap \Sigma_2$ *is a geodesic line. Then the following hold.*

(1) *If* ℓ' *is a geodesic in* $\tilde{\mathcal{X}}$ *such that* $\ell \cap \ell' \neq \emptyset$*, then either* $\ell' \subset \ell$ *or* $\ell \cap \ell'$ *is a singleton.*

(2) *If* ℓ' *is a geodesic in* Σ_i *(*$i = 1$ *or* 2*) such that* $\ell \cap \ell'$ *is a singleton* $\{y\}$ *in* $\operatorname{int} \ell'$*, then* y *is a transversal intersection point of* ℓ *and* ℓ'*, and the two components of* $\ell' \setminus \{y\}$ *are contained in distinct components of* $\Sigma_i \setminus \ell$*.*

(3) *Let* H *be a peripheral hyperplane in* $\tilde{\mathcal{X}}$*, such that* $\ell \cap H \neq \emptyset$*. Then* $\ell \cap H$ *consists of a single point,* w*, and* $\pi_H^{-1}(w) = \ell$*, where* $\pi_H : \tilde{\mathcal{X}} \to H$ *is the projection.*

Proof. (1) Since $\ell \cap \ell'$ is a convex subset of ℓ, $\ell \cap \ell'$ is either a singleton or a non-degenerate geodesic (a geodesic strictly bigger than a singleton). If $\ell \cap \ell'$ is a non-degenerate geodesic, then ℓ' must be contained in the geodesic line ℓ, because every point in ℓ has a Euclidean neighborhood in $\tilde{\mathcal{X}}$ by Proposition 2.6.6(1-b) and Remark 2.6.2(1), and because, in the Euclidean space, every geodesic has no branching (see Figure 2.6(a)).

(2) This follows from the fact that the point $y \in \ell \subset \Sigma_i$ has a Euclidean neighborhood in Σ_i (by Proposition 2.6.6(1-b) and Remark 2.6.2(1)) and the fact that every geodesic has no branching in the Euclidean plane (see Figure 2.6(b)).

(3) It follows from Proposition 2.6.1(1), (2) that ℓ intersects H orthogonally at a single point, w, and that $\ell \subset \pi_H^{-1}(w)$. To see the converse inclusion, pick

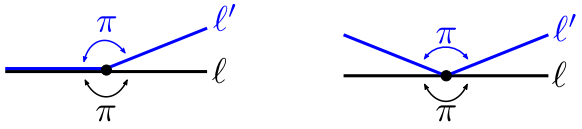

(a) (b)

Figure 2.6: Branching of geodesics. Though branching of geodesic can occur in CAT(0) spaces, it never occurs in Euclidean spaces.

a point z ($\neq w$) of $\pi_H^{-1}(w)$. Then the geodesic segment of $[z,w]$ is orthogonal to H at w (cf. Lemma 2.5.3). Since w has a Euclidean neighborhood in $\tilde{\mathcal{X}}$ by Proposition 2.6.6(2-b), this implies that a small neighborhood of w in $[z,w]$ is contained in ℓ. Hence $[z,w] \subset \ell$ by the assertion (1). Thus $z \in \ell$ and so $\pi_H^{-1}(w) = \ell$. □

The following lemma is used in Sections 2.8 and 2.9.

Lemma 2.6.8. *Let Σ_1 and Σ_2 be disjoint checkerboard hyperplanes in $\tilde{\mathcal{X}}$. Then $\Sigma_1 \cup \Sigma_2$ divides $\tilde{\mathcal{X}}$ into three convex subspaces. To be precise, there are three closed convex subspaces $\mathcal{B}_1$, $\mathcal{B}_{1,2}$ and $\mathcal{B}_2$, such that*

$$\tilde{\mathcal{X}} = \mathcal{B}_1 \cup \mathcal{B}_{1,2} \cup \mathcal{B}_2, \quad \mathcal{B}_1 \cap \mathcal{B}_{1,2} = \Sigma_1, \quad \mathcal{B}_{1,2} \cap \mathcal{B}_2 = \Sigma_2, \quad \mathcal{B}_1 \cap \mathcal{B}_2 = \emptyset.$$

Proof. By Proposition 2.6.4, there are closed convex subspaces $\mathcal{B}_i$ and $\mathcal{B}_i^{\mathfrak{c}}$ such that $\tilde{\mathcal{X}} = \mathcal{B}_i \cup \mathcal{B}_i^{\mathfrak{c}}$ and $\Sigma_i = \mathcal{B}_i \cap \mathcal{B}_i^{\mathfrak{c}}$ ($i = 1, 2$). Since $\Sigma_1 \subset \tilde{\mathcal{X}} \setminus \Sigma_2 = \operatorname{int}\mathcal{B}_2 \sqcup \operatorname{int}\mathcal{B}_2^{\mathfrak{c}}$, we may assume $\Sigma_1 \subset \operatorname{int}\mathcal{B}_2^{\mathfrak{c}}$ and $\Sigma_1 \cap \mathcal{B}_2 = \emptyset$. Similarly, we may assume $\Sigma_2 \subset \operatorname{int}\mathcal{B}_1^{\mathfrak{c}}$ and $\Sigma_2 \cap \mathcal{B}_1 = \emptyset$. Then $\mathcal{B}_1 \cap \mathcal{B}_2$ is disjoint from $\Sigma_1 \cup \Sigma_2 = \partial\mathcal{B}_1 \cup \partial\mathcal{B}_2$, and therefore $\mathcal{B}_1 \cap \mathcal{B}_2 = \operatorname{int}\mathcal{B}_1 \cap \operatorname{int}\mathcal{B}_2$. Hence $\mathcal{B}_1 \cap \mathcal{B}_2$ is a closed, open, proper subset of $\tilde{\mathcal{X}}$. Since $\tilde{\mathcal{X}}$ is connected, this implies $\mathcal{B}_1 \cap \mathcal{B}_2 = \emptyset$. Thus, by setting $\mathcal{B}_{1,2} := \mathcal{B}_1^{\mathfrak{c}} \cap \mathcal{B}_2^{\mathfrak{c}}$, we obtain the desired result. □

2.7 Decompositions of alternating link complements into checkerboard ideal polyhedra

We recall the (topological) ideal polyhedral decomposition of the complement X of a prime alternating link L associated with its prime alternating diagram D, due to Thurston [52], Menasco [32], Takahashi [49] and others, following the description by Aitchison-Rubinstein [7] (see also [39, Theorem 11.6]).

Regard the prime alternating diagram D as a 4-valent graph on the boundary of the 3-ball B^3. Then (B^3, D) is regarded as a (topological) polyhedron (cf. [39, Definition 1.1]). By removing the vertices from (B^3, D), we obtain a (topological) ideal polyhedron, which we denote by $\mathrm{P}(D)$. Each region R of D determines the (ideal) face $\check{R} := R \setminus \{\text{vertices}\}$ of $\mathrm{P}(D)$, and each edge e of D determines the (ideal) edge $\check{e} := \operatorname{int} e$ of $\mathrm{P}(D)$. Prepare two disjoint copies $\mathrm{P}_+(D)$ and $\mathrm{P}_-(D)$ of $\mathrm{P}(D)$, and glue them together by the following "gear

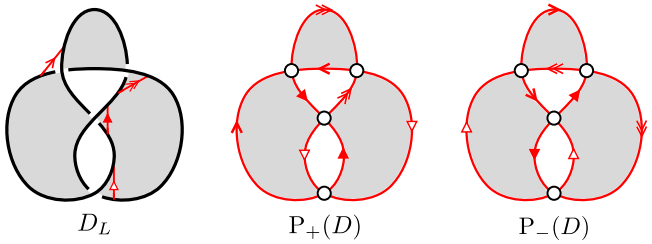

Figure 2.7: The decomposition of the figure-eight knot complement into a pair of checkerboard ideal polyhedra: The shaded regions are black regions and the unshaded regions are white regions.

rule": For each region R of D, the face $\check{R}$ of $\mathrm{P}_+(D)$ is identified with the face $\check{R}$ of $\mathrm{P}_-(D)$ through rotation by one edge in the clockwise or anti-clockwise direction according to whether R is black or white (see Figure 2.7). (Here, we employ the convention that the twisted bands in the black (resp. white) surface are left-handed (resp. right-handed) as in Figure 2.4(a).)

Proposition 2.7.1. *Under the above setting, the resulting space is naturally homeomorphic to the complement X of L. Moreover, the following hold.*

(1) *The image in X of an edge of $\mathrm{P}_\pm(D)$ is an open crossing arc. Moreover, the inverse image of each crossing arc in each of $\mathrm{P}_\pm(D)$ consists of two edges.*

(2) *If R is a black region of D, then the image in X of the face $\check{R}$ of $\mathrm{P}_\pm(D)$ is equal to the closure of the component of $S_b \setminus (S_b \cap S_w)$ corresponding to R. Parallel assertions also hold when R is a white region.*

(3) *For each $\epsilon \in \{+,-\}$, the image of $\mathrm{P}_\epsilon(D)$ in X is equal to the closure of the component of $X \setminus (S_b \cup S_w)$ containing the point v_ϵ.*

Though the natural maps from $\mathrm{P}_\pm(D)$ to X are not injective on the 1-skeletons, their lifts to the universal cover $\tilde{X}$ are homeomorphisms onto their images, each of which is equal to the closure of a component of $\tilde{X} \setminus p_u^{-1}(S_b \cup S_w)$. Thus we obtain a tessellation of $\tilde{X}$ by copies of $\mathrm{P}_+(D)$ and $\mathrm{P}_-(D)$, where the wall is $p_u^{-1}(S_b \cup S_w)$, the union of all checkerboard planes.

By working in the non-positively curved cubed decomposition $\mathcal{X}$ of X and the CAT(0) cubed decomposition $\tilde{\mathcal{X}}$ of $\tilde{X}$, we can refine the above topological picture into the geometric picture explained below.

Recall that the open checkerboard surfaces S_b and S_w in X are isotopic to the hyperplanes $\mathcal{S}_b$ and $\mathcal{S}_w$ in the non-positively curved cubed complex $\mathcal{X}$. They intersect orthogonally along $\mathcal{C} = \mathcal{S}_b \cap \mathcal{S}_w$, the disjoint union of geodesic lines representing open crossing arcs. The union $\mathcal{S}_{bw} := \mathcal{S}_b \cup \mathcal{S}_w$ cuts $\mathcal{X}$ into two connected components. We denote by $\mathcal{P}_+$ and $\mathcal{P}_-$, the closures of the components of $\mathcal{X} \setminus \mathcal{S}_{bw}$ containing the vertices v_+ and v_-, respectively. Then $\mathcal{P}_\pm$ is naturally homeomorphic to the image of $\mathrm{P}_\pm(D)$ in X.

In the universal cover $\tilde{\mathcal{X}}$, both $\tilde{\mathcal{S}}_b = p_u^{-1}(\mathcal{S}_b)$ and $\tilde{\mathcal{S}}_w = p_u^{-1}(\mathcal{S}_w)$ are disjoint unions of checkerboard hyperplanes, and they intersect orthogonally along $\tilde{\mathcal{C}} := \tilde{\mathcal{S}}_b \cap \tilde{\mathcal{S}}_w$. The union $\tilde{\mathcal{S}}_{bw} = \tilde{\mathcal{S}}_b \cup \tilde{\mathcal{S}}_w$ of all checkerboard hyperplanes divides $\tilde{\mathcal{X}}$ into infinitely many "right-angled, cubed, ideal polyhedra", and we obtain the following proposition.

Proposition 2.7.2. *Let $\tilde{\mathcal{P}}_\epsilon$ be the closure of a component of $\tilde{\mathcal{X}} \setminus \tilde{\mathcal{S}}_{bw}$ which projects to $\mathcal{P}_\epsilon \subset \mathcal{X}$ ($\epsilon \in \{+,-\}$). Then $\tilde{\mathcal{P}}_\epsilon$ admits a natural structure of a (topological) ideal polyhedron with respect to which there is an isomorphism $\varphi_\epsilon : \mathrm{P}(D) \to \tilde{\mathcal{P}}_\epsilon$ satisfying the following conditions.*

(1) *For each region R of D, there is a checkerboard hyperplane, $\Sigma_R = \Sigma_R(\tilde{\mathcal{P}}_\epsilon)$, satisfying the following conditions.*

   (a) $\varphi_\epsilon(\check{R}) = \partial\tilde{\mathcal{P}}_\epsilon \cap \Sigma_R$.

   (b) *If R is a black region, then $p_u(\Sigma_R) = \mathcal{S}_b$, and the restriction of the universal covering projection $p_u|_{\Sigma_R} : \Sigma_R \to \mathcal{S}_b$ to the face $\varphi_\epsilon(\check{R})$ is a homeomorphism onto the closure of the component of $\mathcal{S}_b \setminus \mathcal{C}$ corresponding to R. Parallel assertions also hold when R is a white region.*

(2) *For each region R of D, let $\mathcal{B}^{\mathfrak{c}}_{\tilde{R}} = \mathcal{B}^{\mathfrak{c}}_{\tilde{R}}(\tilde{\mathcal{P}}_\epsilon)$ be the checkerboard half-space bounded by Σ_R that contains $\tilde{\mathcal{P}}_\epsilon$. Then $\tilde{\mathcal{P}}_\epsilon = \bigcap_R \mathcal{B}^{\mathfrak{c}}_{\tilde{R}}$, where R runs over the regions of D. In particular, $\tilde{\mathcal{P}}_\epsilon$ is convex in the CAT(0) space $\tilde{\mathcal{X}}$.*

(3) *Let e be an edge of D and let R_1 and R_2 be the regions of D sharing e. Then the two faces $\varphi_\epsilon(\check{R}_1)$ and $\varphi_\epsilon(\check{R}_2)$ intersect orthogonally along the edge $\varphi_\epsilon(\check{e})$. The edge $\varphi_\epsilon(\check{e})$ projects to a geodesic line in $\mathcal{X}$ representing an open crossing arc.*

Moreover, φ_+ and φ_- are related as explained below. Note that, for each region R of D, $(p_u \circ \varphi_\pm)|_{\check{R}}$ are homeomorphisms with the same image, and so the composition $(p_u \circ \varphi_-)|_{\check{R}} \circ {(p_u \circ \varphi_+)|_{\check{R}}}^{-1}$ is a well-defined automorphism of the ideal polygon $\check{R}$. This automorphism is a rotation by one edge in the clockwise or anti-clockwise direction according to whether R is black or white.

The proposition is obtained by looking Proposition 2.7.1 in the setting of Proposition 2.6.1. The convexity of $\tilde{\mathcal{P}}_\epsilon$ in (2) is a consequence of Proposition 2.6.4.

Definition and Notation 2.7.3. We call $\tilde{\mathcal{P}}_\epsilon$ a *checkerboard ideal polyhedron* in $\tilde{\mathcal{X}}$. The unique point $\tilde{v}_\epsilon \in p_u^{-1}(v_\epsilon)$ contained in $\tilde{\mathcal{P}}_\epsilon$ is called the *center* of $\tilde{\mathcal{P}}_\epsilon$.

When we do not mind the sign ϵ, we drop it from the symbols, such as $\tilde{\mathcal{P}}_\epsilon$ and φ_ϵ. For a fixed checkerboard ideal polyhedron $\tilde{\mathcal{P}}$ and for a region R of D, we use the following terminology and notation.

(1) The face $\varphi(\check{R})$ of $\tilde{\mathcal{P}}$ is called the *face R of $\tilde{\mathcal{P}}$*.

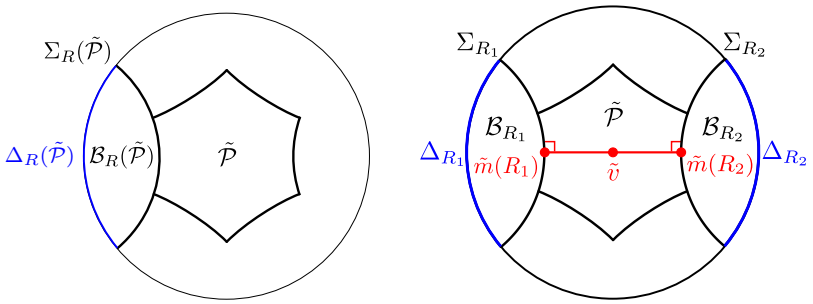

Figure 2.8: (a) $\mathcal{B}_R(\tilde{\mathcal{P}})$ is the checkerboard half-space in $\tilde{\mathcal{X}}$ bounded by the hyperplane $\Sigma_R(\tilde{\mathcal{P}})$ which is *disjoint* from $\operatorname{int}\tilde{\mathcal{P}}$. (This 2-dimensional figure does not reflect the fact that $\tilde{\mathcal{P}}$ is an *ideal* polyhedron.) (b) If R_1 and R_2 are not adjacent, then $\angle_{\tilde{v}}(\tilde{m}(R_1), \tilde{m}(R_2)) = \pi$, and hence $[\tilde{m}(R_1), \tilde{v}] \cup [\tilde{v}, \tilde{m}(R_2)]$ is a common perpendicular to Σ_{R_1} and Σ_{R_2}. This implies $\mathcal{B}_{R_1}(\tilde{\mathcal{P}}) \cap \mathcal{B}_{R_2}(\tilde{\mathcal{P}}) = \emptyset$.

(2) The *center* $\tilde{m}(R)$ of the face R of $\tilde{\mathcal{P}}$ is defined as follows. By Proposition 2.7.2(1-b), p_u determines a homeomorphism from $\varphi(\check{R})$ to the closure of the component of $\mathcal{S}_{bw} \setminus \mathcal{C}$ containing the center $m(R)$. Then $\tilde{m}(R) \in \varphi(\check{R})$ is the inverse image of $m(R)$.

(3) $\Sigma_R = \Sigma_R(\tilde{\mathcal{P}})$ denotes the checkerboard hyperplane in $\tilde{\mathcal{X}}$ containing the face R of $\tilde{\mathcal{P}}$.

(4) $\mathcal{B}_R = \mathcal{B}_R(\tilde{\mathcal{P}})$ and $\mathcal{B}_R^{\mathrm{c}} = \mathcal{B}_R^{\mathrm{c}}(\tilde{\mathcal{P}})$ denote the checkerboard half-spaces in $\tilde{\mathcal{X}}$ bounded by $\Sigma_R(\tilde{\mathcal{P}})$, such that $\tilde{\mathcal{P}} \subset \mathcal{B}_R^{\mathrm{c}}(\tilde{\mathcal{P}})$ and $\mathcal{B}_R(\tilde{\mathcal{P}}) \cap \mathcal{B}_R^{\mathrm{c}}(\tilde{\mathcal{P}}) = \Sigma_R(\tilde{\mathcal{P}})$ (see Figure 2.8(a)).

Then we have the following proposition, which plays a key role in the proof of Theorem 2.1.2.

Proposition 2.7.4. *Let $\tilde{\mathcal{P}} \subset \tilde{\mathcal{X}}$ be a checkerboard ideal polyhedron, and let R_1 and R_2 be distinct regions of D. Then $\mathcal{B}_{R_1} = \mathcal{B}_{R_1}(\tilde{\mathcal{P}})$ and $\mathcal{B}_{R_1} = \mathcal{B}_{R_2}(\tilde{\mathcal{P}})$ are disjoint if and only if R_1 and R_2 are not adjacent.*

Proof. Let $\tilde{v}$ be the center of $\tilde{\mathcal{P}}$, and let $\tilde{m}(R_i)$ be the center of the face R_i of $\tilde{\mathcal{P}}$ $(i = 1, 2)$. Then the geodesic segment $[\tilde{v}, \tilde{m}(R_i)]$ is perpendicular to $\Sigma_{R_i} = \Sigma_{R_i}(\tilde{\mathcal{P}})$ by Proposition 2.6.1(4) (cf. Remark 2.6.2(2)) and Remark 2.5.2. Note that there is a natural isomorphism $\operatorname{Lk}(\tilde{v}, \tilde{\mathcal{X}}) \cong \operatorname{Lk}(v, \mathcal{M})$, where $v = p_u(\tilde{v})$. Thus, by Remark 2.6.2(4), $\angle_{\tilde{v}}(\tilde{m}(R_1), \tilde{m}(R_2))$ is equal to $\pi/2$ or π according to whether R_1 and R_2 are adjacent or not. Hence, if R_1 and R_2 are not adjacent, then $[\tilde{m}(R_1), \tilde{v}] \cup [\tilde{v}, \tilde{m}(R_2)]$ is a geodesic which is perpendicular to the checkerboard hyperplanes Σ_{R_1} and Σ_{R_2} at their endpoints. (In fact, it is a local geodesic by [16, Remark I.5.7 and Theorem I.7.39] and so it is a geodesic by [16, Proposition II.1.4(2)].) Hence, by Lemma 2.5.4, it is a shortest path between

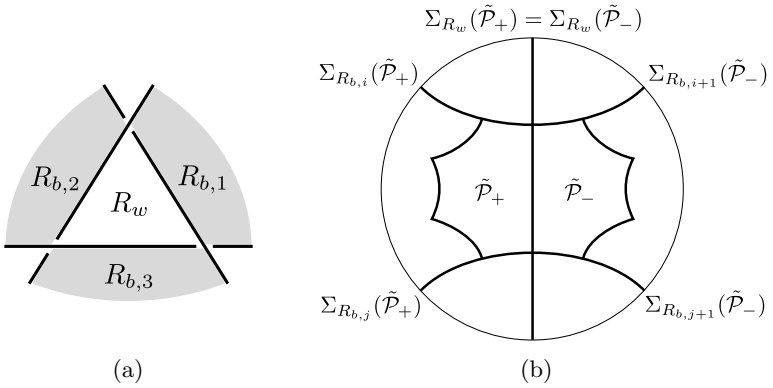

Figure 2.9: The checkerboard polyhedra $\tilde{\mathcal{P}}_+$ and $\tilde{\mathcal{P}}_-$ share a face that is contained in the checkerboard hyperplane $\Sigma_{R_w}(\tilde{\mathcal{P}}_+) = \Sigma_{R_w}(\tilde{\mathcal{P}}_-)$. Then $\Sigma_{R_{b,i}}(\tilde{\mathcal{P}}_+) = \Sigma_{R_{b,i+1}}(\tilde{\mathcal{P}}_-)$.

the hyperplanes, and in particular, Σ_{R_1} and Σ_{R_2} are disjoint. By Lemma 2.6.8, $\Sigma_{R_1} \cup \Sigma_{R_2}$ divides $\tilde{\mathcal{X}}$ into three closed convex subspaces $\mathcal{B}_1$, $\mathcal{B}_{1,2}$ and $\mathcal{B}_2$, that satisfy the condition in the lemma. Since $\tilde{\mathcal{P}}$ intersects both Σ_{R_1} and Σ_{R_2}, we have $\tilde{\mathcal{P}} \subset \mathcal{B}_{1,2}$. This implies that $\mathcal{B}_i = \mathcal{B}_{R_i}$ $(i = 1, 2)$. Hence $\mathcal{B}_{R_1}$ and $\mathcal{B}_{R_2}$ are disjoint (see Figure 2.8(b)).

On the other hand, if the regions R_1 and R_2 are adjacent in D, then the faces R_1 and R_2 of $\tilde{\mathcal{P}}$ are adjacent. Thus $\Sigma_{R_1} \cap \Sigma_{R_2}$ is a geodesic line (cf. Proposition 2.6.6(1)) and hence $\mathcal{B}_{R_1}$ and $\mathcal{B}_{R_2}$ are not disjoint. □

At the end of this section, we note the following observation (see Figure 2.9), which is used in Section 2.9.

Lemma 2.7.5. *Let R_w be a white region of D and $R_{b,i}$ $(1 \le i \le n)$ be the black regions of D which are adjacent to R_w and which are arranged around R_w in this cyclic order with respect to the anti-clockwise orientation of ∂R_w. Let $\tilde{\mathcal{P}}_\pm \subset \tilde{\mathcal{X}}$ be the checkerboard ideal polyhedra, such that $\tilde{\mathcal{P}}_+ \cap \tilde{\mathcal{P}}_-$ is the face R_w of both $\tilde{\mathcal{P}}_+$ and $\tilde{\mathcal{P}}_-$. Then we have $\Sigma_{R_{b,i}}(\tilde{\mathcal{P}}_+) = \Sigma_{R_{b,i+1}}(\tilde{\mathcal{P}}_-)$ and $\mathcal{B}_{R_{b,i}}(\tilde{\mathcal{P}}_+) = \mathcal{B}_{R_{b,i+1}}(\tilde{\mathcal{P}}_-)$, where the index i is considered with modulo n. When the colors black and white are interchanged, similar assertion holds.*

Proof. For $\epsilon \in \{+, -\}$, let φ_ϵ be the isomorphism from $\mathrm{P}(D)$ to the checkerboard ideal polyhedron $\tilde{\mathcal{P}}_\epsilon$. Then $\varphi_+(\check{R}_w) = \varphi_-(\check{R}_w)$ by the assumption. Consider the edge $e_i := R_w \cap R_{b,i}$ of D. Then, by the last assertion of Proposition 2.7.2, we see that $\varphi_+(\check{e}_i) = \varphi_-(\check{e}_{i+1})$ and that it is a common edge of the faces $\varphi_+(\check{R}_{b,i})$ and $\varphi_-(\check{R}_{b,i+1})$. Since $\tilde{\mathcal{P}}_\pm$ are right-angled cubed polyhedra (cf. Proposition 2.7.2(3)), this implies that the two faces are contained in a single checkerboard hyperplane, which is equal to $\Sigma_{R_{b,i}}(\tilde{\mathcal{P}}_+) = \Sigma_{R_{b,i+1}}(\tilde{\mathcal{P}}_-)$. Since $\tilde{\mathcal{P}}_+$ and $\tilde{\mathcal{P}}_-$ share the common face $\varphi_+(\check{R}_w) = \varphi_-(\check{R}_w)$, we also have $\mathcal{B}_{R_{b,i}}(\tilde{\mathcal{P}}_+) = \mathcal{B}_{R_{b,i+1}}(\tilde{\mathcal{P}}_-)$. □

2.8 Butterflies and checkerboard ideal polyhedra

The complement X of a hyperbolic alternating link L with a prescribed prime alternating diagram D admits two distinct geometric structures given as:

- the complete hyperbolic manifold $\mathbb{H}^3/G$, and
- the underlying space of the non-positively curved cubed complex $\mathcal{X}$ that is constructed from a prime alternating diagram D of L.

We fix homeomorphisms

$$(X, M) \cong (\mathbb{H}^3/G, (\mathbb{H}^3 \setminus \mathcal{Q})/G) \cong (|\mathcal{X}|, |\mathcal{M}|),$$

and identify the relevant spaces through the homeomorphisms. Here $\mathcal{Q}$ is the disjoint union of the open horoballs bounded by the horospheres $\{H_p\}_{p\in \mathrm{PFix}(G)}$ introduced in Section 2.4 (the paragraph after Lemma 2.4.2). This identification induces the following G-equivariant identifications of the universal covering spaces

$$(\tilde{X}, \tilde{M}) = (\mathbb{H}^3, \mathbb{H}^3 \setminus \mathcal{Q}) = (|\tilde{\mathcal{X}}|, |\tilde{\mathcal{M}}|).$$

In particular, each horosphere $H_p \subset \mathbb{H}^3$ is regarded as a peripheral plane contained in $\partial\tilde{\mathcal{M}}$ in the CAT(0) space $\tilde{\mathcal{X}}$; so we call it the *peripheral plane centered at* p.

We also assume that the quasi-fuchsian checkerboard surfaces S_b and S_w in the hyperbolic manifold $X = \mathbb{H}^3/G$ (cf. Sections 2.3 and 2.4) are the hyperplanes $\mathcal{S}_b$ and $\mathcal{S}_w$, respectively, in the non-positively curved cubed complex $\mathcal{X}$ (cf. Sections 2.6 and 2.7). Thus each checkerboard plane $\Sigma \subset \mathbb{H}^3$ is a checkerboard hyperplane in the CAT(0) cubed complex $\tilde{\mathcal{X}}$.

For a checkerboard ideal polyhedron $\tilde{\mathcal{P}} \subset \tilde{\mathcal{X}} = \mathbb{H}^3$, let $\hat{\mathcal{P}}$ be the closure of $\tilde{\mathcal{P}}$ in $\bar{\mathbb{H}}^3 = \mathbb{H}^3 \cup \hat{\mathbb{C}}$. Then the isomorphism $\varphi : \mathrm{P}(D) \to \tilde{\mathcal{P}}$ (between topological ideal polyhedra) extends to an isomorphism $\hat{\varphi} : (B^3, D) \to \hat{\mathcal{P}}$ (between topological polyhedra), because $\tilde{X} \setminus \tilde{M}$ is identified with the disjoint family of open horoballs $\mathcal{Q}$ centered at points in $\mathrm{PFix}(G)$. For each vertex c of D, the ideal point $p := \hat{\varphi}(c)$ belongs to $\mathrm{PFix}(G)$, and we call p the *ideal vertex of* $\tilde{\mathcal{P}}$ *corresponding to* c. We also call c the *vertex of* D *corresponding to the ideal vertex* p *of* $\tilde{\mathcal{P}}$.

We introduce the following notation for objects in the closure $\bar{\mathbb{H}}^3$ of the hyperbolic space, building on Definition and Notation 2.7.3 for objects in the CAT(0) cubed complex $\tilde{\mathcal{X}}$ (cf. Figure 2.8(a)).

Notation 2.8.1. Let $\tilde{\mathcal{P}} \subset \tilde{\mathcal{X}}$ be a checkerboard ideal polyhedron, and R a region of the diagram D.

1. $\bar{\Sigma}_R = \bar{\Sigma}_R(\tilde{\mathcal{P}})$ denotes the checkerboard disk properly embedded in $\bar{\mathbb{H}}^3$ obtained as the closure of $\Sigma_R(\tilde{\mathcal{P}}) \subset \tilde{\mathcal{X}} = \mathbb{H}^3$.
2. $\bar{\mathcal{B}}_R = \bar{\mathcal{B}}_R(\tilde{\mathcal{P}})$ and $\bar{\mathcal{B}}^{\mathfrak{c}}_R = \bar{\mathcal{B}}^{\mathfrak{c}}_R(\tilde{\mathcal{P}})$ denote the 3-balls in $\bar{\mathbb{H}}^3$ obtained as the closures of the checkerboard half-spaces $\mathcal{B}_R(\tilde{\mathcal{P}})$ and $\mathcal{B}^{\mathfrak{c}}_R(\tilde{\mathcal{P}})$. Note that $\tilde{\mathcal{P}} \subset \bar{\mathcal{B}}^{\mathfrak{c}}_R(\tilde{\mathcal{P}})$ and $\bar{\mathcal{B}}_R(\tilde{\mathcal{P}}) \cap \bar{\mathcal{B}}^{\mathfrak{c}}_R(\tilde{\mathcal{P}}) = \bar{\Sigma}_R(\tilde{\mathcal{P}})$.

3. $\Delta_R(\tilde{\mathcal{P}})$ denotes the disk in $\hat{\mathbb{C}}$ defined by $\Delta_R(\tilde{\mathcal{P}}) := \bar{\mathcal{B}}_R(\tilde{\mathcal{P}}) \cap \hat{\mathbb{C}}$.

Then we have the following lemma.

Lemma 2.8.2. *Let $\tilde{\mathcal{P}}_1$ and $\tilde{\mathcal{P}}_2$ be checkerboard ideal polyhedra, and let R_1 and R_2 be regions of D. If the checkerboard half-spaces $\mathcal{B}_{R_1}(\tilde{\mathcal{P}}_1)$ and $\mathcal{B}_{R_2}(\tilde{\mathcal{P}}_2)$ in $\mathbb{H}^3$ are disjoint, then the two disks $\Delta_{R_1}(\tilde{\mathcal{P}}_1)$ and $\Delta_{R_2}(\tilde{\mathcal{P}}_2)$ have disjoint interiors in $\hat{\mathbb{C}}$.*

Proof. By Corollary 2.3.2, the pair $(\bar{\mathbb{H}}^3, \bar{\mathcal{B}}_{R_i})$, with $\mathcal{B}_{R_i} = \mathcal{B}_{R_i}(\tilde{\mathcal{P}}_i)$, is homeomorphic to the standard pair (B^3, B^3_+) of the unit 3-ball B^3 in $\mathbb{R}^3$ and the closed upper half-ball $B^3_+ = \{(x, y, z) \in B^3 \mid z \geq 0\}$ $(i = 1, 2)$. Thus a point $x \in \hat{\mathbb{C}}$ belongs to the interior of $\Delta_{R_i} := \Delta_{R_i}(\tilde{\mathcal{P}}_i)$ if and only if there is a neighborhood U of x in $\bar{\mathbb{H}}^3$ such that $U \cap \mathbb{H}^3 \subset \mathcal{B}_{R_i}$ $(i = 1, 2)$. So x belongs to $\operatorname{int}\Delta_{R_1} \cap \operatorname{int}\Delta_{R_2}$ if and only if there is a neighborhood U of x in $\bar{\mathbb{H}}^3$ such that $U \cap \mathbb{H}^3 \subset \mathcal{B}_{R_1} \cap \mathcal{B}_{R_2}$. Hence, if $\mathcal{B}_{R_1} \cap \mathcal{B}_{R_2} = \emptyset$ then $\operatorname{int}\Delta_{R_1} \cap \operatorname{int}\Delta_{R_2} = \emptyset$. □

Proposition 2.7.4 together with Lemma 2.8.2 implies the following proposition, which plays a key role in the proof of Theorem 2.2.1.

Proposition 2.8.3. *Let $\tilde{\mathcal{P}} \subset \tilde{\mathcal{X}}$ be a checkerboard ideal polyhedron, and let R_1 and R_2 be distinct regions of D. If R_1 and R_2 are not adjacent, then $\Delta_{R_1}(\tilde{\mathcal{P}})$ and $\Delta_{R_2}(\tilde{\mathcal{P}})$ have disjoint interiors in $\hat{\mathbb{C}}$.*

Remark 2.8.4. In Lemma 2.8.2 and Proposition 2.8.3, the converses also hold. Actually, Proposition 2.8.3 reflects only a small part of a very interesting statement in Agol's slide [3], which we read as follows. Aitchison and Rubinstein (cf. [6]) studied patterns of the intersections of the limit circles $\{\partial_\infty \Sigma\}$ of the checkerboard hyperplanes in the ideal boundary $\partial_\infty \tilde{\mathcal{X}}$ of the CAT(0) space $\tilde{\mathcal{X}}$: Put a circle around each region of D, then the limit circles $\{\partial_\infty(\Sigma_R(\tilde{\mathcal{P}}))\}_R$ "have this intersection pattern" in $\partial_\infty \tilde{\mathcal{X}}$ (see Figure 2.10). We hope to give more detailed interpretation of this statement in a subsequent paper.

The following characterization of butterflies is used repeatedly in the proof of Theorem 2.2.1.

Lemma 2.8.5. *Let $p \in \mathrm{PFix}(G)$ be a parabolic fixed point and $\tilde{\mathcal{P}}$ an ideal checkerboard polyhedron which has p as an ideal vertex. Let c be the vertex of D corresponding to p, and let $\{R^-, R^+\}$ be a pair of regions that contain c and have the same color. Then, after replacing $R^\pm$ with $R^\mp$ if necessary, the pair $\{\Delta_{R^-}(\tilde{\mathcal{P}}), \Delta_{R^+}(\tilde{\mathcal{P}})\}$ forms a butterfly $\mathrm{BF}(p)$ at p (in the sense of Notation 2.4.10). Conversely, every butterfly is obtained in this way.*

Proof. Consider the compact right-angled polyhedron $\tilde{\mathcal{P}}_0$ obtained from $\tilde{\mathcal{P}}$ through truncation along the peripheral planes $\{H_p\}$ (see Figure 2.11). Then, for each ideal vertex p of $\tilde{\mathcal{P}}$, the intersection $\tilde{\mathcal{P}} \cap H_p$ forms a square in $\partial\tilde{\mathcal{P}}_0$, one of whose diagonals projects to a meridian (see Figure 2.11). By using this fact, we can see that the meridian $\mu_p \in G$ maps the checkerboard hyperplane $\Sigma_{R^-}(\tilde{\mathcal{P}})$ to the checkerboard hyperplane $\Sigma_{R^+}(\tilde{\mathcal{P}})$, if necessary after replacing $R^\pm$ with $R^\mp$. We

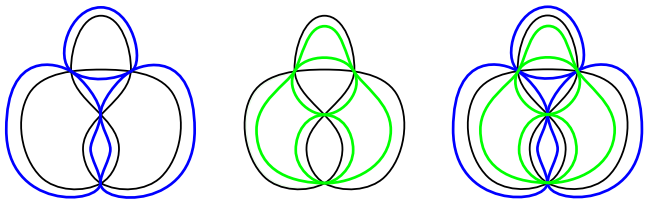

Figure 2.10: Put a circle C_R around each region R of the diagram D, so that C_R bounds a disk containing R and passes though the vertices on ∂R. The figures (a) and (b) illustrates the circles $\{C_R\}$ where R runs over the black or white regions, respectively. By overlaying these two figures, we obtain the figure (c). According to [3], the figure (c) "illustrates" the intersection pattern of the limit circles $\{\partial_\infty(\Sigma_R(\tilde{\mathcal{P}}))\}_R$, where R runs over the regions of D.

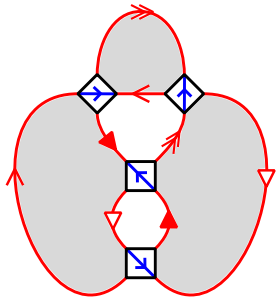

Figure 2.11: The truncation $\tilde{\mathcal{P}}_0$ of the checkerboard ideal polyhedron $\tilde{\mathcal{P}} = \tilde{\mathcal{P}}_+$. The blue diagonal arcs in the squares project to meridians.

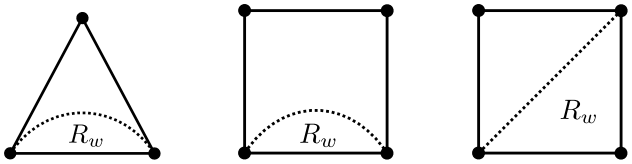

Figure 2.12: The plane graph $\mathcal{G}$ dual to the black regions. The complementary region of $\mathcal{G}$ labeled R_w determines the desired white region R_w.

can further see that μ_p maps the ball pair $(\bar{\mathcal{B}}_{R^-}(\tilde{\mathcal{P}}), \bar{\mathcal{B}}^{\mathfrak{c}}_{R^-}(\tilde{\mathcal{P}}))$ to the ball pair $(\bar{\mathcal{B}}^{\mathfrak{c}}_{R^+}(\tilde{\mathcal{P}}), \bar{\mathcal{B}}_{R^+}(\tilde{\mathcal{P}}))$. This implies that $\{\Delta_{R^-}(\tilde{\mathcal{P}}), \Delta_{R^+}(\tilde{\mathcal{P}})\}$ is a butterfly at p.

To see the converse, let $\mathrm{BF}(p) = \{\Delta_j^-, \Delta_{j+1}^+\} = \{\Delta_j^-(p), \Delta_{j+1}^+(p)\}$ be a butterfly, where we use notations in Definition 2.4.6. Consider the infinite strip in the peripheral plane (or the horosphere) $H_p \subset p_u^{-1}(\partial\mathcal{M})$ bounded by the lines $\ell_j(p) = \Sigma_j(p) \cap H_p$ and $\ell_{j+1}(p) = \Sigma_{j+1}(p) \cap H_p$ (see Figure 2.2). Let $\tilde{\mathcal{P}}$ be a checkerboard ideal polyhedron which has p as an ideal vertex, such that $\tilde{\mathcal{P}} \cap H_p$ is a square contained in the strip. Then there are regions R^- and R^+ of D containing the vertex c of D corresponding to the ideal vertex p of $\tilde{\mathcal{P}}$, such that $\Sigma_j(p) = \Sigma_{R^-}(\tilde{\mathcal{P}})$ and $\Sigma_{j+1}(p) = \Sigma_{R^+}(\tilde{\mathcal{P}})$. Then we see $\mathrm{BF}(p) = \{\Delta_j^-, \Delta_{j+1}^+\} = \{\Delta_{R^-}(\tilde{\mathcal{P}}), \Delta_{R^+}(\tilde{\mathcal{P}})\}$. □

At the end of this subsection, we prove the following elementary lemma concerning prime alternating diagrams of hyperbolic alternating links, which is used in Section 2.9.

Lemma 2.8.6. *Let D be a prime alternating diagram of a hyperbolic alternating link $L \subset S^3$. Then the following hold.*

(1) *D has at least three black regions.*

(2) *Suppose D has precisely three black regions. Then there is a white region R_w, such that R_w is a bigon and the black regions adjacent to R_w are distinct (to be precise, the black regions that contain one of the two edges of R_w are distinct).*

(3) *Suppose D has precisely four black regions. Then there is a white region R_w, such that either (a) R_w is a bigon and the black regions adjacent to R_w are distinct, or (b) R_w is a 3-gon and the black regions adjacent to R_w are all distinct.*

Parallel statements also hold when black and white are interchanged.

Proof. Let $\mathcal{G}$ be the plane graph whose vertices are the black regions and whose edges correspond to the crossings. Observe that $\mathcal{G}$ is connected and has no loop edge nor a cut edge, because the diagram D is connected and prime.

(1) By using the above observation, we see that D has at least two black regions. If D has only two black regions, then L is the $(2, \pm n)$-torus link, where n is the number of the edges of $\mathcal{G}$, a contradiction. Hence D has at least three black regions.

(2) Suppose D has precisely three black regions. Then, by using the observation above, we see that $\mathcal{G}$ has a 3-cycle. If $\mathcal{G}$ is equal to the 3-cycle then L is the $(2, \pm 3)$-torus knot, a contradiction. Hence, there is an additional edge and so $\mathcal{G}$ has multiple edges. Then we see that the white region, R_w, determined by an innermost pair of multiple edges satisfies the desired condition (see Figure 2.12(a)).

(3) Suppose D has precisely four black regions. Then, as in (2), we see that $\mathcal{G}$ has a 4-cycle. Since L is hyperbolic, $\mathcal{G}$ is strictly bigger than the 4-cycle. Thus we see that there is a complementary region of $\mathcal{G}$ that is either a bigon or a triangle. Then the white region, R_w, determined by a complementary bigon or triangle satisfies the desired condition (a) or (b), accordingly (see Figure 2.12 (b,c)). □

2.9 Proof of Theorem 2.2.1 and 2.2.2

In this section, we first prove Theorem 2.2.2 and then prove Theorem 2.2.1.

Proof of Theorem 2.2.2. Let L, D, $\{\mu_1, \mu_2\}$ and γ be as in the setting of the theorem, and let $\{p_1, p_2\}$ be the pair of parabolic fixed points corresponding to $\{\mu_1, \mu_2\}$ (cf. Lemma 2.4.9(1)). We regard γ living in the non-positively curved cubed complex $\mathcal{M} \subset \mathcal{X}$. Then there is a lift $\tilde{\gamma}$ of γ in the universal cover $\tilde{\mathcal{M}} \subset \tilde{\mathcal{X}}$ which joins the peripheral planes H_{p_1} and H_{p_2} centered at p_1 and p_2, respectively (cf. Lemma 2.4.9(2)). We may assume $\tilde{\gamma}$ satisfies the following conditions.

(A1) $\tilde{\gamma}$ is an arc properly embedded in $\tilde{\mathcal{M}} \subset \tilde{\mathcal{X}}$ that is disjoint from $\tilde{\mathcal{C}} = \tilde{\mathcal{S}}_b \cap \tilde{\mathcal{S}}_w$ and transversal to $\tilde{\mathcal{S}}_{bw} = \tilde{\mathcal{S}}_b \cup \tilde{\mathcal{S}}_w$. Moreover, for $i = 1, 2$, the endpoint $x_i := \partial\tilde{\gamma} \cap H_{p_i}$ is disjoint from the family of lines $\tilde{\mathcal{S}}_{bw} \cap H_{p_i}$ (see Figure 2.2(a)).

(A2) The cardinality $\iota(\tilde{\gamma})$ of $\tilde{\gamma} \cap \tilde{\mathcal{S}}_{bw} = \tilde{\gamma} \cap (\tilde{\mathcal{S}}_{bw} \setminus \tilde{\mathcal{C}})$ is minimal among all arcs properly embedded in $\tilde{\mathcal{M}}$ joining the boundary components H_{p_1} and H_{p_2} of $\tilde{\mathcal{M}}$ and satisfying the condition (A1).

We orient $\tilde{\gamma}$ so that $x_1 \in H_{p_1}$ and $x_2 \in H_{p_2}$ are the initial point and the terminal point, respectively.

In the remainder of the paper, we use the following terminology. For a connected topological space Y and its connected subspaces Y_1, Y_2 and Z, we say that Z *separates* Y_1 and Y_2 (in Y), if Y_1 and Y_2 are contained in distinct components of $Y \setminus Z$. We say that Z *weakly separates* Y_1 and Y_2 (in Y), if Y_1 and Y_2 are contained in the closures of distinct components of $Y \setminus Z$.

Case I. $\iota(\tilde{\gamma}) > 0$. Throughout the treatment of this case, geodesics are those with respect to the CAT(0) metric of the cubed complex $\tilde{\mathcal{X}}$.

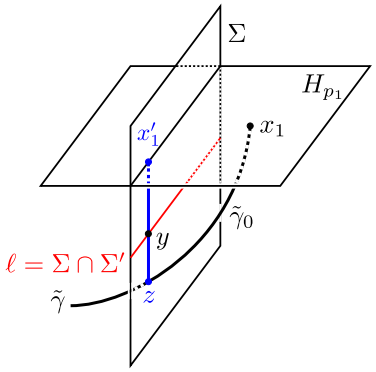

Figure 2.13: If a checkerboard hyperplane $\Sigma' \neq \Sigma$ intersects $[x_1', z]$, then it separates H_{p_1} and z, and hence intersects $\tilde{\gamma}_0$.

Lemma 2.9.1. *Any checkerboard hyperplane intersects $\tilde{\gamma}$ in at most one point.*

Proof. Assume that there is a checkerboard hyperplane Σ which intersects $\tilde{\gamma}$ in more than one points. Pick two successive intersection points z_1 and z_2 of $\tilde{\gamma}$ with Σ, and let $\tilde{\gamma}_0$ be the subarc of $\tilde{\gamma}$ bounded by z_1 and z_2. Since Σ is convex (Proposition 2.6.4), the geodesic segment $[z_1, z_2]$ is contained in Σ.

Claim 2.9.2. *If a checkerboard hyperplane Σ' different from Σ intersects $[z_1, z_2]$, then (i) $\Sigma' \cap [z_1, z_2]$ consists of a single transversal intersection point in (z_1, z_2) and (ii) $\Sigma' \cap \operatorname{int} \tilde{\gamma}_0 \neq \emptyset$.*

Proof. Let $\Sigma' \neq \Sigma$ be a checkerboard hyperplane which intersects $[z_1, z_2]$. Then $\ell := \Sigma \cap \Sigma' \supset [z_1, z_2] \cap \Sigma' \neq \emptyset$, and so ℓ is a geodesic line (cf. Proposition 2.6.6(1)) which intersects $[z_1, z_2]$. Since $z_1, z_2 \notin \ell$ by the condition (A1), $\Sigma' \cap [z_1, z_2] = \ell \cap [z_1, z_2]$ is a singleton $\{y\}$ for some $y \in (z_1, z_2)$ by Corollary 2.6.7(1). By Corollary 2.6.7(2), the two components of $[z_1, z_2] \setminus \{y\}$ are contained in distinct components of $\Sigma \setminus \ell$. Hence the condition (i) holds. This also implies that Σ' separates the endpoints z_1 and z_2 of $\tilde{\gamma}_0$. Hence (ii) also holds. □

Let $\tilde{\gamma}'$ be an arc obtained from $\tilde{\gamma}$ by replacing $\tilde{\gamma}_0$ with $[z_1, z_2]$ and then pushing (a neighborhood in the resulting arc of) $[z_1, z_2]$ off Σ, by using a regular neighborhood of Σ. Then $\tilde{\gamma}'$ is properly homotopic to $\tilde{\gamma}$, and we may assume $\tilde{\gamma}'$ satisfies the condition (A1). Moreover, Claim 2.9.2 implies that $\iota(\tilde{\gamma}') \leq \iota(\tilde{\gamma}) - 2$, a contradiction. □

We now prove a key lemma for the treatment of Case 1.

Lemma 2.9.3. *Any checkerboard hyperplane which intersects $\tilde{\gamma}$ separates H_{p_1} and H_{p_2} in $\tilde{\mathcal{X}}$.*

Proof. Let Σ be a checkerboard hyperplane which intersects $\tilde{\gamma}$. By Lemma 2.9.1 and the condition (A1), $\Sigma \cap \tilde{\gamma}$ consists of a single transversal intersection point

$z \in \operatorname{int}\tilde{\gamma}$. Thus we have only to show that Σ is disjoint from H_{p_1} and H_{p_2}. Suppose to the contrary that Σ intersects one of H_{p_1} and H_{p_2}, say, H_{p_1} (see Figure 2.13). Let $\tilde{\gamma}_0$ be the subarc of $\tilde{\gamma}$ bounded by the initial point $x_1 \in H_{p_1}$ of $\tilde{\gamma}$ and the intersection point $z \in \Sigma \cap \tilde{\gamma}$. Let $x_1' \in \Sigma \cap H_{p_1}$ be the projection, in the CAT(0) space Σ, of z to the geodesic line $\Sigma \cap H_{p_1}$. Since Σ intersects H_{p_1} orthogonally (Proposition 2.6.6(2)), we see that the geodesic segment $[x_1', z]$ intersects H_{p_1} orthogonally. Thus x_1' is the projection, in the CAT(0) space $\tilde{\mathcal{X}}$, of z to H_{p_1} by Lemma 2.5.3.

Claim 2.9.4. *If a checkerboard hyperplane Σ' different from Σ intersects $[x_1', z]$, then (i) $\Sigma' \cap [x_1', z]$ consists of a single transversal intersection point in (x_1', z) and (ii) $\Sigma' \cap \operatorname{int}\tilde{\gamma}_0 \neq \emptyset$.*

Proof. Let $\Sigma' \neq \Sigma$ be a checkerboard hyperplane which intersects $[x_1', z]$. Then, as in the proof of Claim 2.9.2, $\ell := \Sigma \cap \Sigma'$ is a geodesic line which intersects $[x_1', z]$. Since $z \notin \ell \cap \tilde{\gamma}$ by the condition (A1), $\ell \cap [x_1', z]$ is a singleton $\{y\}$ for some $y \in [x_1', z)$ by Corollary 2.6.7(1). If $y = x_1'$, then $\{x_1'\} = H_{p_1} \cap \Sigma \cap \Sigma'$ and so $[x_1', z] \subset \pi_{H_{p_1}}^{-1}(x_1') = \ell$ by Corollary 2.6.7(3), a contradiction to the fact that $z \notin \ell \cap \tilde{\gamma}$. Thus $\ell \cap [x_1', z]$ is a singleton $\{y\}$ for some $y \in (x_1', z)$. So, by Corollary 2.6.7(2), we obtain the conclusion (i). This also implies that x_1' and z belong to distinct components of $\Sigma \setminus \ell$, and hence Σ' separates $x_1' \in H_{p_1}$ and z. Moreover, Σ' is disjoint from H_{p_1} as shown below. Suppose to the contrary that $\Sigma' \cap H_{p_1} \neq \emptyset$. Then Σ' intersects H_{p_1} orthogonally (Proposition 2.6.6(2)), and we see by the argument preceding Claim 2.9.4 that the projection, y_1, of y, in the CAT(0) space Σ', to $\Sigma' \cap H_{p_1}$ is equal to the projection of y in the CAT(0) space $\tilde{\mathcal{X}}$ to H_{p_1}, which is equal to x_1'. Hence $x_1' = y_1$ belongs to Σ', and therefore $x_1' \in \Sigma' \cap \Sigma = \ell$, a contradiction to the fact that $[x_1', z] \cap \Sigma' = \{y\} \subset (x_1', z)$. Hence Σ' is disjoint from H_{p_1} as desired. Since Σ' separates $x_1' \in H_{p_1}$ and z, this implies that Σ' separates H_{p_1} and z. Since $\tilde{\gamma}_0$ joins the point $x_1 \in H_{p_1}$ and z, $\tilde{\gamma}_0$ must intersect Σ'. Thus the conclusion (ii) holds. □

Let $\tilde{\gamma}'$ be an arc obtained from $\tilde{\gamma}$ by replacing $\tilde{\gamma}_0$ with $[x_1', z]$ and then pushing (a neighborhood in the resulting arc of) $[x_1', z]$ off Σ. Then $\tilde{\gamma}'$ is properly homotopic to $\tilde{\gamma}$, and we may assume $\tilde{\gamma}'$ satisfies the condition (A1). Moreover, Claim 2.9.4 implies that $\iota(\tilde{\gamma}') \leq \iota(\tilde{\gamma}) - 1$, a contradiction. □

Let y_1 be the first intersection point of $\tilde{\gamma}$ with $\tilde{\mathcal{S}}_{bw}$, and $\tilde{\mathcal{P}}_1$ the checkerboard ideal polyhedron that contains the subarc of $\tilde{\gamma}$ bounded by x_1 and y_1. Similarly, let y_2 be the last intersection point of $\tilde{\gamma}$ with $\tilde{\mathcal{S}}_{bw}$, and $\tilde{\mathcal{P}}_2$ the checkerboard ideal polyhedron that contains the subarc of $\tilde{\gamma}$ bounded by x_2 and y_2 (see Figure 2.14(a)). (If $\iota(\tilde{\gamma}) = 1$ then $y_1 = y_2$ but $\tilde{\mathcal{P}}_1 \neq \tilde{\mathcal{P}}_2$.) For $i = 1, 2$, recall the isomorphism $\hat{\mathcal{P}}_i \cong (B^3, D)$, and let c_i be the vertex of D corresponding to the ideal vertex p_i of $\hat{\mathcal{P}}_i$, and let R_i be the region of D such that $\Sigma_{R_i} = \Sigma_{R_i}(\tilde{\mathcal{P}}_i)$ contains y_i (Definition and Notation 2.7.3). Note that the region R_i does not contain the vertex c_i by Lemma 2.9.3.

For simplicity, we assume that R_1 is a black region. For $i = 1, 2$, let $R_i^{\pm}$ be the black regions of D that contain the vertex c_i, and consider the disks

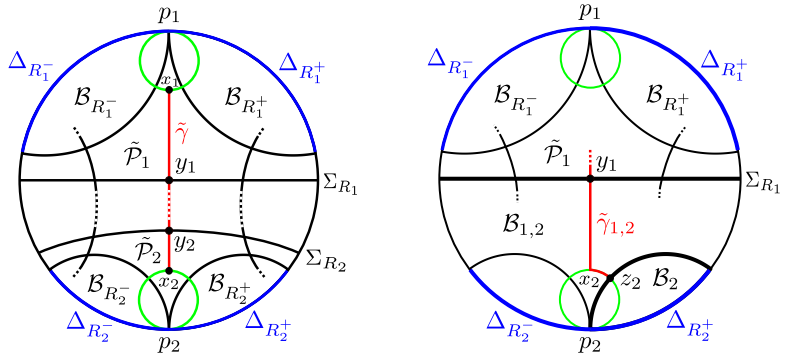

Figure 2.14: (a) The checkerboard hyperplane $\Sigma_{R_1}(\tilde{\mathcal{P}}_1)$ separates $\mathcal{B}_{R_1^-} \cup \mathcal{B}_{R_1^+}$ and $\mathcal{B}_{R_2^-} \cup \mathcal{B}_{R_2^+}$. Note that $\mathcal{B}_{R_1} = \mathcal{B}_{R_1}(\tilde{\mathcal{P}}_1)$ is the region in $\tilde{\mathcal{X}} = \mathbb{H}^3$ "below" Σ_{R_1}. (b) The arc $\tilde{\gamma}_{1,2}$, that is the union of the arc $\delta \subset H_{p_2}$ and the subarc of $\tilde{\gamma}$ bounded by y_1 and x_2, intersects Σ_{R_1} and $\Sigma_{R_2^\epsilon}$ only at the endpoints. Here $\epsilon = +$.

$\Delta_{R_i^\pm} := \Delta_{R_i^\pm}(\tilde{\mathcal{P}}_i)$ in $\hat{\mathbb{C}}$ (see Notation 2.8.1 and Figure 2.8(a)). Then $\mathrm{BF}(p_i) := \{\Delta_{R_i^-}, \Delta_{R_i^+}\}$ forms a butterfly at p_i by Lemma 2.8.5 (after replacing $R_i^\pm$ with $R_i^\mp$ if necessary). Set $\Sigma_{R_i^\pm} := \Sigma_{R_i^\pm}(\tilde{\mathcal{P}}_i)$ and $\mathcal{B}_{R_i^\pm} := \mathcal{B}_{R_i^\pm}(\tilde{\mathcal{P}}_i)$ (see Figure 2.14(a)). Then we have the following lemma.

Lemma 2.9.5. (1) $\mathcal{B}_{R_2^-} \cup \mathcal{B}_{R_2^+} \subset \mathcal{B}_{R_1}$, *where* $\mathcal{B}_{R_1} = \mathcal{B}_{R_1}(\tilde{\mathcal{P}}_i)$

(2) $\mathcal{B}_{R_1^-} \cup \mathcal{B}_{R_1^+}$ *and* $\mathcal{B}_{R_2^-} \cup \mathcal{B}_{R_2^+}$ *are disjoint.*

(3) $\Delta_{R_2^-} \cup \Delta_{R_2^+} \subset \Delta_{R_1}$, *where* $\Delta_{R_1} = \Delta_{R_1}(\tilde{\mathcal{P}}_1)$.

(4) $|\mathrm{BF}(p_1)| = \Delta_{R_1^-} \cup \Delta_{R_1^+}$ *and* $|\mathrm{BF}(p_2)| = \Delta_{R_2^-} \cup \Delta_{R_2^+}$ *have disjoint interiors.*

Proof. (1) For each $\epsilon \in \{-, +\}$, Σ_{R_1} is distinct from $\Sigma_{R_2^\epsilon}$, because $\Sigma_{R_2^\epsilon} \cap H_{p_2} \neq \emptyset$ whereas $\Sigma_{R_1} \cap H_{p_2} = \emptyset$ by Lemma 2.9.3. This implies that Σ_{R_1} is disjoint from $\Sigma_{R_2^\epsilon}$ (because they are distinct components of $p_u^{-1}(\mathcal{S}_b)$). By Lemma 2.6.8, the disjoint union $\Sigma_{R_1} \sqcup \Sigma_{R_2^\epsilon}$ divides $\tilde{\mathcal{X}}$ into three closed convex subspaces $\mathcal{B}_1$, $\mathcal{B}_{1,2}$ and $\mathcal{B}_2$, such that $\mathcal{B}_1 \cap \mathcal{B}_{1,2} = \Sigma_{R_1}$, $\mathcal{B}_{1,2} \cap \mathcal{B}_2 = \Sigma_{R_2^\epsilon}$ and $\mathcal{B}_1 \cap \mathcal{B}_2 = \emptyset$. Let δ be an arc in the square $H_{p_2} \cap \tilde{\mathcal{P}}_2$ which joins x_2 with a point z_2 in $H_{p_2} \cap \Sigma_{R_2^\epsilon}$ (cf. Figure 2.2(a)), and let $\tilde{\gamma}_{1,2}$ be the union of δ and the subarc of $\tilde{\gamma}$ bounded by y_1 and x_2 (see Figure 2.14(b), where ϵ is assumed to be $+$). Then $\tilde{\gamma}_{1,2}$ is an arc in $\tilde{\mathcal{X}}$ joining y_1 and z_2, such that $\tilde{\gamma}_{1,2} \cap \Sigma_{R_1} = \{y_1\}$ and $\tilde{\gamma}_{1,2} \cap \Sigma_{R_2^\epsilon} = \{z_2\}$. Hence $\tilde{\gamma}_{1,2}$ is contained in $\mathcal{B}_{1,2}$. This implies $\tilde{\mathcal{P}}_2 \subset \mathcal{B}_{1,2}$, because $\operatorname{int} \tilde{\mathcal{P}}_2 \cap (\Sigma_{R_1} \cup \Sigma_{R_2^\epsilon}) = \emptyset$ and $\operatorname{int} \tilde{\mathcal{P}}_2 \cap \operatorname{int} \tilde{\gamma}_{1,2} \neq \emptyset$. Hence we have $\mathcal{B}_2 = \mathcal{B}_{R_2^\epsilon}$. On the other hand, we have $\tilde{\mathcal{P}}_1 \subset \mathcal{B}_1$, because $\tilde{\gamma}_{1,2} \subset \mathcal{B}_{1,2}$ and $\tilde{\gamma}$ intersects Σ_{R_1} transversely at y_1;

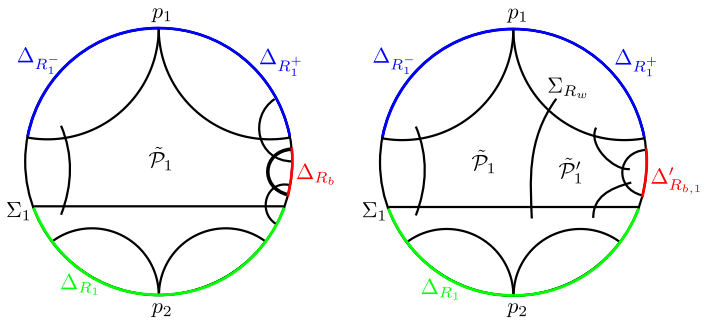

Figure 2.15: (a) If D has more than 3 black regions, then, for a black region R_b distinct from R_1 and $R_1^{\pm}$, the open disk $\operatorname{int}\Delta_{R_b}$ is disjoint from $|\mathrm{BF}(p_1)| \cup |\mathrm{BF}(p_2)|$. (b) If D has precisely 3 black regions, then, for the black region $R_{b,1}$ that is not adjacent to the white bigon R_w, the open disk $\operatorname{int}\Delta'_{R_{b,1}}$, where $\Delta'_{R_{b,1}} = \Delta_{R_{b,1}}(\tilde{\mathcal{P}}_1')$, is disjoint from $|\mathrm{BF}(p_1)| \cup |\mathrm{BF}(p_2)|$.

so $\mathcal{B}_1 = \mathcal{B}^{\epsilon}_{R_1} := \mathcal{B}^{\epsilon}_{R_1}(\tilde{\mathcal{P}}_1)$. Hence $\mathcal{B}^{\epsilon}_{R_1} \cap \mathcal{B}_{R_2^{\epsilon}} = \mathcal{B}_1 \cap \mathcal{B}_2 = \emptyset$, and therefore $\mathcal{B}_{R_2^{\epsilon}} \subset \mathcal{B}_{R_1}$.

(2) Since the black region R_1 does not contain c_1, it is distinct from the black regions $R_1^{\pm}$. Hence $\mathcal{B}_{R_1^{\pm}}$ are disjoint from $\mathcal{B}_{R_1}$ by Proposition 2.7.4. Since $\mathcal{B}_{R_2^-} \cup \mathcal{B}_{R_2^+} \subset \mathcal{B}_{R_1}$ by (1), this implies that $\mathcal{B}_{R_1^{\pm}}$ are disjoint from $\mathcal{B}_{R_2^-} \cup \mathcal{B}_{R_2^+}$.

(3) By (1), we have $\Delta_{R_2^-} \cup \Delta_{R_2^+} = (\bar{\mathcal{B}}_{R_2^-} \cap \hat{\mathbb{C}}) \cup (\bar{\mathcal{B}}_{R_2^+} \cap \hat{\mathbb{C}}) \subset \bar{\mathcal{B}}_{R_1} \cap \hat{\mathbb{C}} = \Delta_{R_1}$.

(4) This follows from (2) and Lemma 2.8.2. □

Lemma 2.9.6. *The open set $O := \hat{\mathbb{C}} \setminus (|\mathrm{BF}(p_1)| \cup |\mathrm{BF}(p_2)|)$ is non-empty.*

Proof. Suppose first that D has more than 3 black regions. Pick a black region R_b of D different from R_1 and $R_1^{\pm}$. Then the interior of the disk $\Delta_{R_b} := \Delta_{R_b}(\tilde{\mathcal{P}}_1)$ is disjoint from the disks Δ_{R_1} and $\Delta_{R_1^{\pm}}$ by Proposition 2.8.3. Since $\Delta_{R_2^-} \cup \Delta_{R_2^+} \subset \Delta_{R_1}$ by Lemma 2.9.5(3), this implies that the open disk $\operatorname{int}\Delta_{R_b}$ is disjoint from $\Delta_{R_1} \cup \Delta_{R_1^-} \cup \Delta_{R_1^+} \supset \Delta_{R_1^-} \cup \Delta_{R_1^+} \cup \Delta_{R_2^-} \cup \Delta_{R_2^+} = |\mathrm{BF}(p_1)| \cup |\mathrm{BF}(p_2)|$ (see Figure 2.15(a)). Hence $\operatorname{int}\Delta_{R_b} \subset O$ and therefore O is non-empty, as desired.

Suppose next that D has at most 3 black regions. Then, by Lemma 2.8.6(1), (2), D has precisely three black regions, $\{R_{b,j}\}_{1 \le j \le 3} = \{R_1, R_1^-, R_1^+\}$ and a white bigon R_w. We may assume $R_{b,1}$ is not adjacent to R_w. Let $\tilde{\mathcal{P}}_1'$ be the checkerboard ideal polyhedron such that $\tilde{\mathcal{P}}_1 \cap \tilde{\mathcal{P}}_1'$ is the common face corresponding to R_w. Set $\Delta_{R_{b,j}} := \Delta_{R_{b,j}}(\tilde{\mathcal{P}}_1)$ and $\Delta'_{R_{b,j}} := \Delta_{R_{b,j}}(\tilde{\mathcal{P}}_1')$ $(1 \le j \le 3)$. (See Figure 2.15(b).)

Claim 2.9.7. *The interior of the disk $\Delta'_{R_{b,1}}$ is disjoint from $\cup_{j=1}^3 \Delta_{R_{b,j}} = \Delta_{R_1} \cup \Delta_{R_1^-} \cup \Delta_{R_1^+}$.*

Proof. By Lemma 2.7.5 and by Notation 2.8.1(3), we see $\Delta'_{R_{b,2}} = \Delta_{R_{b,3}}$ and $\Delta'_{R_{b,3}} = \Delta_{R_{b,2}}$. Hence, by Proposition 2.8.3, $\operatorname{int}\Delta'_{R_{b,1}}$ is disjoint from $\Delta'_{R_{b,3}} \cup \Delta'_{R_{b,2}} = \Delta_{R_{b,2}} \cup \Delta_{R_{b,3}}$. Moreover, $\operatorname{int}\Delta'_{R_{b,1}}$ is also disjoint from $\Delta_{R_{b,1}}$, as explained below. Since $R_{b,1}$ and R_w are not adjacent, Proposition 2.7.4 implies that $\mathcal{B}_{R_{b,1}}(\tilde{\mathcal{P}}_1) \cap \mathcal{B}_{R_w}(\tilde{\mathcal{P}}_1) = \emptyset$. Hence $\mathcal{B}_{R_{b,1}}(\tilde{\mathcal{P}}_1) \subset \tilde{\mathcal{X}} \setminus \mathcal{B}_{R_w}(\tilde{\mathcal{P}}_1) = \operatorname{int}\mathcal{B}_{R_w}(\tilde{\mathcal{P}}'_1)$. Similarly, $\mathcal{B}_{R_{b,1}}(\tilde{\mathcal{P}}'_1) \subset \operatorname{int}\mathcal{B}_{R_w}(\tilde{\mathcal{P}}_1)$. Since $\operatorname{int}\mathcal{B}_{R_w}(\tilde{\mathcal{P}}_1)$ and $\operatorname{int}\mathcal{B}_{R_w}(\tilde{\mathcal{P}}'_1) = \operatorname{int}\mathcal{B}^{\mathfrak{c}}_{R_w}(\tilde{\mathcal{P}}_1)$ are disjoint, $\mathcal{B}_{R_{b,1}}(\tilde{\mathcal{P}}_1)$ and $\mathcal{B}_{R_{b,1}}(\tilde{\mathcal{P}}'_1)$ are disjoint. By Lemma 2.8.2, this implies that $\Delta_{R_{b,1}}$ and $\Delta'_{R_{b,1}}$ have disjoint interiors, and hence $\operatorname{int}\Delta'_{R_{b,1}}$ is disjoint from $\Delta_{R_{b,1}}$. □

Since $\Delta_{R_2^-} \cup \Delta_{R_2^+} \subset \Delta_{R_1}$ by Lemma 2.9.5(3), Claim 2.9.7 implies that the open disk $\operatorname{int}\Delta'_{R_{b,1}}$ is disjoint from $\Delta_{R_1^-} \cup \Delta_{R_1^+} \cup \Delta_{R_2^-} \cup \Delta_{R_2^+} = |\mathrm{BF}(p_1)| \cup |\mathrm{BF}(p_2)|$. Hence $\operatorname{int}\Delta'_{R_{b,1}} \subset O$ and therefore O is non-empty, as desired. □

Thus we have proved that the pair of butterflies $\mathrm{BF}(p_1)$ and $\mathrm{BF}(p_2)$ satisfies the conditions in Proposition 2.4.11. Hence $\{\mu_1, \mu_2\}$ generates a rank 2 free Kleinian group which is geometrically finite. This completes the proof of Theorem 2.2.2 in Case I where $\iota(\tilde{\gamma}) > 0$.

Case II. $\iota(\tilde{\gamma}) = 0$. In this case, the proper arc $\tilde{\gamma} \subset \tilde{\mathcal{M}}$ is contained in $\tilde{\mathcal{P}} \cap \tilde{\mathcal{M}}$ for some ideal checkerboard polyhedron $\tilde{\mathcal{P}}$. Recall the isomorphism $\hat{\varphi} : (B^3, D) \to \hat{\mathcal{P}}$, where $\hat{\mathcal{P}}$ is the closure of $\tilde{\mathcal{P}}$ in $\bar{\mathbb{H}}^3$ (Section 2.8). We identify $\hat{\mathcal{P}}$ with (B^3, D) through the isomorphism. Let c_i be the vertex of D corresponding to the ideal vertex p_i of $\hat{\mathcal{P}}$ $(i = 1, 2)$. Then the equivalence class of the meridian pair $\{\mu_1, \mu_2\}$ is determined by the pair $\{c_1, c_2\}$. Let $\hat{\gamma}$ be an arc in ∂B^3 joining c_1 and c_2, such that $\hat{\gamma}$ intersects the vertex set of D only at their endpoints and that $\operatorname{int}\hat{\gamma}$ is transversal to D. Then the proper homotopy class of $\tilde{\gamma}$ is represented by $\hat{\gamma}$. We assume that the cardinality $\omega(\hat{\gamma})$ of $\operatorname{int}\hat{\gamma} \cap D$ is minimized.

Subcase II-1. $\omega(\hat{\gamma}) > 0$. For $i = 1, 2$, let R_i^- and R_i^+ be the black regions that contain the vertex c_i. Then $\{\Delta_{R_i^-}, \Delta_{R_i^+}\}$ forms a butterfly $\mathrm{BF}(p_i)$ at p_i by Lemma 2.8.5 (see Figure 2.16).

Claim 2.9.8. *The four black regions R_1^-, R_1^+, R_2^- and R_2^+ are distinct.*

Proof. Suppose to the contrary that there is an overlap among the four regions. Since $R_i^- \neq R_i^+$ for $i = 1, 2$, we have $R_1^{\epsilon_1} = R_2^{\epsilon_2}$ for some $\epsilon_1, \epsilon_2 \in \{-, +\}$. Then the vertices c_1 and c_2 are contained in the single region $R_1^{\epsilon_1} = R_2^{\epsilon_2}$. Thus the two vertices are joined by an arc in the region, a contradiction to the assumption $\omega(\hat{\gamma}) > 0$. □

By Claim 2.9.8 and Proposition 2.8.3, the butterflies $\mathrm{BF}(p_1)$ and $\mathrm{BF}(p_2)$ have disjoint interiors. Moreover, the following lemma holds.

Lemma 2.9.9. *The open set $O := \hat{\mathbb{C}} \setminus (|\mathrm{BF}(p_1)| \cup |\mathrm{BF}(p_2)|)$ is non-empty.*

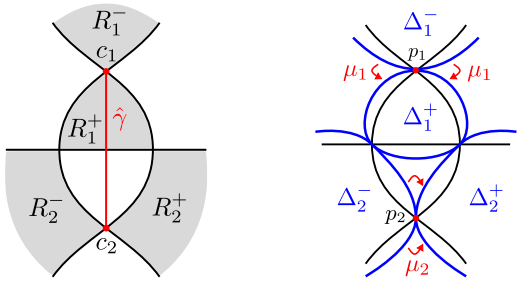

Figure 2.16: The butterflies $\mathrm{BF}(p_1)$ and $\mathrm{BF}(p_2)$ and the actions of the meridians μ_1 and μ_2, in the case $\omega(\hat{\gamma}) > 0$. Here, we employ the model picture of the limit circles described in Remark 2.8.4 and Figure 2.10.

Proof. The proof of this lemma is parallel to that of Lemma 2.9.6. If D has more than four black regions, then a black region R_b different from $R_1^\pm$ and $R_2^\pm$ gives a non-empty open disk $\operatorname{int}\Delta_{R_b}$ disjoint from $|\mathrm{BF}(p_1)| \cup |\mathrm{BF}(p_2)|$ by Proposition 2.8.3. So, we may assume D has precisely four black regions. Then, by Lemma 2.8.6(3), there is a white region R_w which is either a bigon or a 3-gon. In either case, there is a black region, say $R_{b,1}$, that is not adjacent to R_w. Let $\tilde{\mathcal{P}}_1'$ be the checkerboard ideal polyhedron such that $\tilde{\mathcal{P}}_1 \cap \tilde{\mathcal{P}}_1'$ is the common face corresponding to R_w. Then, as in the proof of Claim 2.9.7, we see that the open disk $\operatorname{int}\Delta_{R_{b,1}}(\tilde{\mathcal{P}}_1')$ is disjoint from $|\mathrm{BF}(p_1)| \cup |\mathrm{BF}(p_2)|$. □

Thus the pair of butterflies $\mathrm{BF}(p_1)$ and $\mathrm{BF}(p_2)$ satisfies the conditions in Proposition 2.4.11. Hence $\{\mu_1, \mu_2\}$ generates a rank 2 free Kleinian group which is geometrically finite. This completes the proof of Theorem 2.2.2 in the case where $\iota(\tilde{\gamma}) = 0$ and $\omega(\hat{\gamma}) > 0$.

Subcase II-2. $\omega(\hat{\gamma}) = 0$. In this case, there is a region R of D that contains $\hat{\gamma}$ and the vertices c_1 and c_2. Recall that γ is not properly homotopic to a crossing arc by the assumption of the theorem. This implies that $\hat{\gamma}$ is not homotopic relative to the endpoints to an edge of R (i.e., the vertices c_1 and c_2 are not adjacent in ∂R), because, for any edge e of D, the composition $p_u \circ \varphi : \mathrm{P}(D) \to p_u(\tilde{\mathcal{P}}) \subset X$ maps the ideal edge $\check{e}$ to an open crossing arc (cf. Proposition 2.7.2(3) and Figure 2.7).

For simplicity, assume that R is a white region. For $i = 1, 2$, let $R_i^\pm$ be the black regions that contain the crossing c_i. Then $\{\Delta_{R_i^-}, \Delta_{R_i^+}\}$ forms a butterfly $\mathrm{BF}(p_i)$ at p_i by Lemma 2.8.5 (see Figure 2.17).

Claim 2.9.10. *The four black regions R_1^-, R_1^+, R_2^- and R_2^+ are distinct.*

Proof. Suppose to the contrary that there is an overlap among the 4 regions. Then as in the proof of Claim 2.9.8, we have $R_1^{\epsilon_1} = R_2^{\epsilon_2}$ for some $\epsilon_1, \epsilon_2 \in \{-, +\}$. Since c_1 and c_2 are not adjacent in ∂R, the edges $e_i := R \cap R_i^{\epsilon_i}$ $(i = 1, 2)$ are distinct. Thus we can find a simple loop C in the union of the white region R

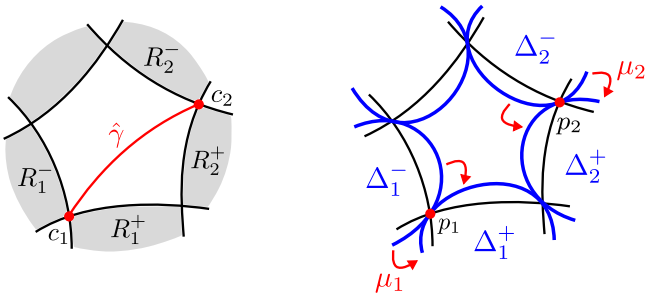

Figure 2.17: The butterflies $\mathrm{BF}(p_1)$ and $\mathrm{BF}(p_2)$ and the actions of the meridians μ_1 and μ_2, in the case $\omega(\hat{\gamma}) = 0$ and γ is not a crossing arc. Here, we employ the model picture of the limit circles described in Remark 2.8.4 and Figure 2.10.

and the black region $R_1^{\epsilon_1} = R_2^{\epsilon_2}$, which intersects D transversely in precisely two points, one in $\operatorname{int} e_1$ and the other in $\operatorname{int} e_2$. Since $e_1 \neq e_2$, both disks bounded by C contains a vertex of D. This contradicts the primeness of the diagram D. □

The proof of Lemma 2.9.9 works in the current setting, and so, we see that the open set $O = \hat{\mathbb{C}} \setminus (|\mathrm{BF}(p_1)| \cup |\mathrm{BF}(p_2)|)$ is non-empty. Thus the pair of the butterflies $\mathrm{BF}(p_1)$ and $\mathrm{BF}(p_2)$ satisfies the conditions in Proposition 2.4.11. Hence $\{\mu_1, \mu_2\}$ generates a rank 2 free Kleinian group which is geometrically finite.

This completes the proof of Theorem 2.2.2. □

Proof of Theorem 2.2.1. Let $L \subset S^3$ be a hyperbolic 2-bridge link, γ an essential proper path in the link exterior M, $\{\mu_1, \mu_2\}$ a non-commuting meridian pair in the link group G represented by γ, and $\{p_1, p_2\}$ the corresponding pair of parabolic fixed points. Assume that γ is not properly homotopic to the upper or lower tunnel of L. We show that $\{\mu_1, \mu_2\}$ generates a rank 2 free Kleinian group which is geometrically finite.

If necessary by taking the mirror image of L, we may assume that L admits the prime alternating diagram D in Figure 2.18, where $(a_1, a_2, \ldots, a_n)$ is a sequence of positive integers with $n \geq 2$, $a_1 \geq 2$ and $a_n \geq 2$. D consists of n twist regions $A_1, A_2, \cdots, A_n$, where A_i consists of a_i right-hand or left-hand half-twists according to whether i is odd or even. By Theorem 2.2.2, we have only to treat the case where γ is a crossing arc with respect to the diagram D. Let A_i be the twist region that contains the crossing corresponding to the crossing arc γ. If $i = 1$ or n, then γ is isotopic to the upper or lower tunnel accordingly. So, $2 \leq i \leq n-1$.

Suppose i is odd. Apply the flype to D as illustrated in Figure 2.19, and let D' be the resulting prime alternating diagram. Then the image of the crossing arc γ by the flype is an arc γ' contained in a region R' of D', such that the corresponding arc $\hat{\gamma}'$ in the polyhedron (B^3, D') joins crossings c_1' and c_2' of R' which are not adjacent in $\partial R'$. Hence, we can apply the arguments in Subcase

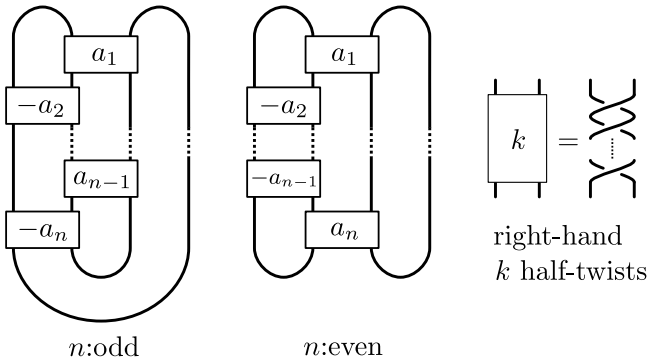

Figure 2.18: The standard prime alternating diagram D of a hyperbolic 2-bridge link L

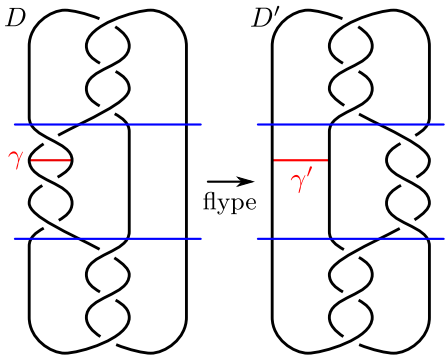

Figure 2.19: The flype maps the crossing arc γ in the diagram D to an arc which is not a crossing arc in the new diagram D'.

II-2 in the proof of Theorem 2.2.2 to show that $\{\mu_1, \mu_2\}$ generates a rank 2 free group which is geometrically finite.

Suppose i is even. Then we first modify D by an ambient isotopy in S^2 (which is not an ambient isotopy in $\mathbb{R}^2$) as in Figure 2.20, and then apply the flype as in Figure 2.20. Then we can again apply the arguments in Subcase II-2 in the proof of Theorem 2.2.2 and to obtain the same conclusion.

This completes the proof of Theorem 2.2.1. □

2.10 Rational links in the projective 3-space and the proof of Theorem 2.1.3

In this section, we first define the rational links in P^3 (Definition 2.10.2) and present their basic properties including classification and hyperbolization (Propo-

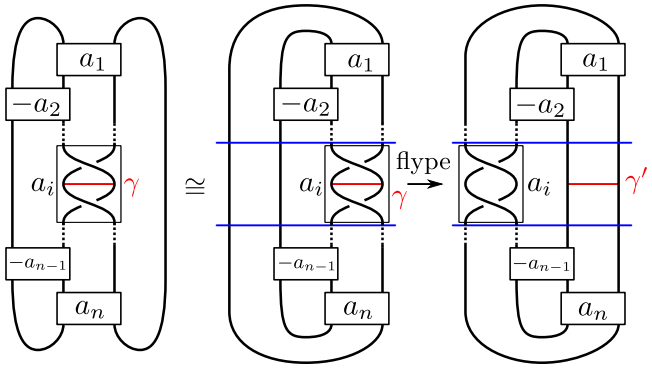

Figure 2.20: If i is even, then first modify D by an ambient isotopy in S^2 into the middle diagram and then apply the flype.

sitions 2.10.3 and 2.10.5). Then we give a detailed description of Theorem 2.1.3(3) in Remark 2.10.6, and prove the theorem.

We recall the definition of a rational tangle following [14, Chapter 18] and [9, Section 2]. Let $\boldsymbol{B}^3 := \{(x, y, z) \in \mathbb{R}^3 \mid x^2 + y^2 + z^2 \leq 2\}$ be the round 3-ball in $\mathbb{R}^3 \subset \hat{\mathbb{R}}^3 := \mathbb{R}^3 \cup \{\infty\}$, whose boundary contains the set P^0 consisting of the four marked points

$$\mathrm{SW} := (-1, -1, 0), \quad \mathrm{SE} := (1, -1, 0), \quad \mathrm{NE} := (1, 1, 0), \quad \mathrm{NW} := (-1, 1, 0).$$

For $r \in \hat{\mathbb{Q}} := \mathbb{Q} \cup \{\infty\}$, the *rational tangle of slope* r is the pair $(\boldsymbol{B}^3, t(r))$, where $t(r)$ is a pair of arcs properly embedded in $\boldsymbol{B}^3$ such that $t(r) \cap \partial \boldsymbol{B}^3 = \partial t(r) = P^0$ as depicted in Figure 2.21(b). Here the "pillowcase" in the figure is the quotient space $(\mathbb{R}^2, \mathbb{Z}^2)/\mathcal{J}$, where $\mathcal{J}$ is the group of isometries of the Euclidean plane $\mathbb{R}^2$ generated by the π-rotations around the points in $\mathbb{Z}^2$, and the pair of arcs on the pillowcase is the image of the lines in $\mathbb{R}^2$ of slope r passing through points in $\mathbb{Z}^2$. We can arrange $t(r)$ so that it is invariant by the π-rotations h_x, h_y and $h_z = h_x h_y$ about the x-, y- and z-axis, respectively.

The 2-*bridge link* $(S^3, K(r))$ *of slope* r is obtained by gluing (disjoint copies of) $(\boldsymbol{B}^3, t(r))$ and $(-\boldsymbol{B}^3, t(\infty))$ via the identity map on $\partial \boldsymbol{B}^3$. (Here $\boldsymbol{B}^3$ inherits the natural orientation of $\hat{\mathbb{R}}^3$.) Thus we may regard

$$K(r) = t(r) \cup \iota(t(\infty)) \subset \boldsymbol{B}^3 \cup \iota(\boldsymbol{B}^3) = \hat{\mathbb{R}}^3,$$

where ι is the inversion of $\hat{\mathbb{R}}^3$ in $\partial \boldsymbol{B}^3$. Let $\mathcal{D}$ be the *Farey tessellation*, that is, the tessellation of the upper half-space $\mathbb{H}^2$ by ideal triangles which are obtained from the ideal triangle with the ideal vertices $0, 1, \infty \in \hat{\mathbb{Q}}$ by repeated reflection in the edges. Let $\mathrm{Aut}(\mathcal{D})$ be the automorphism group of $\mathcal{D}$ and $\mathrm{Aut}^+(\mathcal{D})$ the orientation-preserving subgroup of $\mathrm{Aut}(\mathcal{D})$. The following proposition reformulates (i) the classification of 2-bridge links established by Schubert [46] and (ii) the hyperbolization of alternating link complements proved by

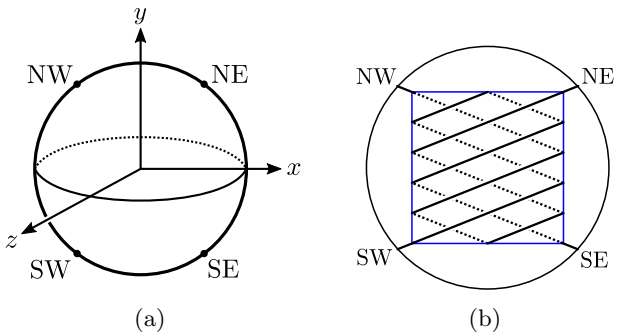

Figure 2.21: (a) The 3-ball $\boldsymbol{B}^3$ with the set P^0 of the four marked points. (b) The rational tangle $(\boldsymbol{B}^3, t(r))$ with $r = 2/5$. Note that the vertical axis is the y-axis, not the z-axis.

Menasco [32, Corollary 2] by using Thurston's uniformization theorem of Haken manifolds [51], applied to 2-bridge link complements.

Proposition 2.10.1. (1) *For two rational numbers $r, r' \in \hat{\mathbb{Q}}$, there is a homeomorphism $\psi : S^3 \to S^3$ such that $\psi(K(r)) = K(r')$ if and only if there is an element $\xi \in \mathrm{Aut}(\mathcal{D})$ that maps $\{r, \infty\}$ to $\{r', \infty\}$. Moreover, ψ can be chosen to be orientation-preserving if and only if either (i) ξ is orientation-preserving and $(\xi(r), \xi(\infty)) = (r', \infty)$ or (ii) ξ is orientation-reversing and $(\xi(r), \xi(\infty)) = (\infty, r')$.*

(2) *$K(r)$ is hyperbolic if and only if $d(\infty, r) \geq 3$, where d is the edge path distance in the 1-skeleton of $\mathcal{D}$.*

Now, we define the rational links in P^3 and state their basic properties.

Definition 2.10.2. For $r \in \hat{\mathbb{Q}}$, the *rational link of slope r in the projective 3-space* P^3 is the pair $(P^3, K_P(r)) := (\boldsymbol{B}^3, t(r))/\sim$, where $\sim$ identifies x and $-x$ for every $x \in \partial \boldsymbol{B}^3$. The inverse image $\tilde{K}_P(r)$ of $K_P(r)$ in the universal cover S^3 of P^3 is called the *covering link* of $K_P(r)$.

Proposition 2.10.3. *The covering link of a rational link $K_P(r)$ in P^3 is equivalent to the 2-bridge link $K(\tilde{r})$ with $\tilde{r} = \eta_r(r)$, where η_r is an element of $\mathrm{Aut}^+(\mathcal{D})$ such that $\eta_r(-r) = \infty$. (In other words, $\tilde{r}$ is characterized by the property that $(\tilde{r}, \infty) = (\eta_r(r), \eta_r(-r))$ for some $\eta_r \in \mathrm{Aut}^+(\mathcal{D})$.)*

Here, we assume that P^3 inherits the natural orientation of $\boldsymbol{B}^3 \subset \hat{\mathbb{R}}^3 \cong S^3$, and so the covering projection $S^3 \to P^3$ is orientation-preserving. Two links in an oriented 3-manifold are *equivalent* if there is an orientation-preserving homeomorphism of the ambient 3-manifold that maps one to the other.

Proof of Proposition 2.10.3. Identify $S^3 := \{(z_1, z_2) \in \mathbb{C}^2 \mid |z_1|^2 + |z_2|^2 = 1\}$ with the spherical join $S^1_1 * S^1_2$ of the circles $S^1_1 := S^3 \cap (\mathbb{C} \times 0)$ and $S^1_2 := S^3 \cap (0 \times \mathbb{C})$ (cf. [16, Definition I.5.13]). Then we can identify $\hat{\mathbb{R}}^3$ with S^3 so that the following conditions are satisfied (see Figure 2.22(a)).

1. The great circle $\partial \boldsymbol{B}^3 \cap \{y = 0\}$ is identified with S^1_1, and the compactified y-axis is identified with S^1_2. Moreover $\boldsymbol{B}^3$ is identified with the spherical join $S^1_1 * J_2$, where $J_2 := \{(0, z_2) \in S^1_2 \mid -\pi/2 \leq \arg(z_2) \leq \pi/2\}$.

2. The π-rotations h_x, h_y, h_z of $\hat{\mathbb{R}}^3$, respectively, are identified with the involutions on S^3 defined by

$$h_x(z_1, z_2) = (\bar{z}_1, \bar{z}_2), \quad h_y(z_1, z_2) = (-z_1, z_2), \quad h_z(z_1, z_2) = (-\bar{z}_1, \bar{z}_2).$$

3. Let f be the generator of the covering transformation group of the covering $S^3 \to P^3$, given by $f(z_1, z_2) = (-z_1, -z_2)$. Then f viewed on $\hat{\mathbb{R}}^3$ is the composition of the antipodal map $(x, y, z) \mapsto (-x, -y, -z)$ and the inversion ι in $\partial \boldsymbol{B}^3$.

Then the the covering link $\tilde{K}_P(r) \subset S^3$ of $K_P(r) \subset P^3$ is given by $\tilde{K}_P(r) = t(r) \cup f(t(r)) \subset \boldsymbol{B}^3 \cup f(\boldsymbol{B}^3) = S^3$, and it is invariant by the action of the subgroup $\langle h_x, h_y, f \rangle \cong (\mathbb{Z}/2\mathbb{Z})^3$ of $\mathrm{Isom}^+(S^3)$. Note that $f(t(r)) = fh_z(t(r))$, where fh_z, which is given by $fh_z(z_1, z_2) = (\bar{z}_1, -\bar{z}_2)$, is the π-rotation of $S^3 = S^1_1 * S^1_2$ whose axis is the spherical join $S^0_1 * iS^0_2$, where $S^0_1 = \{(\pm 1, 0)\}$ and $iS^0_2 = \{(0, \pm i)\}$. The axis of fh_z viewed in $\hat{\mathbb{R}}^3$ is the great circle $\partial \boldsymbol{B}^3 \cap \{z = 0\}$, which passes through the set P^0. Hence the action of fh_z on $(S^3, \tilde{K}_P(r))$ is conjugate to the involution illustrated in Figure 2.22(b), where $\tilde{K}_P(r)$ is represented as the "sum" of the two rational tangles of slope r. Note that the right rational tangle in the figure corresponds to the image of $(\boldsymbol{B}^3, t(-r))$ by the inversion ι. So, we have $(S^3, \tilde{K}_P(r)) \cong (\boldsymbol{B}^3, t(r)) \cup \iota(\boldsymbol{B}^3, t(-r))$.

Now, let $\eta_r \in \mathrm{Aut}^+(\mathcal{D})$ and $\tilde{r} \in \hat{\mathbb{Q}}$ be such that $(\tilde{r}, \infty) = (\eta_r(r), \eta_r(-r))$. Recall the isomorphism $\mathrm{Aut}^+(\mathcal{D}) \cong \mathrm{SL}(2, \mathbb{Z})$, and let $A \in \mathrm{SL}(2, \mathbb{Z})$ be the matrix corresponding to η_r. Then the linear map $A : \mathbb{R}^2 \to \mathbb{R}^2$ maps the lines of slope r (resp. $-r$) to the lines of slope $\tilde{r}$ (resp. ∞). Thus A induces an orientation-preserving auto-homeomorphism of the pillowcase $(\mathbb{R}^2, \mathbb{Z}^2)/\mathcal{J}$ which maps the pair of proper arcs of "slope" r (resp. $-r$) to the pair of proper arcs of slope $\tilde{r}$ (resp. ∞). This homeomorphism induces an orientation-preserving auto-homeomorphism of $(\partial \boldsymbol{B}^3, P^0)$ via the natural identification $(\partial \boldsymbol{B}^3, P^0) \cong (\mathbb{R}^2, \mathbb{Z}^2)/\mathcal{J}$. By using the fact that $t(s) \subset \boldsymbol{B}^3$ is boundary parallel for every $s \in \hat{\mathbb{Q}}$, we can extend the homeomorphism to an orientation-preserving homeomorphism from $(S^3, \tilde{K}_P(r)) \cong (\boldsymbol{B}^3, t(r)) \cup \iota(\boldsymbol{B}^3, t(-r))$ to $(S^3, K(\tilde{r})) = (\boldsymbol{B}^3, t(\tilde{r})) \cup \iota(\boldsymbol{B}^3, t(\infty))$. □

Remark 2.10.4. By using [44, Proof of Lemma II.3.3(3) and Figure II.3.4], we obtain the following expression of $\tilde{r}$. Consider a continued fraction expansion

$$r = a_0 + [a_1, a_2, \cdots, a_n] = a_0 + \cfrac{1}{a_1 + \cfrac{1}{a_2 + \ddots + \cfrac{1}{a_n}}}.$$

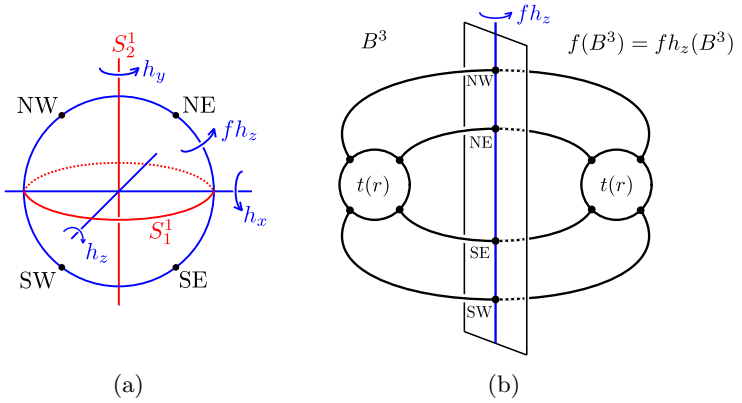

(a) (b)

Figure 2.22: In (a), the axis of the π-rotation fh_z is the great circle $\partial \boldsymbol{B}^3 \cap \{z = 0\}$, and it passes through the four marked points. In (b), ∂B^3 is the central vertical plane and the axis of fh_z is the vertical line. The free involution f is the composition of the π-rotations fh_z and h_z, where $\mathrm{Fix}(fh_z) \cup \mathrm{Fix}(h_z)$ forms a Hopf link.

Then

$$\tilde{r} = \begin{cases} (-1)^{n-1}[a_n, \cdots, a_1, 2a_0, a_1, \cdots, a_n] & \text{if } a_0 \neq 0, \\ (-1)^{n-1}[a_n, \cdots, a_2, 2a_1, a_2, \cdots, a_n] & \text{if } a_0 = 0. \end{cases}$$

Moreover, if $\tilde{r} = \tilde{q}/\tilde{p}$ with $\gcd(\tilde{p}, \tilde{q}) = 1$ then $\tilde{q}^2 \equiv 1 \pmod{2\tilde{p}}$.

Propositions 2.10.1 and 2.10.3 imply the following proposition for rational links in P^3.

Proposition 2.10.5. (1) *$K_P(r)$ is trivial (i.e., it bounds a disk in P^3) if and only if $r = 0$ or ∞.*

(2) *For $r, r' \in \hat{\mathbb{Q}}$, there is a homeomorphism $\psi : P^3 \to P^3$ such that $\psi(K_P(r)) = K_P(r')$ if and only if $r' = \pm r$ or $\pm 1/r$. Moreover, ψ can be chosen to be orientation-preserving if and only if $r' = r$ or $-1/r$.*

(3) *$K_P(r)$ is hyperbolic if and only if $\min(d(0, r), d(\infty, r)) \geq 2$, equivalently, $r \notin \mathbb{Z} \cup \{\infty\} \cup \{1/p \mid p \in \mathbb{Z} \setminus \{0\}\}$.*

Proof. (1) Recall that $t(r)$ is boundary parallel in $\boldsymbol{B}^3$, namely, there is a pair of disjoint disks Δ in $\boldsymbol{B}^3$, such that $t(r) \subset \partial\Delta$ and $\mathrm{cl}(\partial\Delta \setminus t(r)) = \Delta \cap \partial \boldsymbol{B}^3$. If $r = 0$ or ∞, then the antipodal map interchanges the components of $\mathrm{cl}(\partial\Delta \setminus t(r))$, and so Δ descends to a disk in P^3 bounded by $K_P(r)$. Hence $K_P(r)$ is trivial if $r = 0$ or ∞. Conversely, suppose that $K_P(r)$ is trivial. Then its covering link $K(\tilde{r})$ is the 2-component trivial link, and so $\tilde{r} = \infty$. This implies $r = 0$ or ∞ by Proposition 2.10.3.

(2) If $r' = -1/r$, then $(\boldsymbol{B}^3, t(r'))$ is obtained from $(\boldsymbol{B}^3, t(r))$ by $\pi/2$-rotation about the z-axis. Since its restriction to $\partial \boldsymbol{B}^3$ is commutative with the antipodal map, it induces an orientation-preserving homeomorphism $\psi : P^3 \to P^3$ such

that $\psi(K_P(r)) = K_P(r')$. Similarly, if $r' = -r$, then $(\boldsymbol{B}^3, t(r'))$ is obtained from $(\boldsymbol{B}^3, t(r))$ by the reflection in the xy-plane. Since its restriction to $\partial\boldsymbol{B}^3$ is commutative with the antipodal map, it induces an orientation-reversing homeomorphism $\psi : P^3 \to P^3$ such that $\psi(K_P(r)) = K_P(r')$. The if part of (2) follows from these two observations.

Next, we prove the only if part of (2). By (1), we may assume none of r and r' is equal to 0 or ∞. Then the following hold.

(a) Let $\nu_0 \in \mathrm{Aut}(\mathcal{D})$ be the reflection of $\mathcal{D}$ in the Farey edge $\overline{0\infty}$, i.e., ν_0 is the element of $\mathrm{Aut}(\mathcal{D})$ such that $\nu_0(x) = -x$ for every $x \in \hat{\mathbb{Q}}$. Then, for any $r \in \hat{\mathbb{Q}} \setminus \{0, \infty\}$, ν_0 is the unique reflection of $\mathcal{D}$ that interchanges r and $-r$.

(b) If $\xi \in \mathrm{Aut}(\mathcal{D})$ is commutative with ν_0, then the action of ξ on $\hat{\mathbb{Q}}$ is given by $\xi(x) = x$, $-x$, $1/x$ or $-1/x$. Here ξ is orientation-preserving if and only if $\xi(x) = x$ or $-1/x$.

The observation (a) implies that, for any $r \in \hat{\mathbb{Q}} \setminus \{0, \infty\}$, if η_r is an element of $\mathrm{Aut}^+(\mathcal{D})$ such that $(\eta_r(r), \eta_r(-r)) = (\tilde{r}, \infty)$, then $\nu_r := \eta_r \nu_0 \eta_r^{-1}$ is the unique reflection of $\mathcal{D}$ that interchanges $\tilde{r}$ and ∞.

Now suppose that there is a homeomorphism $\psi : P^3 \to P^3$ such that $\psi(K_P(r)) = K_P(r')$, where $r, r' \in \hat{\mathbb{Q}} \setminus \{0, \infty\}$. Then ψ lifts to a homeomorphism $\tilde{\psi} : S^3 \to S^3$ which maps the covering link $K(\tilde{r})$ of $K_P(r)$ to the covering link $K(\tilde{r}')$ of $K_P(r')$. By Proposition 2.10.1(1), there is an automorphism $\xi \in \mathrm{Aut}(\mathcal{D})$ which maps $\{\tilde{r}, \infty\}$ to $\{\tilde{r}', \infty\}$. By the uniqueness of the reflections ν_r and $\nu_{r'}$, we have $\nu_{r'} = \xi \nu_r \xi^{-1}$. Again, by the uniqueness of the reflection ν_0, this in turn implies that the conjugation of ν_0 by $\xi_0 := \eta_{r'}^{-1} \xi \eta_r$ is ν_0, i.e., ν_0 and ξ_0 are commutative. Hence, by the observation (b), the action of ξ_0 on $\hat{\mathbb{Q}}$ is given by $\xi_0(x) = x$, $-x$, $1/x$ or $-1/x$. On the other hand, $r' = \eta_{r'}^{-1}(\tilde{r}')$ is equal to either $\eta_{r'}^{-1}(\xi(\tilde{r})) = \eta_{r'}^{-1}(\xi(\eta_r(r))) = \xi_0(r)$ or $\eta_{r'}^{-1}(\xi(\infty)) = \eta_{r'}^{-1}(\xi(\eta_r(-r))) = \xi_0(-r)$. Since ξ_0 is equal to one of the four transformations in the above, we see that r' is equal to $\pm r$ or $\pm 1/r$ as desired. This completes the proof of the first assertion of (2). The second assertion of (2) can be proved by refining the above arguments by using the second assertion of Proposition 2.10.1(1).

(3) Since $K_P(r)$ is hyperbolic if and only if $K(\tilde{r})$ is hyperbolic, Proposition 2.10.1(2) implies that $K_P(r)$ is hyperbolic if and only if $d(\infty, \tilde{r}) \geq 3$. On the other hand, since the Farey edge $\overline{0\infty}$ separates $-r$ and r, we have

$$d(\infty, \tilde{r}) = d(-r, r) = 2\min(d(\infty, r), d(0, r)).$$

Hence $K_P(r)$ is hyperbolic if and only if $\min(d(\infty, r), d(0, r)) \geq 2$. It is obvious that the latter condition is equivalent to the condition $r \notin \mathbb{Z} \cup \{\infty\} \cup \{1/p \mid p \in \mathbb{Z} \setminus \{0\}\}$. □

By Proposition 2.10.5, we have the following description of the statement (3) of Theorem 2.1.3.

Remark 2.10.6. In the setting of Theorem 2.1.3(3), the following hold. $X = \mathbb{H}^3/G$ is the complement of a hyperbolic rational link $K_P(r)$ in P^3 for some $r \in \hat{\mathbb{Q}} \setminus (\mathbb{Z} \cup \{\infty\} \cup \{1/p \mid p \in \mathbb{Z} \setminus \{0\}\})$, $\Gamma = \langle \mu_1, \mu_2 \rangle$ is an index 2 subgroup of G, and $\mathbb{H}^3/\Gamma$ is the complement of the 2-bridge link $K(\tilde{r})$, where $\tilde{r}$ is characterized by the property that $(\tilde{r}, \infty) = (\eta(r), \eta(-r))$ for some $\eta \in \mathrm{Aut}^+(\mathcal{D})$. In the group $\Gamma = \pi_1(S^3 \setminus K(\tilde{r}))$, $\{\mu_1, \mu_2\}$ is equivalent to the upper or lower meridian pair of the 2-bridge link $K(\tilde{r})$. In the group $G = \pi_1(P^3 \setminus K_P(r))$, $\{\mu_1, \mu_2\}$ is a meridian pair of the rational link $K_P(r)$, such that $G/\langle \mu_1, \mu_2 \rangle \cong \pi_1(P^3) \cong \mathbb{Z}/2\mathbb{Z}$.

The following proposition, obtained by using the result of Millichap-Worden [34, Corollary 1.2] on the commensurable classes of hyperbolic 2-bridge links, plays a key role in the proof of Theorem 2.1.3.

Proposition 2.10.7. *If the complement of a hyperbolic 2-bridge link $K(\tilde{r})$ non-trivially covers an orientable, complete hyperbolic manifold X, then X is the complement of a hyperbolic rational link $K_P(r)$ in P^3, and $K(\tilde{r})$ is the covering link of $K_P(r)$. Thus the covering is a double covering, and $\tilde{r}$ is characterized by the property that $(\tilde{r}, \infty) = (\eta(r), \eta(-r))$ for some $\eta \in \mathrm{Aut}^+(\mathcal{D})$. Moreover, the image of the upper and lower meridian pairs of the link group of $K(\tilde{r})$ in $\pi_1(X)$ are meridian pairs of $K_P(r)$.*

Proof. By [34, Corollary 1.2], a hyperbolic 2-bridge link complement covers a hyperbolic manifold X non-trivially, then it is a regular covering. The isometry group of hyperbolic 2-bridge link complements are calculated by [8, Proposition 4.1] (cf. [43, Theorem 4.1]). As suggested by Boileau-Weidmann [12, Lemma 15], the calculation implies that (i) the complement of the hyperbolic 2-bridge link $K(\tilde{r})$ with $\tilde{r} = \tilde{q}/\tilde{p}$ admits an orientation-preserving free isometry if and only if $\tilde{q}^2 \equiv 1 \pmod{2\tilde{p}}$ and (ii) any such hyperbolic 2-bridge link complement admits a unique orientation-preserving free isometry. In fact, the orientation-preserving isometry group $\mathrm{Isom}^+(S^3 \setminus K(\tilde{r}))$ for such a 2-bridge link $K(\tilde{r})$ is isomorphic to $(\mathbb{Z}/2\mathbb{Z})^3$. Moreover, it extends to the $(\mathbb{Z}/2\mathbb{Z})^3$-action of $(S^3, K(\tilde{r}))$ generated by $\{h_x, h_y, f\}$ as illustrate in Figure 2.22; we can easily check that f is the unique element which acts on the link complement (and also on S^3) freely. (See Bonahon-Siebenmann [14, Chapter 18] for nice description of link symmetries as rigid motions of S^3.) This fact together with Proposition 2.10.3 implies the first assertion. The last assertion is obvious. □

Proof of Theorem 2.1.3. Let $X = \mathbb{H}^3/G$ and $\{\mu_1, \mu_2\}$ be as in Theorem 2.1.3, and let $\Gamma = \langle \mu_1, \mu_2 \rangle$ be the subgroup of G generated by $\{\mu_1, \mu_2\}$. Then, since $\Gamma < G$ is torsion-free, Theorem 2.1.1 implies that Γ is either a rank 2 free group or a hyperbolic 2-bridge link group. In the former case, the conclusion (1) holds. In the latter case, $X = \mathbb{H}^3/G$ is covered by the hyperbolic 2-bridge link complement $\mathbb{H}^3/\Gamma$. Hence, by Proposition 2.10.7, either (i) $\Gamma = G$ and the conclusion (2) holds by Theorem 2.1.2 (or Theorem 2.1.1) or (ii) Γ is a proper subgroup of G and the conclusion (3) holds. This completes the first assertion of Theorem 2.1.3.

In order to prove the second assertion, assume that $X = \mathbb{H}^3/G$ has finite volume and Γ is a rank 2 free group. Suppose to the contrary that Γ is geometrically infinite. Since the codomain X of the covering $p : \hat{X} = \mathbb{H}^3/\Gamma \to X = \mathbb{H}^3/G$ has finite volume and since $\hat{X}$ is tame by the tameness theorem ([4, 15, 18, 47]), the covering theorem of Canary [19] implies that X has a finite cover X' which fibers over the circle, such that the cover X_S of X' associated to a fiber subgroup satisfies one of the following conditions.

(a) $\hat{X} = X_S$.

(b) $\hat{X}$ is a twisted I-bundle which is doubly covered by X_S.

Suppose first that $\hat{X} = X_S$. Then there is a fuchsian group Γ_0 of co-finite volume, such that (i) the hyperbolic surface $\mathbb{H}^2/\Gamma_0$ is homeomorphic to the fiber surface S of the bundle X' over S^1, and (ii) there is an isomorphism $\rho : \Gamma_0 \to \Gamma$ which is strictly type-preserving, i.e., for $g \in \Gamma_0 < \mathrm{Isom}^+(\mathbb{H}^2)$, $\rho(g)$ is parabolic if and only if g is parabolic. Since Γ is generated by two parabolic elements, S must be a thrice-punctured sphere. This contradicts the assumption that S is a fiber surface of X', because a thrice-punctured sphere does not admit a pseudo-Anosov homeomorphism.

Suppose next that $\hat{X}$ is a twisted I-bundle which is doubly covered by X_S. Then there is a non-orientable hyperbolic surface $F = \mathbb{H}^2/\Gamma_0$, where $\pi_1(F) \cong \Gamma_0 < \mathrm{Isom}(\mathbb{H}^2) < \mathrm{Isom}^+(\mathbb{H}^3)$, and a strictly type-preserving isomorphism $\rho : \Gamma_0 \to \Gamma$. (Here F is homeomorphic to the base space of the twisted I-bundle $\hat{X}$.) This contradicts the fact that there is no non-orientable surface whose fundamental group is generated by peripheral elements. Hence Γ is geometrically finite. □

Bibliography

[1] C. Adams, *Hyperbolic 3-manifolds with two generators*, Comm. Anal. Geom. **4** (1996), no. 1-2, 181–206.

[2] C. Adams, *Noncompact Fuchsian and quasi-Fuchsian surfaces in hyperbolic 3-manifolds*, Algebr. Geom. Topol. **7** (2007), 565–582.

[3] I. Agol, *The classification of non-free 2-parabolic generator Kleinian groups*, Slides of talks given at Austin AMS Meeting and Budapest Bolyai conference, July 2002, Budapest, Hungary.

[4] I. Agol, *Tameness of hyperbolic 3-manifolds*, arXiv:math/0405568.

[5] I. R. Aitchison, E. Lumsden, and J. H. Rubinstein, *Cusp structures of alternating links*, Invent. Math. **109** (1992), no. 3, 473–494.

[6] I. R. Aitchison and J. H. Rubinstein, *An introduction to polyhedral metrics of nonpositive curvature on 3-manifolds*, Geometry of low-dimensional manifolds, 2 (Durham, 1989), 127–161, London Math. Soc. Lecture Note Ser., **151**, Cambridge Univ. Press, Cambridge, 1990.

[7] I. R. Aitchison and J. H. Rubinstein, *Combinatorial cubings, cusps and dodecahedral knots*, Topology '90 (Columbus, OH, 1990), 17–26, Ohio State Univ. Math. Res. Inst. Publ., 1, de Gruyter, Berlin, 1992.

[8] S. Aimi, D. Lee, S. Sakai, and M. Sakuma, *Classification of parabolic generating pairs of Kleinian groups with two parabolic generators*, Rend. Istit. Mat. Univ. Trieste **52** (2020), 477–511.

[9] H. Akiyoshi, K. Ohshika, J. Parker, M. Sakuma, and H. Yoshida, *Classification of non-free Kleinian groups generated by two parabolic transformations*, Trans. Amer. Math. Soc. **374** (2021), no. 3, 1765–1814.

[10] H. Akiyoshi, M. Sakuma, M. Wada, and Y. Yamashita, *Punctured torus groups and 2-bridge knot groups (I)*, Lecture Notes in Mathematics **1909**, Springer, Berlin, 2007.

[11] R. J. Aumann, *Asphericity of alternating knots*, Ann. of Math. (2) **64** (1956), 374–392.

[12] M. Boileau and R. Weidmann, *The structure of* 3*-manifolds with two-generated fundamental group*, Topology **44** (2005), no. 2, 283–320.

[13] M. Boileau and B. Zimmermann, *The* π*-orbifold group of a link*, Math. Z. **200** (1989), 187–208.

[14] F. Bonahon and L. Siebenmann, *New geometric splittings of classical knots, and the classification and symmetries of arborescent knots*, `http://www-bcf.usc.edu/~fbonahon/Research/Publications.html`

[15] B. H. Bowditch, *Notes on tameness*, Enseign. Math. **56** (2010), 229–285.

[16] M. Bridson and A. Haefliger, *Metric spaces of non-positive curvature*, Grundlehren der Mathematischen Wissenschaften **319**, Springer-Verlag, Berlin, 1999. xxii+643 pp.

[17] R. Byrd and R. Harlander, *On the Dehn complex of virtual links*, J. Knot Theory Ramifications **22** (2013), no. 7, 1350033, 13 pp.

[18] D. Calegari and D. Gabai, *Shrinkwrapping and the taming of hyperbolic 3-manifolds*, J. Amer. Math. Soc. **19** (2006), 385–446.

[19] R. D. Canary, *A covering theorem for hyperbolic* 3*-manifolds and its applications*, Topology **35** (1996), no. 3, 751–778.

[20] A. Elzenaar, G. Martin, J. Schillewaert, *Approximations of the Riley slice*, arXiv:2111.03230 [math.GT].

[21] D. Farley, *A proof of Sageev's theorem on hyperplanes in CAT(0) cubical complexes*, Topology and geometric group theory, 127–142, Springer Proc. Math. Stat., **184**, Springer, [Cham], 2016.

[22] D. Futer, E. Kalfagianni,and J. Purcell, *quasi-fuchsian state surfaces*, Trans. Amer. Math. Soc. **366** (2014), no. 8, 4323–4343.

[23] J. Greene, *Alternating links and definite surfaces*, Duke Math. J. **166** (2017), 2133–2151.

[24] F. Haglund and D. Wise, *Special cube complexes*, Geom. Funct. Anal. **17** (2008), no. 5, 1551–1620.

[25] J. Harlander, *Hyperbolic alternating virtual link groups*, Groups Geom. Dyn. **6** (2012), 83–96.

[26] J. Harlander and S. Rosebrock, *Generalized knot complements and some aspherical ribbon disc complements*, J. Knot Theory Ramifications **12** (2003), no. 7, 947–962.

[27] J. Howie, *A characterisation of alternating knot exteriors*, Geom. Tool. **21** (2017), no. 4, 2353–2371.

[28] D. Lee and M. Sakuma, *Parabolic generating pairs of genus-one* 2*-bridge knot groups*, J. Knot Theory Ramifications **25** (2016), 1650023, 21 pp.

[29] B. Maskit, *Kleinian groups*, Grundlehren der mathematischen Wissenschaften, **287**, Springer-Verlag, Berlin, 1988. xiv+326

[30] B. Maskit and G. Swarup, *Two parabolic generator Kleinian groups*, Israel J. Math. **64** (1988), no. 3, 257–266 (1989).

[31] K. Matsuzaki and M. Taniguchi, *Hyperbolic manifolds and Kleinian groups*, Oxford Mathematical Monographs. Oxford Science Publications. The Clarendon Press, Oxford University Press, New York, 1998. x+253 pp.

[32] W. Menasco, *Closed incompressible surfaces in alternating knot and link complements*, Topology **23** (1984), no. 1, 37–44.

[33] W. Menasco and M. Thistlethwaite, *The classification of alternating links*, Ann. of Math. (2) **138** (1993), no. 1, 113–171.

[34] C. Millichap and W. Worden, *Hidden symmetries and commensurability of* 2*-bridge link complements*, Pacific J. Math. **285** (2016), 453–484.

[35] D. Mumford, C. Series and D. Wright, *Indra's pearls. The vision of Felix Klein*, Cambridge University Press, New York, 2002. xx+396 pp.

[36] M. Ozawa, *Non-triviality of generalized alternating knots*, J. Knot Theory Ramifications **15** (2006), no. 3, 351–360.

[37] M. Ozawa, *Essential state surfaces for knots and links*, J. Aust. Math. Soc. **91** (2011), no. 3, 391–404.

[38] J. Parker and S. P. Tan, *Caroline Series and Hyperbolic Geometry*, Notices Amer. Math. Soc. **70** (2023), no. 3, 380–389.

[39] J. S. Purcell, *Hyperbolic knot theory*, Graduate Studies in Mathematics, **209**. American Mathematical Society, Providence, RI, 2020. xviii+369 pp.

[40] M. Sageev, *Ends of group pairs and non-positively curved cube complexes*, Proc. London Math. Soc. (3) **71** (1995), no. 3, 585–617.

[41] S. Sakai, *A characterization of alternating link exteriors in terms of cubed complexes*, J. Knot Theory Ramifications **27** (2018), no. 8, 1850047, 8 pp.

[42] S. Sakai and M. Sakuma, *Combinatorial local convexity implies convexity in finite dimensional CAT(0) cubed complexes*, arXiv:2302.10500v3 [math.GT].

[43] M. Sakuma, *The geometries of spherical Montesinos links*, Kobe J. Math. **7** (1990), 167–190.

[44] M. Sakuma and J. Weeks, *Examples of canonical decompositions of hyperbolic link complements*, Japan. J. Math. (N.S.) **21** (1995), 393–439.

[45] M. Sakuma and Y. Yokota, *An application of non-positively curved cubings of alternating links*, Proc. Amer. Math. Soc. **146** (2018), no. 7, 3167–3178.

[46] H. Schubert, *Knoten mit zwei Brücken*, Math. Z. **65** (1956), 133–170.

[47] T. Soma, *Existence of ruled wrappings in hyperbolic 3-manifolds*, Geom. Topol. **10** (2006), 1173–1184.

[48] StackExchanges, *Convex subcomplexes of CAT(0) cubical complexes*, `https://mathoverflow.net/questions/194235/convex-subcomplexes-of-cat0-cubical-complexes`

[49] M. Takahashi, *On the concrete construction of hyperbolic structures of* 3*-manifolds*, Tsukuba J. Math. **9** (1985), no. 1, 41–83.

[50] D. Thurston, *Hyperbolic volume and the Jones polynomial*, Notes from lectures at the Grenoble summer school Invariants des noeuds et de variétés de dimension 3 , June 1999, available from http://pages.iu.edu/ dpthurst/speaking/Grenoble.pdf.

[51] W. Thurston, *Three-dimensional manifolds, Kleinian groups and hyperbolic geometry*, Bull. Amer. Math. Soc. (N.S.) **6** (1982), no. 3, 357–381.

[52] W. Thurston, *The geometry and topology of three-manifolds*, available from http://library.msri.org/books/gt3m/

[53] Y. Yokota, *On the potential functions for the hyperbolic structures of a knot complement*, Invariants of knots and 3-manifolds (Kyoto, 2001), 303–311, Geom. Topol. Monogr., **4**, Geom. Topol. Publ., Coventry, 2002.

[54] Y. Yokota, *On the complex volume of hyperbolic knots*, J. Knot Theory Ramifications **20** (2011), 955–976.

[55] D. T. Wise, *Non-positively curved squared complexes, aperiodic tilings, and non-residually finite groups*, PhD thesis, Princeton University (1996).